NASA/TM–2002–210006, Vol. 2

The Second SIMBIOS Radiometric Intercomparison (SIMRIC-2), March-November 2002

G. Meister, P. Abel, K. Carder, A. Chapin, D. Clark, J. Cooper, C. Davis, D. English, G. Fargion, M. Feinholz, R. Frouin, F. Hoge, D. Korwan, G. Lazin, C. McClain, S. McLean, D. Menzies, A. Poteau, J. Robertson, J. Sherman, K. Voss, J. Yungel

National Aeronautics and
Space Administration

Goddard Space Flight Center
Greenbelt, Maryland 20771

August 2003

The Second SIMBIOS Radiometric Intercomparison (SIMRIC-2), March-November 2002

Gerhard Meister, SIMBIOS Project / Futuretech Corp., NASA Code 970.1, Greenbelt, Maryland

Peter Abel, Charles McClain, NASA, Goddard Space Flight Center, Greenbelt, Maryland

Kendall Carder, David English, College of Marine Science, University of South Florida, St. Petersburg, Florida

Dennis Clark, Oceanic Research and Applications Div., NOAA/NESDIS/ORA, Silver Springs, Maryland

John Cooper, Raytheon Information Technology and Science Services, NASA Code 920.1, Lanham, Maryland

Curtiss Davis, Daniel Korwan, Naval Research Laboratory, Washington, District of Columbia

Giulietta Fargion, SIMBIOS Project / Science Applications International Corporation, Greenbelt, Maryland

Michael Feinholz, Physical Oceanography, Moss Landing Marine Laboratories, Moss Landing, California

Robert Frouin, Antoine Poteau, Scripps Institution of Oceanography, University of California in San Diego, California

Frank Hoge, James Yungel, AOL Project, Wallops Flight Facility, NASA Code 972

Scott McLean, Jennifer Sherman, Gordana Lazin, Satlantic Inc., Halifax, Canada

David Menzies, Institute for Computational Earth System Science at the University of California in Santa Barbara, California

James Robertson, Biospherical Instruments Inc., San Diego, California

Kenneth Voss, Albert Chapin, Atmospheric and Ocean Optics, Physics Department, University of Miami, Florida

Abstract

The second SIMBIOS (Sensor Intercomparison and Merger for Biological and Interdisciplinary Oceanic Studies) Radiometric Intercomparison (SIMRIC-2) was carried out in 2002. The purpose of the SIMRICs is to ensure a common radiometric scale among the calibration facilities that are engaged in calibrating *in-situ* radiometers used for ocean color related research and to document the calibration procedures and protocols. The SeaWiFS Transfer Radiometer (SXR-II) measured the calibration radiances at six wavelengths from 411nm to 777nm in the ten laboratories participating in the SIMRIC-2. The measured radiances were compared with the radiances expected by the laboratories. The agreement is within the combined uncertainties for all but two laboratories. Likely error sources were identified in these two laboratories and corrective measures were implemented. NIST calibrations in December 2001 and January 2003 showed changes ranging from -0.6% to +0.7% for the six SXR-II channels. Two independent light sources were used to monitor changes in the SXR-II responsivity between the NIST calibrations. A 2% variation of the responsivity of channel 1 of the SXR-II was detected, and the SXR-II responsivity was corrected using the monitoring data. This report also presents a comparison of directional reflectance calibrations of a Spectralon plaque by different calibration facilities.

Contents

Chapter 1

Introduction

Optical remote sensing of the earth has become an important data source for various science fields, from biology, geography, and geology to meteorology, oceanography and climate research. Especially for climate studies, it is important to obtain global data sets that cover large time periods of 10 years or more. The only technique to obtain global data sets is satellite data. Unfortunately, satellite life spans are usually on the order of five years or less. For surfaces covered by land, the longest time series available so far is the NOAA (National Oceanic and Atmospheric Administration) AVHRR (Advanced Very High Resolution Radiometer) time series, which combines the data from four satellites into a continuous dataset covering twenty years from 1981 to 2001. No comparable dataset is available for oceans.

The Sensor Intercomparison and Merger for Biological and Interdisciplinary Oceanic Studies (SIMBIOS) Project has a worldwide, ongoing ocean color data collection program, plus an operational data processing and analysis capability. The SIMBIOS Program goal is to assist the international ocean color community in developing a multi-year time-series of calibrated radiances which transcends the spatial and temporal boundaries of individual missions.

The specific objectives of the SIMBIOS Program are: (1) to quantify the relative accuracies of the ocean color products from each mission, (2) to work with each project to improve the level of confidence and compatibility among the products, and (3) to develop methodologies for generating merged level-3 products. SIMBIOS has identified the primary instruments to be used for developing global data sets. These instruments are Sea-viewing Wide Field-of-view Sensor (SeaWiFS), Ocean Color and Temperature Scanner (OCTS), Polarization and Directionality of the Earth's Reflectances (POLDER) on ADEOS-I and on ADEOS-II, Moderate Resolution Imaging Spectrometer (MODIS) on Aqua and Terra, MISR (on Terra), Medium Resolution Imaging Spectrometer (MERIS), and Global Imager (GLI). The products from other missions (e.g., Ocean Color Imager (OCI) and the two Modular Optoelectronic Scanner (MOS) instruments) will be tracked and evaluated, but are not considered as key data sources for a combined global data set.

The SIMBIOS Program consists of the SIMBIOS Science Team and the SIMBIOS Project Office, [Fargion et al., 2002]. SIMBIOS Science Team Principal Investigators are primarily composed of persons selected under the SIMBIOS NASA Research Announcement (NRA) 1996 (i.e. SIMBIOS Team 1997-1999) and NRA 1999 (i.e. SIMBIOS Team 2000-2003). The present Science Team is grouped under three working areas: 1) Ocean Bio-optical and Sensor Characterization Studies, 2) Data Merger Studies, and 3) Atmospheric Correction Studies. In addition, there are many more US and international co-investigators and collaborators actively participating in the SIMBIOS Program. The SIMBIOS Project incorporates aspects of instrument calibration, algorithm development and evaluation, product merging, data processing, and inter-agency and international coordination, see http://simbios.gsfc.nasa.gov for more information.

To measure ocean color from space is a very difficult task. Only about 10 % of the signal arriving at a space-based sensor originates from the ocean, about 90 % of the signal comes from the atmosphere. An error in the determination of the atmospheric contribution of only 1 % (relative to the atmospheric signal) will lead to an error in the signal from the ocean of 9 % (relative to the ocean signal). Thus in many cases (e.g. SeaWiFS and MODIS) the satellite sensor is calibrated vicariously with *in-situ* data. In the case of SeaWiFS and MODIS, a buoy called MOBY (Marine Optical Buoy,[Clark et al., 2002]) located in the vicinity of Hawaii is used.

The quality of the calibrated satellite data can be checked with match-up analyses from *in-situ* ocean color measurements taken during ship cruises. The SeaWiFS and the SIMBIOS Project jointly maintain a database

called SeaBASS (SeaWiFS Bio-optical Archive and Storage System, http://seabass.gsfc.nasa.gov) that contains *in-situ* data from more than 600 cruises from all over the world. The quality of this database is obviously directly related to the quality and comparability of the stored *in-situ* data. Two kinds of activities are performed by the SIMBIOS program to ensure an adequate quality of the SeaBASS database: First, measurement protocols are developed [Mueller et al., 2003] and their usage by the science community is encouraged. Second, calibration round-robin intercomparison experiments are conducted by the SIMBIOS Project. The participating laboratories include academic institutions, government agencies and instrument manufacturers that either directly or indirectly contribute to SeaBASS. The purpose of these round-robins is to

1. verify that all laboratories are on the same radiometric scale
2. detect and correct problems at any individual laboratory in a timely fashion
3. encourage the common use of calibration protocols
4. identify areas where the calibration protocols need to be improved
5. document the calibration procedures specific to each laboratory.

This report documents the results from the second SIMBIOS round-robin, the SIMRIC-2. The SIMBIOS Radiometric Intercomparison (SIMRIC) series was started by the SIMBIOS Project as a successor to the SIRREX (SeaWiFS Intercalibration Round-Robin Experiment) series. SIRREX-6 [Riley and Bailey, 1998] was a joint venture of the SeaWiFS and the SIMBIOS projects, during which 10 laboratories were visited by NASA personnel, who carried 2 radiance and 2 irradiance radiometers and had them calibrated at each laboratory. The calibration coefficients were compared, and it was found that the average agreement was about $\pm$ 2 %, but there were some outliers up to 8 %.

For the SIMRIC-1 [Meister et al., 2002], [Meister et al., 2003], SIMBIOS staff visited 7 laboratories (Naval Research Laboratories, Washington, DC; Scripps Institute of Oceanography, University of California, San Diego; Biospherical Instruments Inc., CA; ICESS at the University of California, Santa Barbara; HOBI Labs, CA; NASA Code 920.1, GSFC, MD; Satlantic Inc., Canada) with a radiometer designed and calibrated by the National Institute of Standards (NIST), the SeaWiFS Transfer Radiometer II (SXR-II). The radiometric stability of the SXR-II was monitored by portable light sources, the OCS-5002 from YES, Inc., and the SQM-II from Satlantic, Inc. The radiances produced by the laboratories for calibration were measured in the six SXR-II channels from 411 nm to 777 nm and compared to the radiances expected by the laboratories. Typically, the measured radiances were higher than the expected radiances by 0 to 2 %. This level of agreement is satisfactory. Several issues were identified, where the calibration protocols need to be improved, especially the reflectance calibration of the reference plaques and the distance correction when using the irradiance standards at distances greater than 50 cm. The responsivity of the SXR-II changed between 0.1 % (channel 1) and 1.6 % (channel 2) from December 2000 to December 2001. Monitoring the SXR-II with a portable light source showed a linear drift of the calibration, except for channel 1, where a 2 % drop occured in summer.

For the SIMRIC-2, all the laboratories participating in the SIMRIC-1 except for HOBI Labs where visited again, and four more laboratories joined the participants: NASA Code 972, Wallops Flight Facility, MD; Moss Landing Marine Laboratories, CA (MOBY); University of South Florida, St. Petersburg; University of Miami, FL. This report documents the calibration procedures in the new laboratories only, those laboratories that already participated in the SIMRIC-1 have been described in the SIMRIC-1 report [Meister et al., 2002], and only new developments are documented. This report presents and discusses the differences of the radiances expected by the laboratories and the radiances measured by the SXR-II.

The structure of this document is as follows: chapter 2 introduces the SIMBIOS equipment used for this study. The focus of this chapter is the radiometric stability of the SXR-II. The calibration facilities and procedures of the SIMRIC-2 participants are described in chapter 3, as well as the SXR-II specific measurement procedures. The comparison results are described in chapter 4. Results from reflectance calibrations of Spectralon are presented in chapter 5. A discussion of the results of SIMRIC-2 can be found in chapter 6. The SIMRIC-1 results were derived with preliminary SXR-II calibration coefficients for the NIST December 2001 calibration. The final SIMRIC-1 results with the final calibration coefficients from NIST are given in the appendix, section A. A list of the participants and their addresses is given in the appendix, section B.

Chapter 2

Calibration of the SeaWiFS Transfer Radiometer II

2.1 SXR-II

The SeaWiFS Transfer Radiometer II (SXR-II, S/N 104) is a portable transfer radiometer with 6 wavelength channels. It has been designed by the Optical Technology Division at the NIST. It was built by Reyer Corp., New Market, MD. Its primary purpose is to measure radiances produced by calibration light sources in laboratories in order to assess the calibration accuracy of the respective laboratory. See [Meister et al., 2002] and [Johnson et al., 1998] for a complete description.

The SXR-II has been calibrated three times at the Optical Technology Division at the NIST, Gaithersburg, MD at the SIRCUS (Spectral Irradiance and Radiance Calibration with Uniform Sources) facility [Brown et al., 2000]. The calibrations were made in December 2000, December 2001 and January 2003. The calibration factors are given in Table 2.1. No calibration report was delivered by NIST until May 2003 for either calibration. A preliminary estimation of the uncertainties is given in Table 2.2. Some estimates were copied from the uncertainties for the original SXR [Johnson et al., 1998]. Although we use the same terminology for the uncertainty contributions as in [Johnson et al., 1998], the nature of some of these contributions is different: the size-of-source effect (u_a) is the uncertainty associated with the on-axis cavity measurement (see section 3.3), and the long-term drift (u_d) is the uncertainty after the linear interpolation in time of the calibration coefficients. We expect to be able to give a better estimate of the uncertainties once the calibration reports are available. For the moment, the combined uncertainty for the SXR-II is estimated to be 0.8 % (k=1) by taking the root of the sum of the squares of the contributions listed in Table 2.2 (law of error propagation). We estimate that for channels 1 and 6 an additional 0.5% uncertainty should be included to account for a worse temporal stability (for time periods on the order of several days/weeks) as compared to the other channels. Adding this uncertainty quadratically yields a combined uncertainty of about 1.0% for channels 1 and 6. It is surprising that the two channels with the worst temporal stability for time periods on the order of several days/weeks are the most stable over the two year calibration history, see Fig. 2.1. The changes in calibration coefficients from December 2001 to January 2003 for the two SXR-II calibrations on SIRCUS are within ±0.7%, see Table 2.1 and Fig. 2.1, which is much smaller than the changes from December 2000 to December 2001 (up to 1.6%, see also table A.1, page 59).

To calculate the calibration coefficients at a certain date of a SIMRIC-2 measurement, the calibration coefficients are linearly interpolated in time between the December 2001 and the January 2003 calibrations. The error associated with this procedure (u_d) is about 0.5% (see section 2.4 below). The temporal evolution of the calibration coefficients was adjusted to represent features seen in the monitoring data, see below, section 2.4.3.

Fig. 2.2 shows the responsivity of the SXR-II channels as a function of wavelength for the in-band wavelengths, this means for those wavelengths with a high responsivity, for the SIRCUS calibrations from December 2000, December 2001, and January 2003. The out-of-band response is shown in Fig. 2.1 in [Meister et al., 2002]. The data have been normalized to the maximum value. It can be seen that there is almost no spectral shift in the responsivities between the three calibrations.

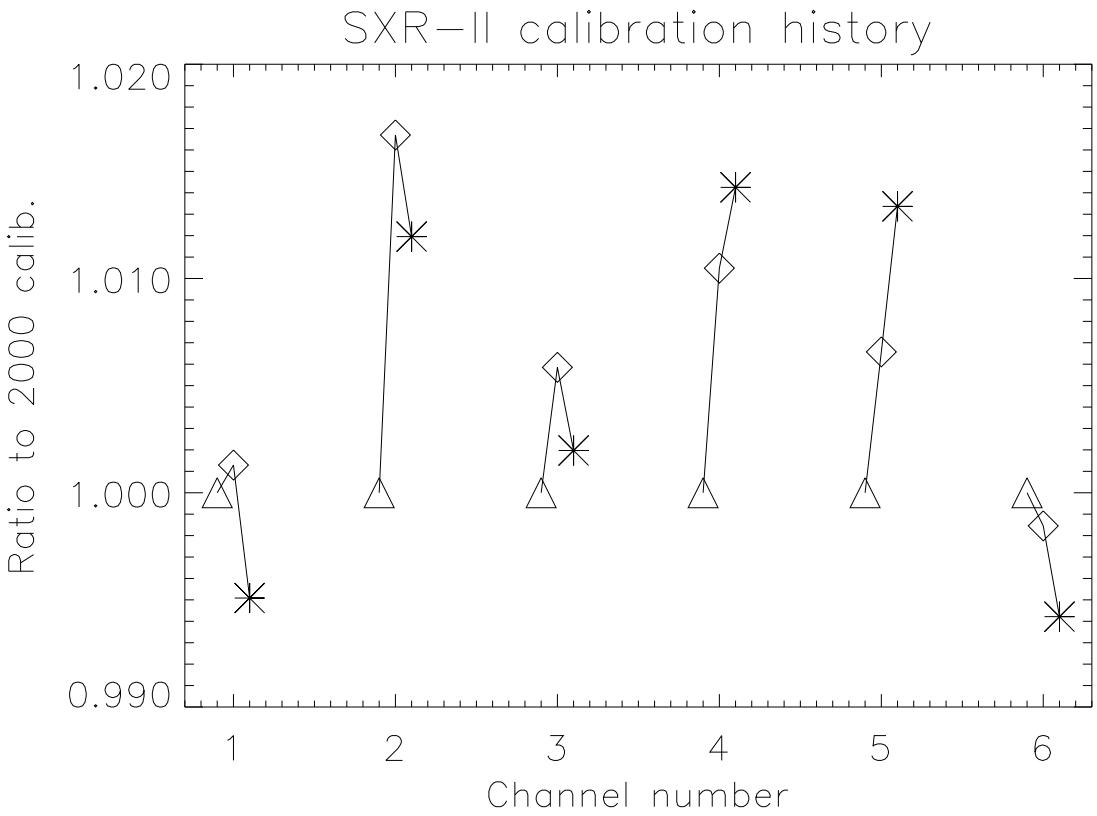

Figure 2.1: *The NIST calibration coefficients for the SXR-II for the three SIRCUS calibrations, normalized to the first calibration. Triangles show the December 2000 calibration (equals 1 by definition), diamonds show the December 2001 calibration, and stars show the January 2003 calibration. Comparing the December 2001 and January 2003 calibrations, the biggest decrease is seen in channel 1 (the calibration coefficient dropped by 0.6%, i.e. the responsivity increased), the biggest increase is seen in channel 5 (the calibration coefficient increased by 0.7%, i.e. the responsivity decreased). The values of the calibration coefficients for 2000 and 2001 are printed in the appendix, section A, for 2002 in Table 2.1.*

	Channel 1	Channel 2	Channel 3	Channel 4	Channel 5	Channel 6
λ_m [nm]	410.69	441.51	487.58	546.89	661.91	776.71
$< \mathrm{D}_{\mathrm{cs}}^{2002} >$	0.651887	0.936835	0.117723	0.204956	0.178774	0.017619
$\Delta < \mathrm{D} > (2002-2001)$ [%]	-0.6	-0.5	-0.4	0.4	0.7	-0.4
L_s	16.6	11.8	92.7	53.9	61.7	615.2

Table 2.1: *SXR-II calibration coefficients* $< \mathrm{D_{cs}} >$ $[\mathrm{V\,cm^2 sr\,nm}/\mu\mathrm{W}]$ *for gain 1 on the SXR-II amplifier (multiplied by -1, the radiometer provides negative voltages) and moment wavelengths* λ_m *for the 6 SXR-II channels. The coefficients from January 2003 are called* $< \mathrm{D}_{\mathrm{cs}}^{2002} >$ *for consistency in terminology with the two previous calibration coefficients (*$< \mathrm{D}_{\mathrm{cs}}^{2000} >$ *and* $< \mathrm{D}_{\mathrm{cs}}^{2001} >$*), which are given in the appendix, Table A.1, page 59. The difference* Δ *in the coefficients between the two dates is calculated as* $< \mathrm{D}_{\mathrm{cs}}^{2002} >$ *minus* $< \mathrm{D}_{\mathrm{cs}}^{2001} >$ *and given in %. The saturation radiances* $L_s[\mu\mathrm{W}/(\mathrm{cm^2 sr\,nm})]$ *in the bottom line are conservative estimates.*

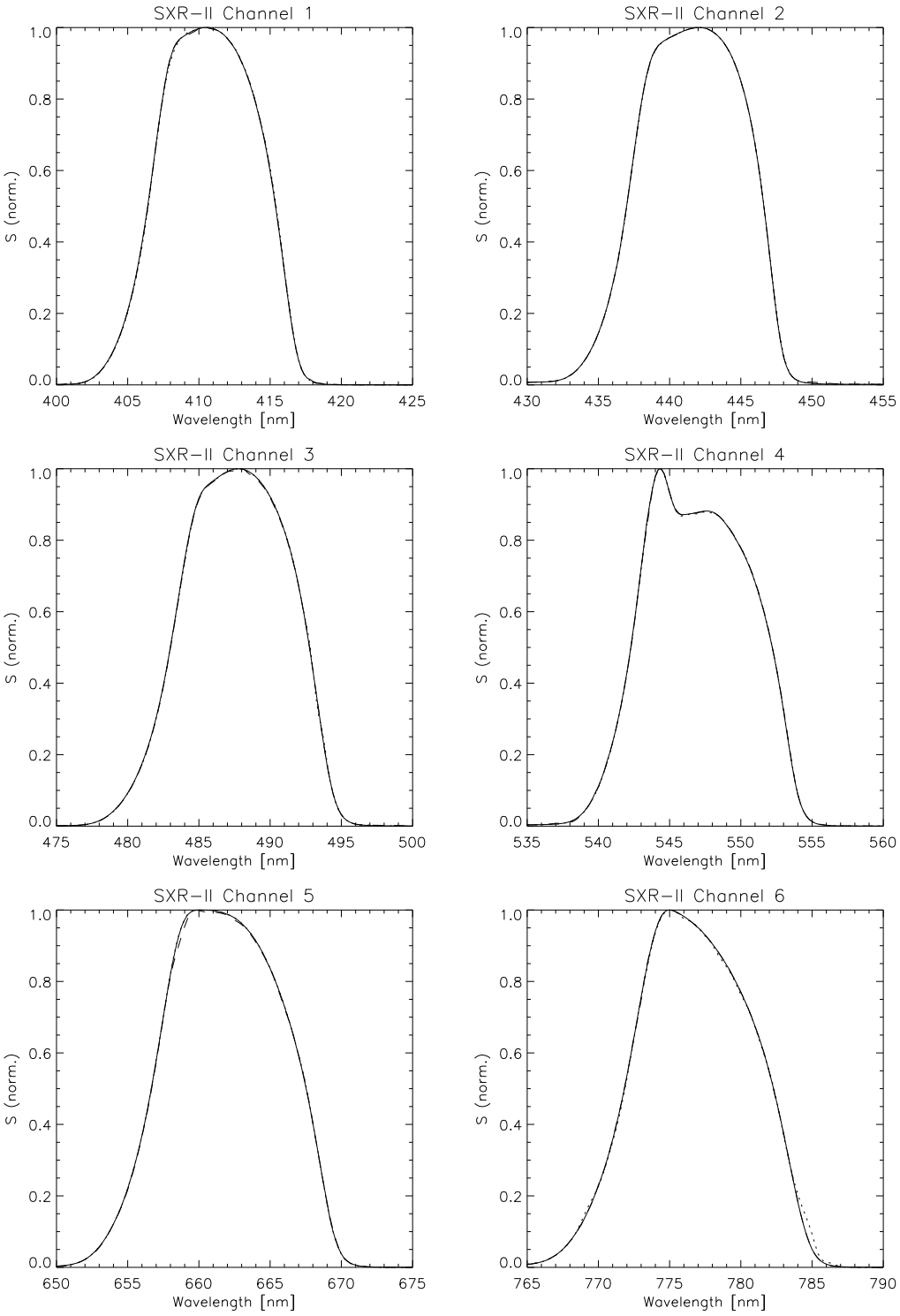

Figure 2.2: *Responsivity $S(\lambda)$ (see eq. 4.2, page 34) of the SXR-II channels as a function of wavelength (interpolated values, normalized to the maximum value). The solid line shows S from the SIRCUS January 2003 calibration, the dashed line from the SIRCUS December 2001 calibration (see e.g. channel 5), the dotted line from the SIRCUS December 2000 calibration (see e.g. channel 6). It is hard to identify any change in most channels from these plots.*

u_D [%]	u_d[%]	u_{flux} [%]	u_{rep} [%]	u_a [%]	u_{setup} [%]	u_c [%]
0.5	0.5	0.1	0.1	0.2	0.3	0.8

Table 2.2: *Preliminary uncertainty estimates for SXR-II channels 2 to 5. The uncertainties* $u_D, u_d, u_{\text{flux}}, u_{\text{rep}}, u_a$, *relate to the calibration coefficient D, the drift of the calibration coefficient, the nonlinearity, the repeatability, the size-of-source effect, respectively (see [Johnson et al., 1998] for a description of these errors in the original SXR). The statistical error from averaging over several scans/samples and the error produced by the amplifier for different gains are negligible (*$< 0.1\%$*).* u_{setup} *is the uncertainty from aligning the SXR-II.* u_c *is the combined uncertainty. For channels 1 and 6,* u_c *is about 1.0%, see text.*

SXR-II wavelength [nm]	411	442	488	547	662	777
OCS-5002 LoBank	0.0161	0.0314	0.0703	0.147	0.332	0.424
OCS-5002 HiBank	0.169	0.310	0.638	1.19	2.17	2.43
OCS-5002 Both Banks	0.182	0.336	0.691	1.30	2.44	2.78
SQM-II LoBank	0.0996	0.199	0.414	0.541	0.738	1.52
SQM-II HiBank	0.260	0.526	1.11	1.48	2.01	4.13
SQM-II Both Banks	0.360	0.731	1.54	2.05	2.78	5.71

Table 2.3: Radiances of the OCS-5002 and the SQM-II at the SXR-II wavelengths. Radiance unit is $\mu\text{W}/(\text{cm}^2\text{sr nm})$.

2.2 OCS-5002

The OCS-5002 (Optical Calibration Source) is an SQM-type (SeaWiFS Quality Monitor) portable stable light source for monitoring the radiometric stability of oceanographic radiometers. The original SQM has been designed by NASA and NIST, see [Johnson et al., 1998b] for a detailed description. The OCS-5002 (S/N 102) of the SIMBIOS Project has been produced by Yankee Environmental System, Turner Falls, Massachusetts.

The OCS-5002 has two sets of 8 bulbs each. There is no individual bulb control, a set is either completely turned on or off. The light output of the second set (called *HiBank* in this report) is about 10 (6) times brighter in the blue (red) than the light output of the first set (called *LoBank* in this report), see Table 2.3 for the absolute radiance values at the SXR-II wavelengths in comparison to the SQM-II (described below). Both sets can also be used simultaneously. The radiometer to be tested for stability is either mounted into the exit aperture or put in front of the exit aperture, see Fig. 2.3.

The OCS-5002 has been redesigned from the original SQM. The major departures from the original design are the integration of all subsystems into one system, the addition of an LED status display, and the removal of the preheater. A serial port provides the capability of monitoring the system with a PC, the LabView based software is provided and gives a graphical representation of the monitored variables of the OCS-5002 covering the recent 10 minutes. The log file of the OCS-5002 monitored variables contains 13 fields:

1. Date and time
2. LoBank current set point
3. LoBank current
4. LoBank register (factory diagnostic tool)
5. HiBank current set point
6. HiBank current
7. HiBank register (factory diagnostic tool)
8. Internal monitor red (center wavelength about 625 nm, FWHM from about 600 nm to 675 nm)
9. Internal monitor white (center wavelength about 525 nm, FWHM from about 375 nm to 650 nm)

10. Internal monitor blue (center wavelength about 425 nm, FWHM from about 375 nm to 475 nm)
11. Shunt temperature
12. Core (case) temperature
13. Detector temperature

The wavelength ranges of the internal monitors are determined by Schott filter combinations and are identical to the original SQM [Johnson et al., 1998b].

A control knob on the back of the OCS-5002 can be set to 5 different positions:

- OFF
- STBY (heater for the electronics is on, internal monitors are temperature stabilized, monitored variables are sent via the serial port)
- LOW (LoBank is on)
- MED (HiBank is on)
- HIGH (LoBank and HiBank are on)

In case the temperature of the case exceeds 35° C, a fan is turned on to cool the case below 35° C.

The usage of the (original) SQM is described in [Mueller et al., 2003] (volume 2, chapter 5), detailed results are presented in [Hooker et al., 1998]. The internal monitors are supposed to be used to correct the light output by dividing the readings from the external radiometer (in this case the SXR-II signal) through the simultaneously measured internal monitor signal.

For the SIMRIC-2, the measured radiances in the SXR-II channels 1 and 2 were adjusted using the blue detector, channels 3 and 4 with the white detector, and channels 5 and 6 with the red detector (although the red detector is not sensitive at 777nm, the wavelength of the SXR-II channel 6). The rationale for the white filter given in [Johnson et al., 1998b] is that it is responsive from 325nm to 800nm and thus monitors the total radiance. In practice, the sensitivity below 375nm and above 650nm is so low that changes in the radiance in those wavelengths do not have a significant impact on the measured signal of the white detector. It may be advisable to choose a narrower wavelength range, to obtain a 'green' detector around 525nm that is not influenced by changes in the red or blue, and is thus more representative of changes in the part of the spectrum between the blue and the red detector.

2.3 SQM-II

The SQM-II is a commercially available version of the SQM available from Satlantic, Halifax, Nova Scotia, Canada. It differs much more from the original SQM design than the OCS-5002. It is described in greater detail in [Meister et al., 2002], its major differences are that the light bulbs are turned away from the exit aperture to illuminate a Spectralon covered light chamber, the intensity of the light bulbs of the LoBank has been increased by a factor of about 3, the flux levels in the blue are increased relative to the red, and there is only one internal monitor. The internal monitor of the SIMBIOS Project's SQM-II (S/N 0006) showed an unexplained increase in 2001 of about 10 %, although the SXR-II measurements of the SQM-II did not show a comparable increase. The increase has continued in 2002 at a much slower rate and is again not correlated to the SXR-II measurements, see Fig. 2.8 below. This strange detector behavior has not occurred in any of the other SQM-IIs produced so far. Maybe the relatively high temperatures that occurred when both HiBank and LoBank were used simultaneously in 2001 (75° C at the lamp ring for both banks compared to 63° for HiBank alone) have caused the filter of the detector to change, but this can only be speculated.

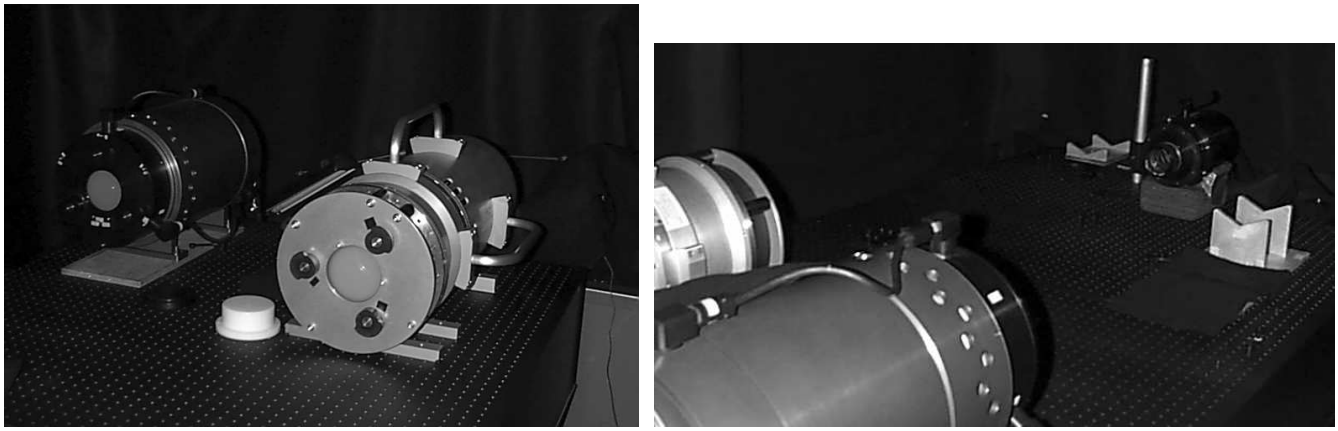

Figure 2.3: *Left: the OCS-5002 (right) and the SQM-II (left) on the optical table in the SIMBIOS Optical Laboratory at NASA Goddard Space Flight Center. Right: there are two separate mounts for the SXR-II to view the SQMs. The SXR-II is in a temporary mount in the picture, between the two fixed mounts.*

2.4 Stability monitoring

2.4.1 Method

A time series of measurements of the SQMs with the SXR-II was taken in the SIMBIOS Optical Laboratory at NASA Goddard Space Flight Center, Greenbelt, MD. The facilities can be seen in Fig. 2.3. The room is not at a stable temperature. The baffling material is felt, which has a bidirectional reflectance factor $R(0°/45°)$ (see section 5) of about 0.02 in the wavelength range of the SXR-II. The SQM-II and the OCS-5002 are placed next to each other on an optical table. The SXR-II is placed on the other end of the optical table. The distance SXR-II/SQM-II is 1 m, the distance SXR-II/OCS-5002 is 1.3 m.

For a measurement of the OCS-5002 with the SXR-II, the following measurement protocol is used:

- Turn on SXR-II, ILX temperature controller and Fluke voltmeter, at least 4 hours before taking measurements, preferably on the day preceding the measurements. Make sure SXR-II optics are set to $f/1.4$ and 1.5 m (the image as seen through the SXR-II eyepiece appears sharp at a 1.5 m setting, although the actual distance to the OCS-5002 is 1.3 m).
- Fine tune SXR-II orientation using SXR-II eyepiece and center of the SQM exit aperture marked on the SQM caps.
- Provide power to OCS-5002.
- Switch the OCS-5002 control knob to 'STBY'. Wait for at least half an hour. Usually the waiting period was extended until the heater for the electronics had heated the SQM to 35° C or at least 30° C. This was done to reduce the warmup period with the bulbs on.
- Start computer logging of OCS-5002 data.
- Measure the OCS dark current with the cap on the exit aperture for 3 minutes.
- Ramp up HiBank by switching the control knob to 'MED'.
- 18 minutes after HiBank rampup, remove cap from exit aperture.

- 20 minutes after HiBank rampup, start signal measurements with the SXR-II. Taking 6 scans usually takes 7 minutes. SXR-II dark current measurements (3 scans each) are taken before and after the signal measurements.
- Close the OCS-5002 exit aperture with cap for at least 1 minute.
- 30 minutes after HiBank rampup, switch control knob to 'LOW', i.e. ramp up the LoBank.
- Repeat the steps described for HiBank above with the LoBank.
- Switch control knob to 'STBY'.
- After the current has been ramped down to 0, measure OCS-5002 dark current for 3 minutes. In the processing of the OCS data, this dark current is subtracted from the internal monitor signals rather than the dark current measured before, because it is closer to the LoBank measurements, which are more sensitive to the dark current.
- Switch control knob to 'OFF'. Cut power from OCS-5002. Stop computer logging of SQM-II data. Backup SXR-II and SQM-II data.

These measurements were done on three consecutive days, once a month.

The protocols for SQM measurements suggest a 1 hour warmup period for HiBank and LoBank each. The warmup period was reduced to 20 minutes to reduce the burn time of the bulbs.

The protocol for the SXR-II/SQM-II measurements has been described in [Meister et al., 2002]. The major difference is that the SQM-II has a 1 hour warmup time for LoBank and HiBank separately. During this warmup, the currents are in a 'coarse-adjust' mode, thus it is not possible to reduce the warmup time. For SIMRIC-2, the SQM-II was measured only once a month to reduce burn time of the bulbs, and because it could be seen in SIMRIC-1 ([Meister et al., 2002], chapter 2.3.2) that the variation on 3 consecutive days was negligible.

2.4.2 Results

The time series of SXR-II measurements in 2002 of the OCS-5002 and the SQM-II is shown in Figs. 2.4, 2.5, 2.6 and 2.9. The SXR-II measured radiances are calculated using the linear interpolation between the December 2001 and January 2003 NIST calibrations described above (section 2). The SQM-II radiances have been normalized to the SXR-II SIRCUS'01 radiances (see below for a definition). The average of the OCS-5002 radiances from March 2002 have been normalized to the average of the SQM-II radiances measured during March 2002, the first month of measurements for the OCS-5002. The ratio of these averages was then applied to all OCS-5002 radiances.

For channel 1 of the SXR-II, variations of 2% are present in the time series of the SQM measurements. The measured variations of the SQM-II and the OCS-5002 radiances are in very good agreement for both light sources and both HiBank and LoBank. This indicates that the source of the variation is the sensor, and not the light sources.

Fig. 2.4 shows that the measured SXR-II channel 2 radiances of the SQM-II HiBank and LoBank and the OCS-5002 HiBank (the later corrected by the OCS-5002 internal blue monitor) show an increase of about 1.0%. The SXR-II channel 2 measured radiance of the OCS-5002 LoBank corrected by the internal blue monitor increased by 1.6%. This might be an indication that e.g. the NIST calibration coefficient from 2001 $< D_{cs}^{2001} >$ is too high. This would smooth the evolution of $< D_{cs} >$ over time for channel 2, see Fig. 2.1. But then the decrease of the OCS-5002 HiBank and LoBank radiances in channel 2 would be significantly different from the decrease in channel 1 and 3 (assuming the NIST calibrations are correct, the decrease is very similar for channels 1,2, and 3, see table 2.5, below). Something similar can be derived from Fig.2.6 for channel 6: SQM-II HiBank and LoBank and the OCS-5002 HiBank show an increase of about 1.0%, but the OCS-5002 LoBank data (Fig. 2.9) do not. We do not think that there is enough evidence to mistrust the NIST calibrations in either case. As we shall see below, if the NIST calibrations are correct, the responsivity of the blue monitor must have decreased by at least 1.0%, see table 2.7. Thus the excellent agreement in channel 1 between increases from March 2002 to January 2003 of the SQM-II HiBank and LoBank radiances and the OCS-5002 HiBank radiance corrected by the blue monitor (all show an increase of about 1.0%) is a coincidence.

There is a 1% spike in the SXR-II channel 5 data from the end of December 2002 to the beginning of January 2003 for all sources (Figs. 2.6 and 2.9). No spike can be seen in the time series of the OCS-5002 internal red monitor data (Fig. 2.7). The SXR-II was opened at the end of December 2002 to remove a screw that had become loose during measurements at NIST to determine the FOV in the middle of December 2002. It was reassembled with

the housing rotated from its original position, which may have caused a misalignment of the SXR-II relative to the sources during the end of December/beginning of January measurements. The SXR-II was reopened and assembled in its original configuration in the middle of January 2003.

It can be seen from Figs. 2.7 and 2.8 that the variations in the OCS-5002 internal monitor data from one measurement to the next is very small, typically about 0.1%, except for the blue detector measurements of the LoBank, which have jumps of up to 1%. This noise is not seen in the SXR-II measurements of the OCS-5002 LoBank (Fig. 2.9). This is the reason why in Figs. 2.4 to 2.6 the OCS-5002 LoBank is not shown, because if the SXR-II measured radiances are corrected with the blue detector of the OCS-5002, the result is dominated by the noise of the blue monitor. It would have been possible to do a correction of the first two SXR-II channels with the white internal detector, but this was not done here.

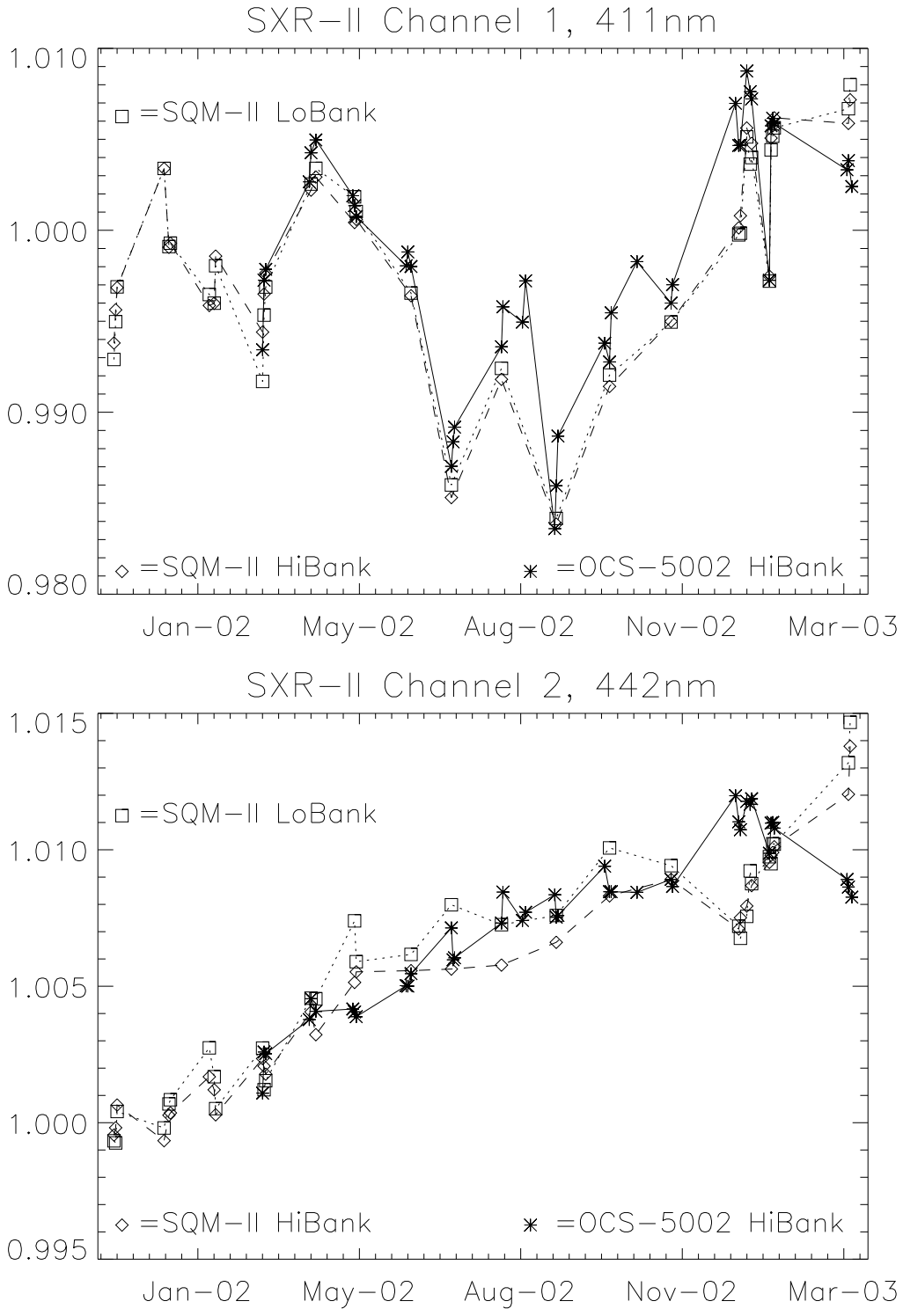

Figure 2.4: *The time series of the SXR-II measured radiances of the SQMs for channel 1 (top) and channel 2 (bottom), measured in the SIMBIOS Optical Laboratory. The values are normalized to the SIRCUS'01 SQM-II radiances. OCS-5002 radiances have been corrected by the OCS internal blue monitor data.*

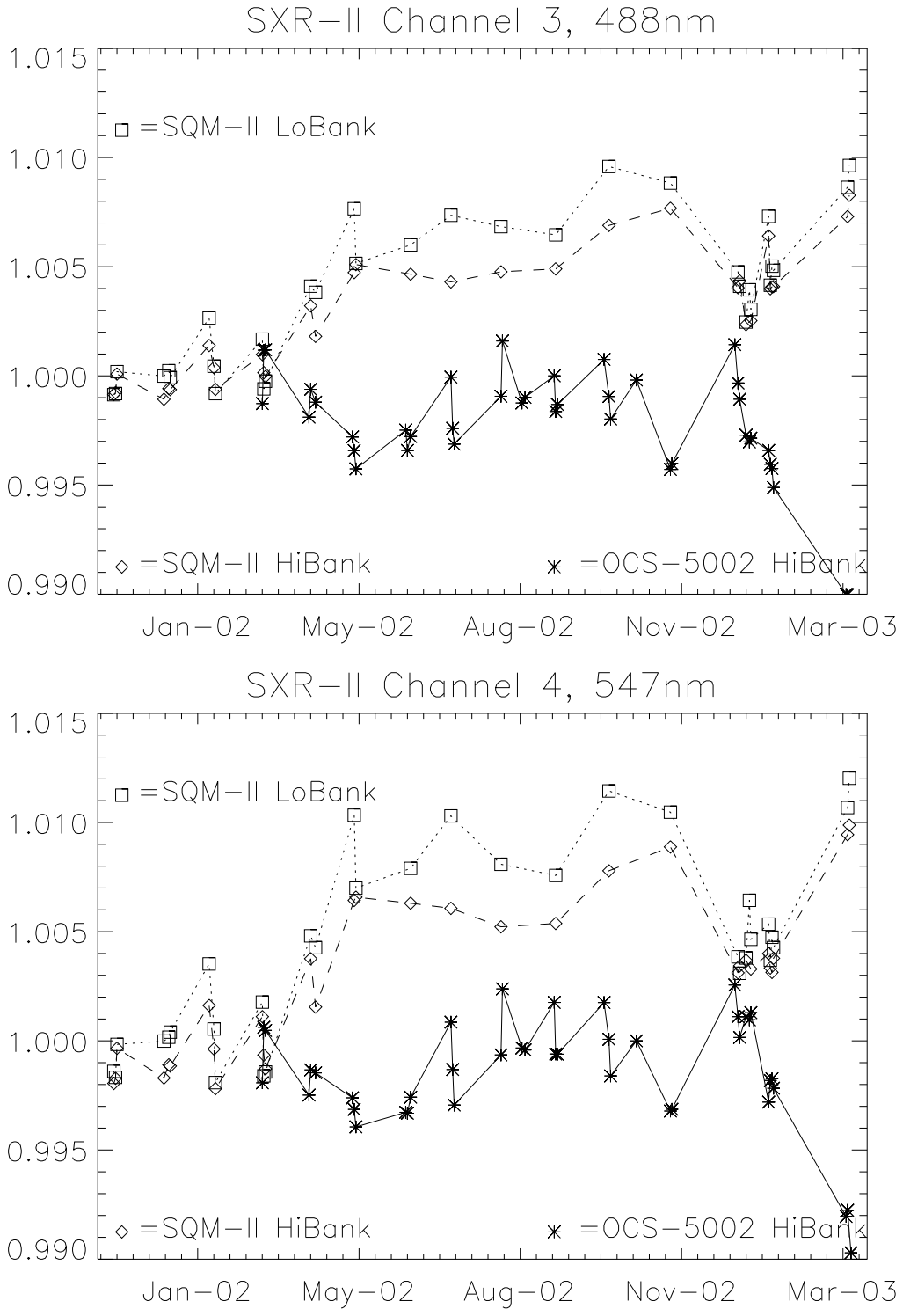

Figure 2.5: *The time series of the SXR-II measured radiances of the SQMs for channel 3 (top) and channel 4 (bottom), measured in the SIMBIOS Optical Laboratory. The values are normalized to the SIRCUS'01 SQM-II radiances. OCS-5002 radiances have been corrected by the OCS internal white monitor data.*

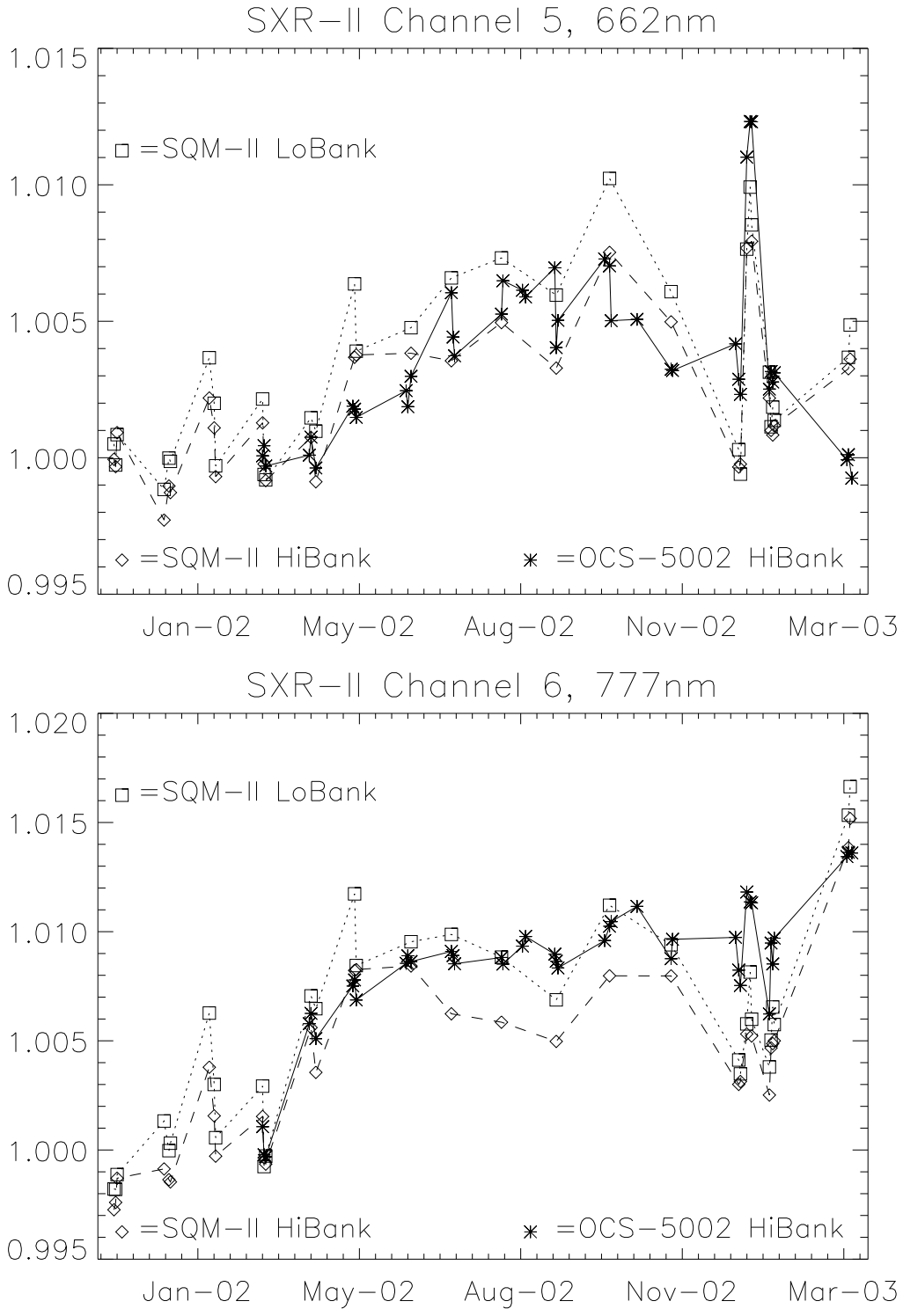

Figure 2.6: *The time series of the SXR-II measured radiances of the SQMs for channel 5 (top) and channel 6 (bottom), measured in the SIMBIOS Optical Laboratory. The values are normalized to the SIRCUS'01 SQM-II radiances. OCS-5002 radiances have been corrected by the OCS internal red monitor data.*

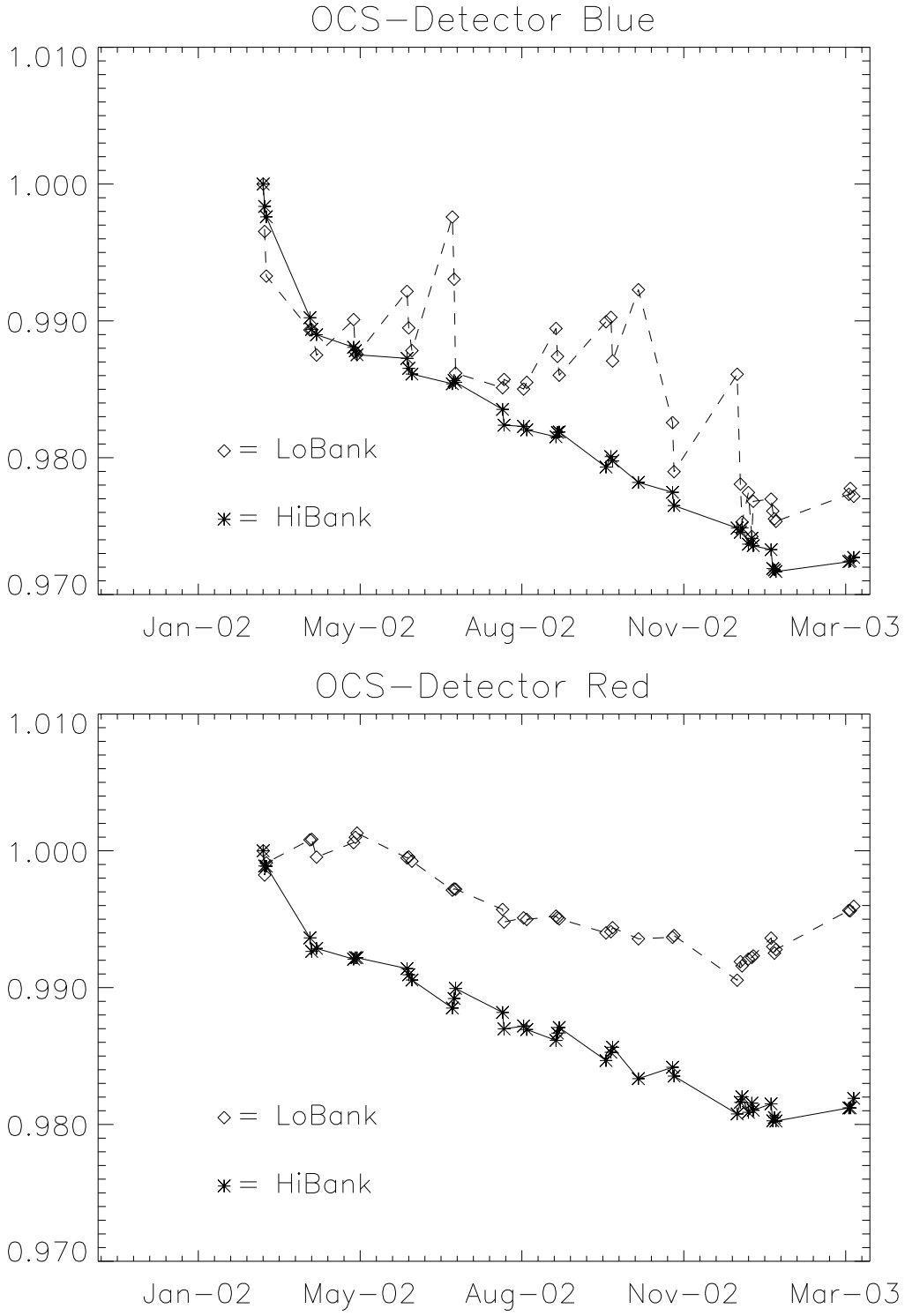

Figure 2.7: *The time series of the internal monitor measurements of the OCS-5002 blue detector (top) and red detector (bottom) for the HiBank (solid line) and LoBank (dashed line), measured in the SIMBIOS Optical Laboratory. The values are normalized to the first measurement.*

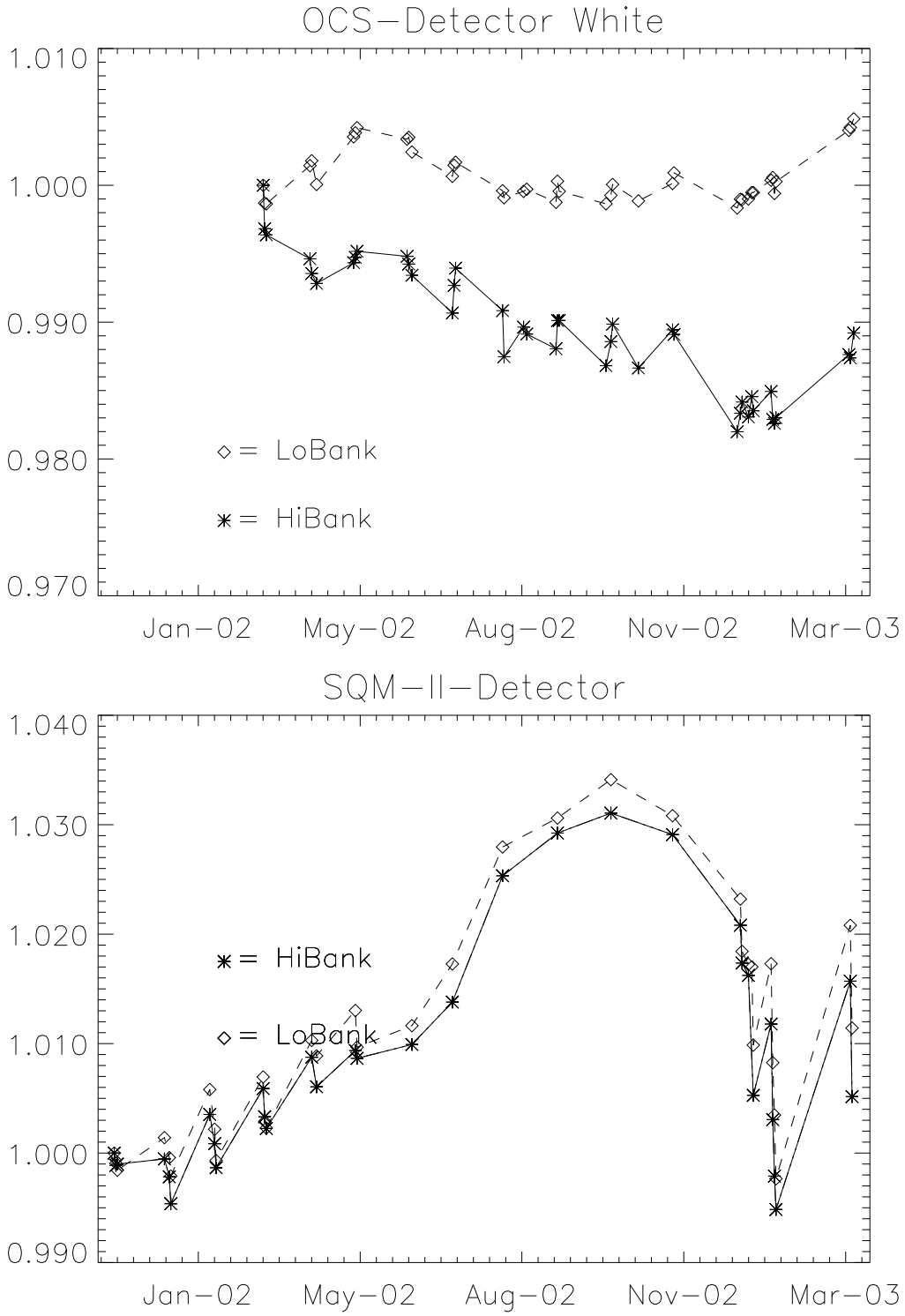

Figure 2.8: *The time series of the internal monitor measurements of the OCS-5002 white detector (top) and the SQM-II internal detector (bottom) for the HiBank (solid line) and LoBank (dashed line), measured in the SIMBIOS Optical Laboratory. The values are normalized to the first measurement.*

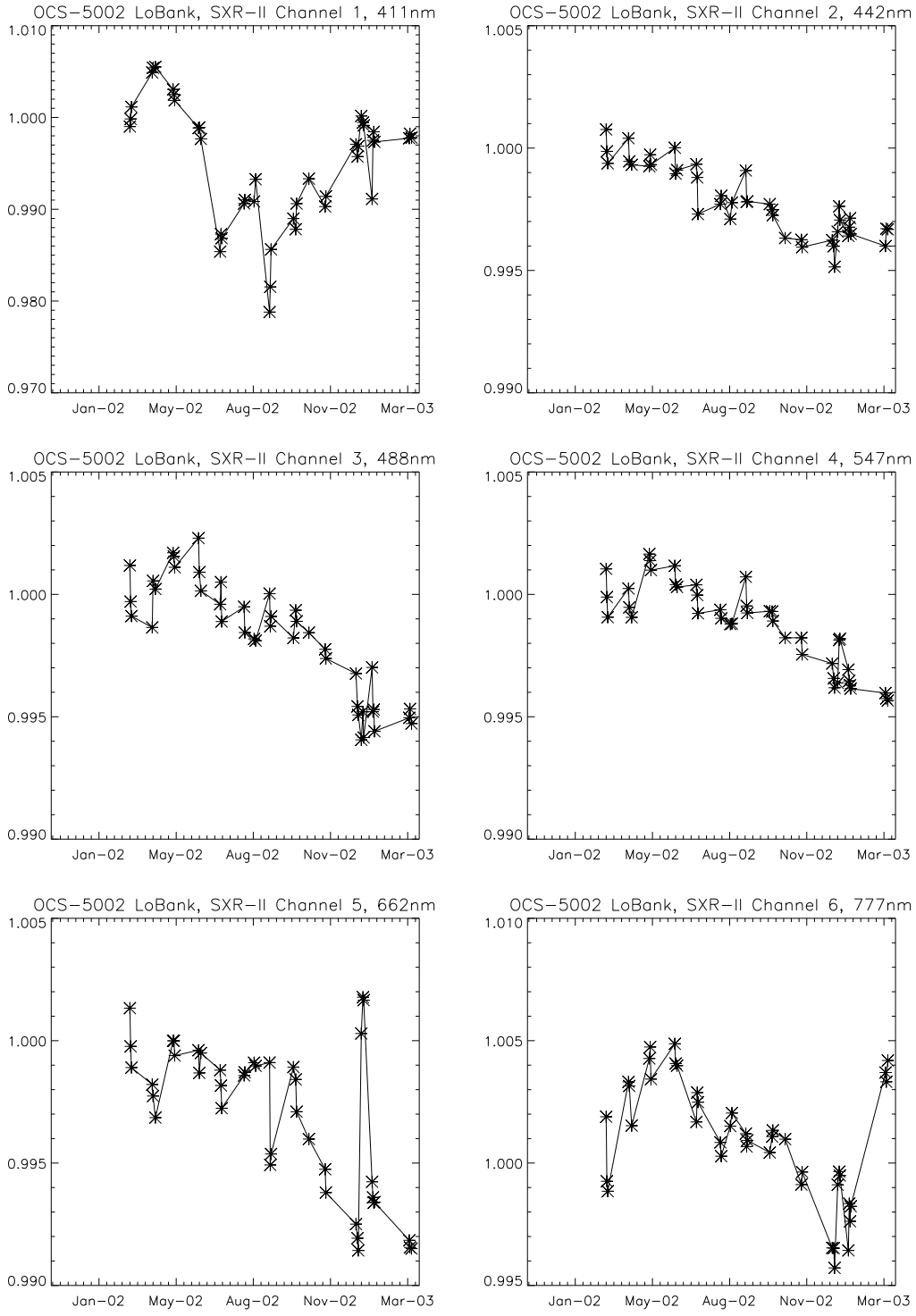

Figure 2.9: *The time series of the SXR-II measured radiances of the OCS-5002 LoBank, measured in the SIMBIOS Optical Laboratory. The OCS-5002 radiances shown here have* **not** *been corrected by the OCS internal monitor data. The OCS-5002 radiances are normalized to the average of the measurements of March 2002.*

2.4.3 Correction to the SXR-II calibration

It was decided to correct the SXR-II calibration with the time series of the SQM-II, because the variations of channel 1 can be seen for all light sources, and there is no variation in the time series of the OCS-5002 internal blue monitor (Figs. 2.4 to 2.7). The OCS-5002 data was not used because its time series starts 2 months after the NIST December 2001 calibration, whereas the SQM-II time series overlaps both SIRCUS calibrations.

The correction requires the SXR-II measured radiance of the SQMs during the SIRCUS calibration. No SQM measurements could be taken exactly during the SIRCUS calibration. Thus to compute the SXR-II SIRCUS'01 radiances, the average was taken over two SQM measurements from two consecutive days preceding the SIRCUS calibration and two measurements on two consecutive days following the SIRCUS calibration. Of each of these two measurements, one was taken in the SIMBIOS Optical Laboratory and one was taken at NIST. The SXR-II was calibrated at SIRCUS for about 30 days.

The main purpose of the SXR-II/SQM monitoring is to detect changes in the SXR-II responsivity between the SIRCUS calibrations. Thus the long term trends of the OCS-5002 and the SQM-II are not important for our purposes. We are interested in the deviations of the SQM time serieses from the long term trend. The long term trend was calculated as a linear interpolation between the measured SQM radiances during the SIRCUS calibrations. Two SQM measurements preceding and two SQM measurements following the SIRCUS calibrations (all in the SIMBIOS Optical Laboratory) were used in the calculation of the end points of the linear trend. The starting point of the OCS-5002 linear trend is the average of the March 2002 measurements. Thus the linear trend is a combination of the change of responsivity of the SXR-II channels measured by SIRCUS (Table 2.1) and the change of the SQM (Tables 2.4 and 2.5). The ratios of the SXR-II measured radiances to this linear trend are shown in Fig. 2.10 for the SQM-II (solid line) and OCS-5002 (dotted line). The dashed lines at 1.005 and 0.995 enclose a range of deviations of $\pm$ 0.5%. It can be seen that

1. channel 2 is well contained within these limits,
2. channel 1 is 1 to 2% lower than the linear trend around August 2002,
3. channels 3, 4, and 5 are about 0.5% higher than the linear trend from May to October 2002,
4. channel 6 shows deviations that vary from +0.5% to -0.5%.

Generally, there is very good agreement between the curves for the OCS-5002 and the SQM-II in Fig. 2.10. All the major trends mentioned above (items 1-4) are present in both curves. Thus it is very likely that these changes are caused by the SXR-II. Although it cannot be ruled out that both SQMs changed synchronously, e.g. because of a change in environmental conditions, like e.g. an increase in humidity, we will assume that these changes are due to the SXR-II and correct all channels for these changes, using the SQM-II data only. *Thus all radiances measured in the laboratories of the SIMRIC-2 participants will be divided by the solid line shown in Fig. 2.10 for the respective date and channel.* The OCS-5002 data will not be used because of the difficulties with channel 1 when extending the March 2002 measurements to the SIRCUS'01 calibration period, see below. It is interesting to note that if the starting point of the OCS-5002 linear trend is calculated with the OCS-5002 data extended to the SIRCUS'01 calibration assuming the SQM-II was stable during that period, the differences between the dashed and the solid line in Fig. 2.10 are significantly reduced for channel 1, the channel that has the largest difference between the two curves (solid line and dotted line). We estimate an uncertainty of the evolvement of the SXR-II calibration between the SIRCUS'01 and the SIRCUS'02 calibrations of 0.3% for all channels.

The OCS-5002 was used starting from March 2002. In order to relate the March 2002 SXR-II measurements of the OCS-5002 to the time of the SIRCUS'01 calibration, theoretically the SQM-II could be used. Fig. 2.11 shows the SXR-II measured radiances of the SQM-II HiBank normalized by the SXR-II SIRCUS'01 SQM-II radiances (see section 2.4.3 for a definition). The SQM-II LoBank yielded similar results (not shown). It can be seen that for channel 1, the SXR-II measured radiances decreased by about 1% from the first measurement after the SIRCUS'01 calibration in December 2001 to the start of the OCS-5002 usage in March 2002. All other channels show much smaller changes. As it is impossible to decide whether the SQM-II or the SXR-II changed, we will *not* use the SQM-II to relate the March 2002 SXR-II measurements of the OCS-5002 to the time of the SIRCUS'01 calibration. However, it seems more probable that the SXR-II changed in channel 1 (411 nm), because both SQM-II HiBank and LoBank yielded similar results, and the SXR-II channel 2 (442 nm) does not show any change at all.

Another indication that the dip in August 2002 of channel seen in Fig. 2.4 is primarily caused by the SXR-II and not by the SQM-II can be derived from a comparison with a NIST calibrated sphere in August 2002. The SXR-II

measured an integrating sphere source at NIST, the NIST Portable Radiance Source (NPR), with only lamp#4 on to avoid saturating the SXR-II. The NPR was calibrated on NIST's Facility for Spectroradiometric Calibrations (FASCAL), and the SXR-II measured the NPR a few days before and a few days after the FASCAL calibration. If the difference of the SQM-II HiBank and LoBank time series from the linear trend (see above) is used to correct the SXR-II measured radiances, the comparisons results for the NPR improve dramatically, see Fig. 2.12. Thus we decided to use this correction for all radiances measured in the laboratories participating in the SIMRIC-2. Note that this correction is not used in the presentation of radiances measured in the SIMBIOS Optical Laboratory in this report.

The OCS-5002 was taken to each participating laboratory and its radiance was measured by the SXR-II. No measurements were taken in the NASA Code 920.1 facility, because measurements were made on the following days in the SIMBIOS Optical Laboratory (long term stability monitoring sessions, June 20th to June 22nd), and the shipping stress on the SXR-II was very limited because the radiometer had simply to be moved from one building to another at Goddard Space Flight Center. Although it would be possible to correct the SXR-II using the measurements on the participating laboratories, we chose not to do this, because the conditions of measurement in the participating laboratories are usually less optimal concerning the setup of the OCS-5002 and ambient light reduction. (The SIMBIOS Optical Laboratory baffling is not optimal either, but the ambient light is not expected to change with time, thus it is sufficient for a time series.) Furthermore we wanted to prevent possible effects of environmental conditions in a specific laboratory (like temperature and humidity) from entering the SXR-II correction, and the connection of the OCS-5002 measurements to the SIRCUS'01 calibration time introduces an additional uncertainty, see above. Fig. 2.13 shows the ratios of the measured radiances (L_m) in the participating laboratories to the average of those measurements in the SIMBIOS Optical Laboratory preceding and following the measurement of L_m. Typically 1 to 2 weeks passed between the measurement of L_m and the measurements in the SIMBIOS Optical Laboratory. It can be seen that there is no systematic trend in the data, except that the ratios for channel 6 are on average 0.2% higher than unity. This can be explained with less ambient light in the SIMBIOS Optical Laboratory, as most baffling materials have a high reflectance at 770 nm. As Fig. 2.13 shows mostly noise, and we believe that the measurements in the SIMBIOS Optical Laboratory are more reliable, we used only measurements from the SIMBIOS Optical Laboratory for the SXR-II correction. In effect, the OCS-5002 data are not used at all because of the missing overlap to the SIRCUS'01 calibration, only the SQM-II data are used.

The changes of the SQM radiances are tabulated in tables 2.4 and 2.5. The radiances of the SQM-II HiBank and LoBank increased quite homogeneously and only by small amounts, between 0.2 and 1.0%, see table 2.4. The OCS-5002 LoBank was the most stable, the OCS-5002 HiBank showed the greatest amount of change. The radiances of the OCS-5002 measured by the SXR-II decreased by between 1.0 and 2.0% for the HiBank, and between 0.1 and 0.6% for the LoBank, see table 2.5. The decrease of the OCS-5002 radiances measured by the OCS-5002 internal monitors is stronger, up to 2.7% for the HiBank and up to 1.9% for the LoBank, see table 2.6. Assuming that the SXR-II measured change is representative for the true change of the OCS radiances in the wavelength range of the OCS internal detectors, the change of the responsivity of the OCS-5002 internal monitors can be calculated, see table 2.7. E.g., according to the SXR-II, the radiance of the OCS-5002 HiBank has decreased by 1.7% in channel 1 (table 2.5). According to the OCS-5002 blue monitor, the HiBank radiance has decreased by 2.7% (table 2.6). This means that the responsivity of the blue monitor has decreased by 1.0% (table 2.7) if the SXR-II channel 1 measured change is regarded as representative. We assigned 1 or 2 SXR-II channels to each of the three OCS-5002 monitors, see table 2.7, matching roughly the wavelengths of the monitors given in [Johnson et al., 1998b]. Averaging over SXR-II channels and HiBank and LoBank, the resulting change of responsivity in the OCS internal blue detector is -1.3%, 0.5% for the white detector, and -0.2% for the red detector. The change of the red (and propably the white) detector is within the uncertainty of the two SIRCUS calibrations of the SXR-II, although it is remarkable that values for the white detector (derived independently for SXR-II channels 3 and 4, table 2.7) are very very similar. The decrease in the responsivity of the blue detector is significant. It is difficult to explain why the change in the blue detector derived from the LoBank (-1.7%) is so much larger than the change derived from the HiBank (-1.0%), for the white detector and the red detector the changes are very consistent between HiBank and LoBank. A possible explanation is a change in the linearity of the blue detector. The changes of the blue monitor responsivity derived from HiBank and LoBank are very consistent between SXR-II channels 1 and 2.

SXR-II λ [nm]	410.69	441.51	487.58	546.89	661.91	776.71
SQM-II HiBank [%]	0.5	1.0	0.5	0.5	0.2	0.6
SQM-II LoBank [%]	0.4	0.9	0.5	0.4	0.2	0.5

Table 2.4: Change of the SXR-II measured radiance of the SQM-II HiBank and LoBank from January 2002 to January 2003. There was an increase in all bands for both HiBank and LoBank.

SXR-II λ [nm]	410.69	441.51	487.58	546.89	661.91	776.71
OCS-5002 HiBank [%]	-1.7	-1.8	-2.0	-1.7	-1.6	-1.0
OCS-5002 LoBank [%]	-0.3	-0.3	-0.4	-0.3	-0.6	-0.1

Table 2.5: Change of the SXR-II measured radiance of the OCS-5002 HiBank and LoBank from March 2002 to January 2003 (not corrected with the OCS-5002 internal monitor data). There was a decrease in all bands for both HiBank and LoBank.

Internal monitor	Blue (425nm)	White (525nm)	Red (625nm)
OCS-5002 HiBank [%]	-2.7	-1.5	-1.9
OCS-5002 LoBank [%]	-1.9	0.1	-0.6

Table 2.6: Change of the internal monitor measurements of the OCS-5002 HiBank and LoBank from March 2002 to January 2003. There was a decrease in all detectors for both HiBank and LoBank, except for the LoBank measured by the white detector. The approximate center wavelengths are given in brackets for each detector.

Internal monitor	Blue		White		Red	(Red)
SXR-II λ [nm]	410.69	441.51	487.58	546.89	661.91	776.71
OCS-5002 HiBank [%]	-1.0	-0.9	0.5	0.2	-0.3	(-0.9)
OCS-5002 LoBank [%]	-1.7	-1.7	0.6	0.5	0.0	(-0.5)

Table 2.7: Change of the OCS-5002 internal monitor responsivity from March 2002 to January 2003, calculated assuming that the SXR-II measured change of HiBank and LoBank is accurate, assigning SXR-II channel 1 and 2 to the blue detector, channels 3 and 4 to the white detector, and channel 5 to the red detector. The responsivity of the white detector increased, the responsivity of the blue and red detectors decreased. (The responsivity change of the red detector was also calculated based on SXR-II channel 6, but the spectral responsivity of the red detector hardly overlaps with the spectral responsivity of channel 6, thus the values are put in brackets.)

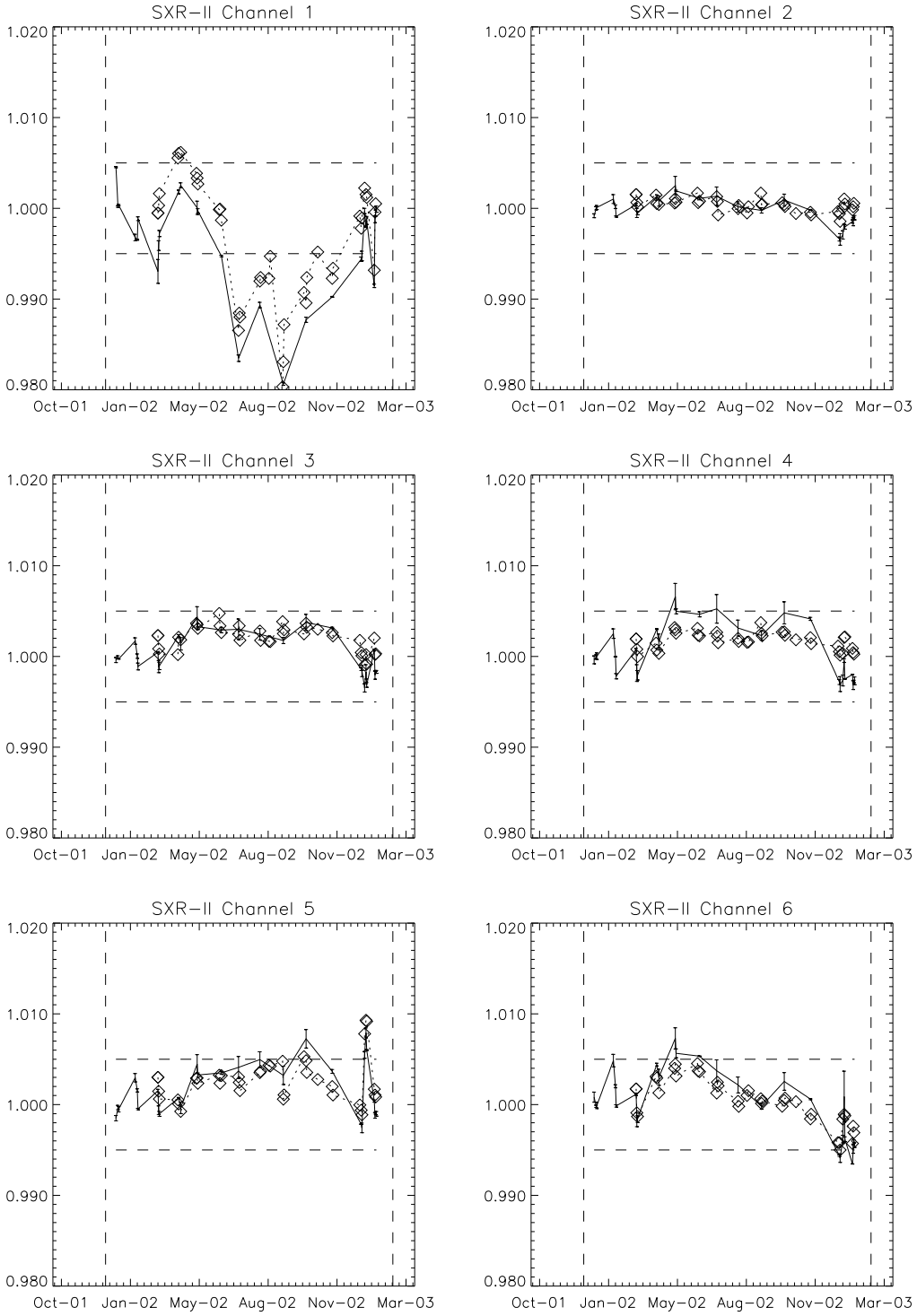

Figure 2.10: *Ratio of the SXR-II measured radiances of the SQM-II (solid line, vertical error bars indicate difference between HiBank and LoBank) and OCS-5002 LoBank (diamonds, connected by dotted line) to the linear trend, see text. The OCS data has not been corrected by the internal monitor data. The horizontal dashed lines show deviations of 0.5%. The times of the SIRCUS calibrations are marked by vertical dashed lines.*

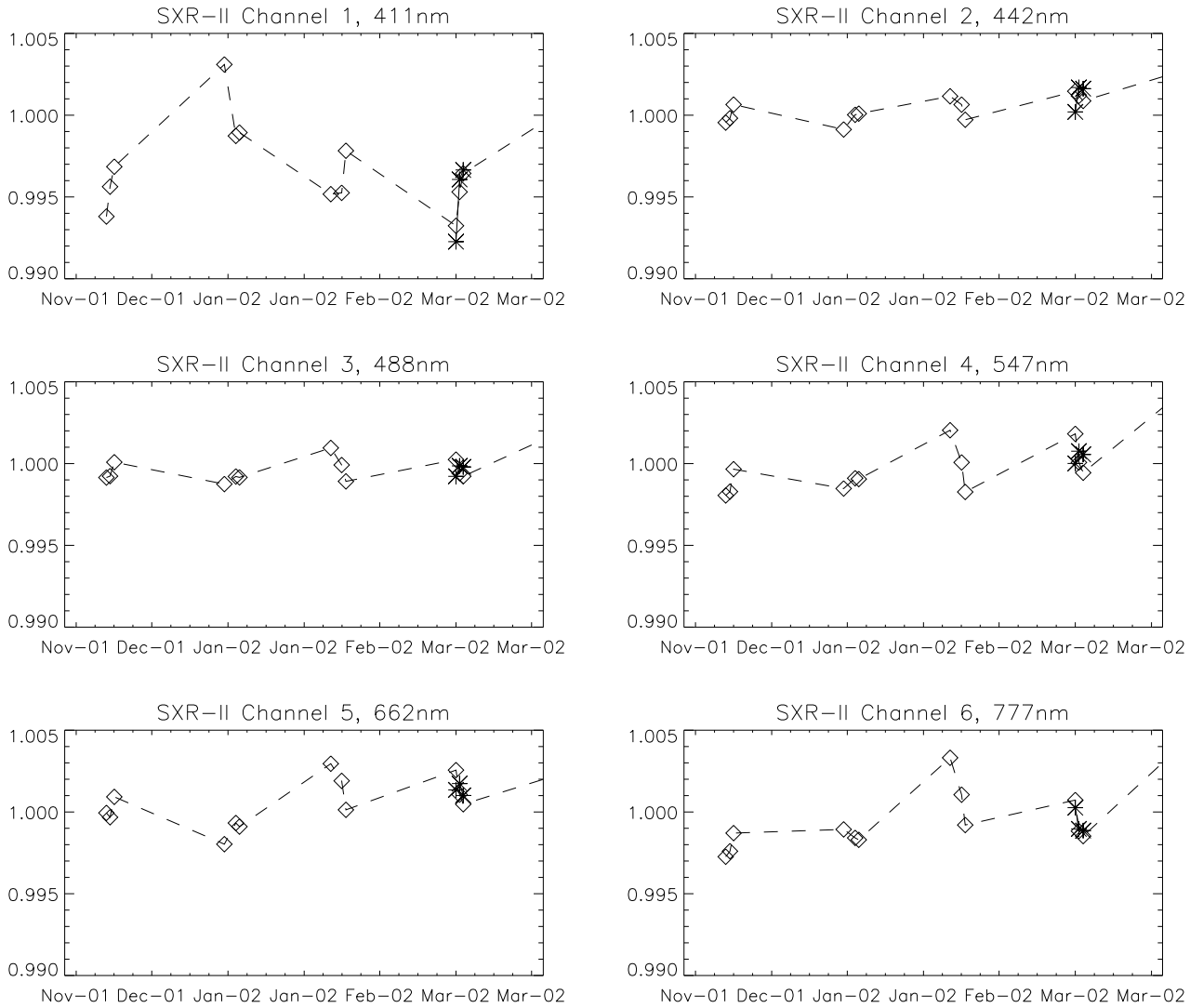

Figure 2.11: *Diamonds show the time series of the SXR-II radiances of the SQM-II HiBank, measured in the SIMBIOS Optical Laboratory. All values are normalized to the the SIRCUS'01 SQM-II radiances. The 3 stars show the March 2002 measurements of the OCS-5002 HiBank. The average of these three measurements is normalized to the average of the corresponding SQM-II measurements from March 2002.*

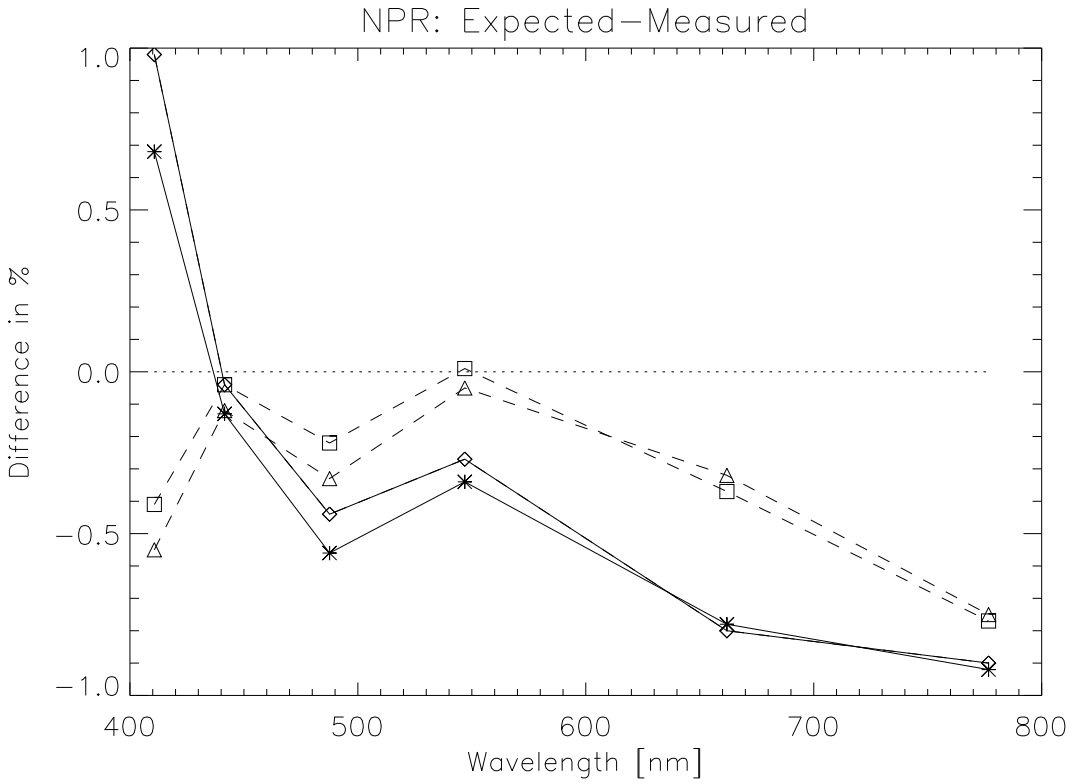

Figure 2.12: *The difference of the expected radiances of the NPR and the SXR-II measured radiances in August 2002. The SXR-II measured radiances have been calculated using a linear interpolation between the SIRCUS calibrations from December'01 and January '03. The solid lines connect the differences calculated without using the SQM-II correction, the dashed lines connect the differences calculated using the SQM-II correction.The stars and triangles show the pre-FASCAL measurements, the diamonds and squares show the post-FASCAL measurements.*

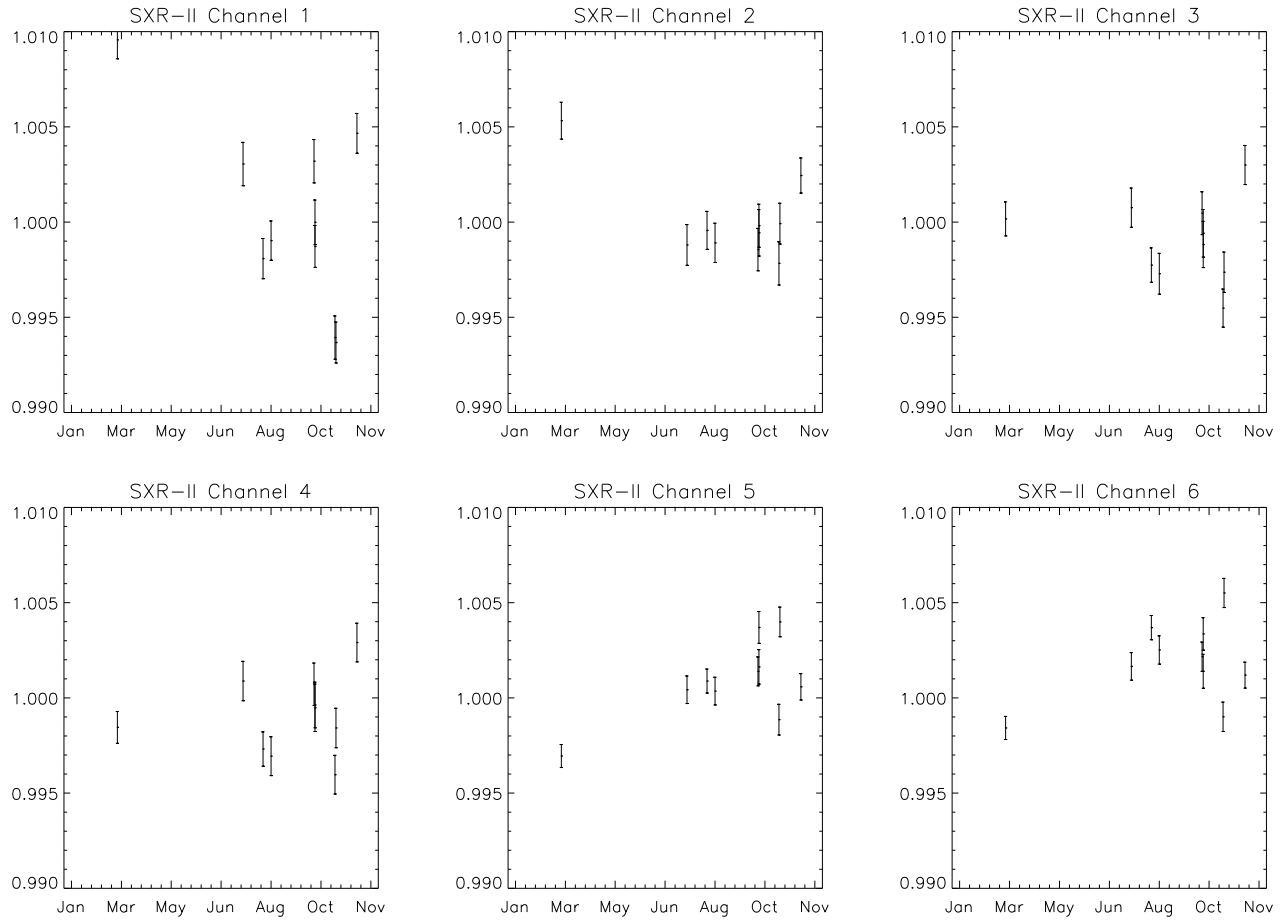

Figure 2.13: *The ratios of the SXR-II measured radiances of the OCS-5002 HiBank in the laboratories participating in the SIMRIC-2 (in the following order: NRL, WFF, MOBY at NIST, MOBY at NIST, UCSB, Scripps, Biospherical, USF, UM, Satlantic) to the average of the SXR-II measured radiance of the OCS-5002 HiBank in the SIMBIOS Optical Laboratory before and after the shipment to the laboratory. The error bars are the uncertainties derived from the standard deviations of the SXR-II measurements and the OCS internal monitor measurements.*

Chapter 3

Documentation of Calibration Techniques

3.1 Introduction

This section documents the calibration procedures performed in each of the participating laboratories. Specifically, the items described include light sources, plaques, transfer radiometers, baffling techniques, installation details and algorithms used. Unless otherwise noted, all laboratories record the burn times for their calibration lamps. All lamps are always warmed up for at least 10 minutes. Table 3.1 gives an overview of the laboratories visited, the dates the measurements took place and the primary calibration standards. In case the calibration facilities have already been described in [Meister et al., 2002], that document is referenced.

3.2 Laboratories

3.2.1 NRL

The same equipment and protocols as described in [Meister et al., 2002] were used. No new calibrations from OL were made. The original OL calibrations were used for F-399 and F-400. During SIMRIC-1, the original OL calibration was used for F-399 as well (no calibration transfer was used, as was erroneously stated in [Meister et al., 2002]).

3.2.2 NASA GSFC Code 920.1

The same equipment and protocols as described in [Meister et al., 2002] were used. The primary standard is still the same FEL lamp with the NIST calibration from 2000.

3.2.3 WFF

At Wallops, lamps manufactured and calibrated by Oriel are used as primary standards. The same 200 W model is used as at HOBI Labs, see [Meister et al., 2002] and Fig. 3.1. The lamps are warmed up for 20 minutes before taking measurements. A Spectralon plaque with a $R(0°/45°)$ reflectance calibration from Labsphere is used. The plaque is viewed by the radiometers at a viewing angle of 45°. When not in use, the plaque is protected by a metal sheath that can be slid over it, see Fig. 3.1. right picture. A curtain between the lamp and the radiometer shields the radiometer from direct illumination. The directional reflectance of the plaque (R(0°/45°)) was calibrated by Labsphere in 1997. After the SIMRIC-2 measurements, the directional reflectance of the plaque was calibrated at NASA Code 920.1. The values for (R(0°/45°)) from NASA Code 920.1 are about 2 % higher than the ones from Labsphere. Wallops is planning to use the values from NASA Code 920.1.

No baffling was used between the lamp and the Spectralon plaque. The use of preliminary baffles during SIMRIC-2 between the lamp and the plaque resulted in a reduction of the SXR-II measured radiances by about 1 %. WFF has added a baffle following the SIMRIC-2, but found no significant change. The lamp is surrounded by black

Laboratory	Acronym	Date	Primary Calibration Source
Naval Research Laboratory, Optical Sensing Section, Code 7212	NRL	3/11/02	FEL calibrated by Optronics Laboratories
NASA Code 920.1 Calibration Facility	NASA Code 920.1	4/24/02	FEL calibrated by NIST
Wallops Flight Facility NASA Code 972	WFF	7/16/02	Irradiance standards calibrated by Oriel
Moss Landing Marine Laboratory	MLML/MOBY	08/02	Spheres calibrated by NIST
Scripps Institution of Oceanography	Scripps	09/26/02	Sphere calibrated by Labsphere
Biospherical Instruments Inc.	Biospherical	09/27/02	FEL calibrated by NIST
Institute for Computational Earth System Science, University of California at Santa Barbara	UCSB	09/25/02	FEL calibrated by NIST
University of South Florida	USF	10/16/02	Sphere at the Univ. of Arizona
University of Miami, Ocean and Atmospheric Optics Laboratory	UM	10/17/02	FEL calibrated by Optronics Laboratories
Satlantic Inc.	Satlantic	11/07/02	FEL calibrated by Optronics Laboratories

Table 3.1: *Overview of the laboratories participating in the SIMRIC-2. The column 'Date' gives the first day of measurements (month/day/year). The last column shows the primary calibration standard.*

painted walls and curtains made of black rubberized fabric from Thorlabs, Inc. (Item # BK 5). The complete setup is shown in Fig. 3.2. A laser and a mirror on the metal sheath (see Fig. 3.1, right picture) reflecting 45° off the incoming direction are used for alignment purposes.

Oriel calibrated the lamp for irradiance. Values interpolated to a 1 nm wavelength interval are used. The lamp was calibrated by Oriel at a distance of 50 cm. During SIMRIC-2 and before, the reference point at the lamp for the distance used at Wallops was the center of the lamp filament. Immediately after the SIMRIC-2, it was realized that the correct reference point is the front of the lamp bracket. Thus the lamp was too close to the plaque by about 6 mm. We calculated that the increase of irradiance resulting from the wrong distance is about 2.4 %. The distance between lamp and plaque is set using the scale on an optical rail that connects the two.

As an additional check, the OL lamp was calibrated at NASA Code 920.1 with the spectroradiometer OL 746 at a distance of 50 cm to the lamp mount (correct distance). Up to 700 nm, the NASA Code 920.1 calibration yielded a 1 % lower irradiance than the Oriel calibration, about 2 % lower above 700 nm, i.e. the results were within the combined uncertainties of NASA Code 920.1 and Oriel. Wallops will keep using the Oriel values.

3.2.4 MLML / MOBY

The Marine Optical Buoy (MOBY) calibration facilities are located in a field station near Honolulu, Hawaii, at Snug Harbor. MOBY is operated by the Moss Landing Marine Laboratory (MLML). The NOAA / University of Hawaii research site in Honolulu manages the Marine-Optical Buoy MOBY. The calibration procedures at MOBY have been described in [Clark et al., 2001]. A hyperspectral radiometer called Marine Optical Spectrographic System (MOS) is used in the buoy to measure underwater radiances. It is replaced every 3 months for service and recalibration. Two spheres from Optronics Laboratories, Inc. (OL) are used as radiance sources to calibrate the MOS in the calibration cabin in Snug Harbor, Honolulu. NIST calibrated FEL lamps are used as irradiance standards for the MOBY irradiance sensors.

In the past, the MLML spheres had been relamped at OL after 50 hours of use. Calibrations were made by OL before and after the relamping. In 2002, the relamping and recalibrations were done at NIST, Gaithersburg,

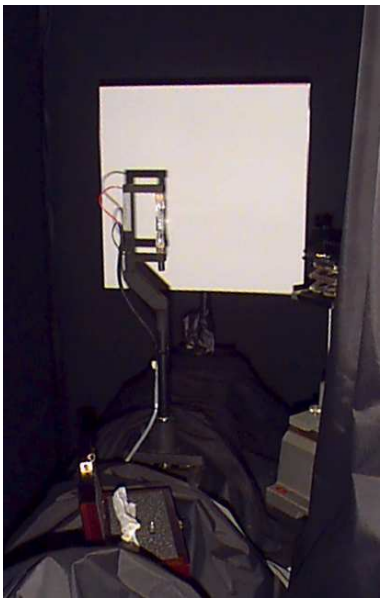

Figure 3.1: *The picture on the left shows the Oriel lamp at Wallops in its bracket in front of the Spectralon plaque. The picture on the right shows James Yungel sliding the metal sheath over the Spectralon plaque. The circular* 45° *reflecting mirror can be seen in the center of the sheath.*

Figure 3.2: *This picture shows the setup at Wallops. An Oriel lamp (obscured by curtains in this picture) illuminates a Spectralon plaque (in the center of the picture, partly obscured by curtains). A radiometer is placed on the right hand side, viewing the plaque at an angle of* 45°*. The curtains on the right separate the area with the radiometer from the control area where PCs and other light emitting equipment can be placed. The whole area is surrounded by black painted wooden walls that prevent light from the outside entering the area.*

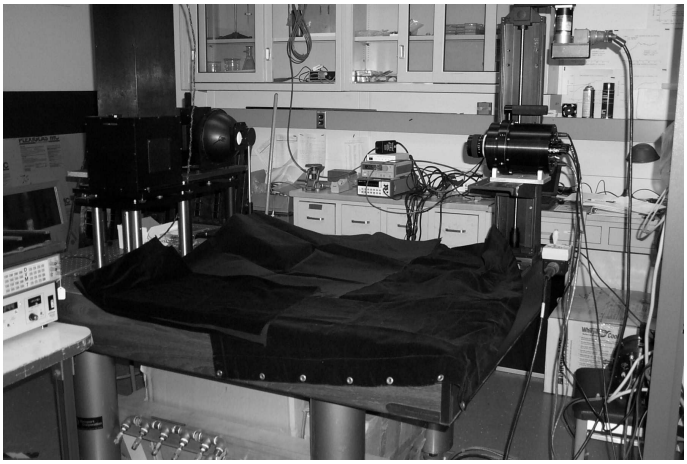

Figure 3.3: *The setup of the two MLML spheres at NIST for the SIMRIC-2. The OL 420 with the vertical rectangular extension is on the left, the OL 425 is on the right, as viewed from the SXR-II. The SXR-II is on a remotely controlled translation stage.*

Maryland. The expected radiances of the MLML spheres for the SIMRIC-2 were calculated with the NIST FASCAL calibration from August 2002. The SIMBIOS Project used this opportunity to measure the MLML spheres at NIST in order to reduce travel expenses and shipping stress on the SXR-II and SQM. The setup is shown in Fig. 3.3. SIMBIOS staff had visited the MOBY field station in Honolulu in 2001 to learn about the MOBY calibration procedures.

The walls of the calibration cabin in Snug Harbor are black, the dimensions are approximately 8 m x 3 m x 2 m (length x width x height). One third of the room can be separated by a black curtain, so that controlling and monitoring equipment (voltmeters, laptops, etc.) do not interfere with the measurement process. The room is air conditioned, with a periodic temperature variation of about 3 deg F. Although the walls are a little specular and several non-black pieces of equipment occupied the cabin, the ambient light is probably very low. No light from the outside enters the cabin (there are no windows and the door locks tightly). The light sources are placed on a rigid table, the radiometers on a separate smaller table, whose height and position is easily adjustable (see Fig. 3.5).

The light sources used are two integrating spheres by OL, the OL420M (S/N 92106057) and the OL425-8-1 (S/N 97101003). The OL420 has an 8 inch diameter integrating sphere and a 45 watt tungsten-halogen lamp. The lamp is placed outside of the sphere, the distance between lamp and sphere can be changed to vary the light output, but is kept constant in practice at 100 cm. In front of the entrance port is an aperture wheel with 6 settings, the two widest settings being 28.57 mm (called W6) and 15.87 mm (called W5). These are the settings used for calibrations by MLML. The second widest setting reduces the radiant flux by a factor of about 3 without affecting the color temperature (according to the manual, no. M000082, revision A, February 1992). The lamp is warmed up for 20 minutes. An OL65DS Power supply from OL operates the 45 W lamp of the OL420 at 6.5 Ampere. Its accuracy is +/- 0.1 % for 6.5 Ampere. There is a rampup period of up to 2 minutes. There is no rampdown period, this means the current to the lamps is shut off immediately, which is generally considered to adversely affect the lamp stability. The uncertainty for the sphere calibrations has been estimated as 2.5 % [Clark et al., 2001].

The second sphere source, the OL 425, is shown in Fig. 3.4. Its design is similar to the OL420: a 45 Watt tungsten halogen lamp can be placed at varying distances (kept constant in practice) from an integrating sphere. An aperture wheel in front of the entrance port is used to achieve different light intensities, again only wheels 5 and 6 are used. The major difference to the OL 420 is that the OL 425 has an internal monitor that records the light intensity in footlamberts. The OL calibration report provides the radiances and the monitor reading in footlamberts during the OL calibration. OL suggests to correct their calibration radiances by the ratio of the monitor reading during the OL calibration and the monitor reading during the user calibration. The photometer amplifier for the monitor and the lamp power supply are contained in a control chassis, see Fig. 3.4. For both spheres, the internal aperture slide 3 is used.

The spheres are routinely monitored using two Standard Lamp Monitors (SLMs). An SLM is a single channel radiometer with an interference filter in front of a silicon photodiode. It was designed by NIST and manufactured

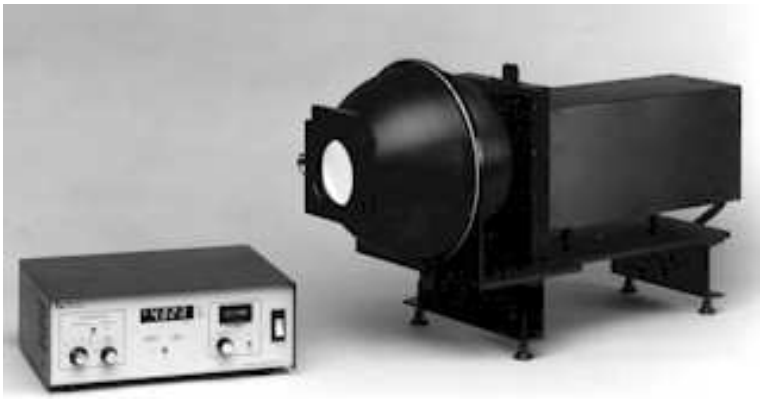

Figure 3.4: *Model picture from the OL website of the OL 425, together with the control chassis. The horizontal rectangular extension contains the lamp. The intensity of the radiance exiting the aperture can be varied by changing the position of the lamp.*

by Reyer Corp., Md. The radiometers can be operated in either radiance mode with a camera lens attachment or in irradiance mode with the camera lens removed and replaced with a Teflon diffuser. The SLM is used in radiance mode at a fixed distance of 51cm to the source. The SLM detector and filter are temperature stabilized at 28.0° C using a thermoelectric temperature controller (ILX Lightwave). The Silicon photodiode detectors are operated in the photocurrent mode, and the photocurrent mode is amplified using an intrinsic transimpedance amplifier. The gain can be varied from 10^4 V/Amp to 10^{10} V/Amp. The FOV is a circle of approximately 2 cm diameter. The centroid wavelengths of the two SLMs are 411.81 nm and 872.14 nm with a bandwidth of 10.78 nm and 12.34 nm, resp. The SLMs are calibrated at NIST, the calibration uncertainty is about 1.5 %. The data from the SLMs is used as a check to verify that the lamps are stable and correctly calibrated (within the uncertainties) at the respective center wavelengths. The lamp calibration data has so far not been corrected with the SLM data, because there has been no indication that this correction is necessary. The alignment of the SLM is done with an eyepiece mounted on top of the SLM. The two instruments are shown in Fig. 3.5.

3.2.5 Scripps

The same equipment and protocols as described in [Meister et al., 2002] were used. No new calibrations were made of the sphere by Labsphere.

3.2.6 Biospherical

The same equipment and protocols as described in [Meister et al., 2002] were used. The Spectralon plaque had been refinished by Labsphere since SIMRIC-1. A new directional reflectance calibration by Labsphere of the plaque was available. Labsphere provides so-called 'uncertified' and 'certified' reflectance values. The uncertified values cover a wavelength range from 250 to 1600 nm, the certified values from 380 nm to 770 nm. Biospherical uses the uncertified values, multiplied by the correction factor 1.028 from [Johnson et al., 1996].

3.2.7 ICESS/UCSB

The equipment and protocols at ICESS/UCSB were described in [Meister et al., 2002]. A reflectance calibration of the Spectralon plaque from 1999 (the '0°/45° Spectral Reflectance Factor') is used. Two additional changes were implemented since the SIMRIC-1. First, a small baffle was attached to the lamp holder, and an additional intermediate baffle (61cm by 66 cm) with a rectangular hole (15cm by 28cm) is placed between the lamp and the plaque, at a distance of 40cm from the lamp. These additional baffles reduced the stray light by about 90% or more. Second, the distance correction for FELs placed at distances from the plaque greater than 50cm described in [Yoon et al., 2003] is used with a value of 3.18mm for the distance correction of the optical center to the front of the pins, see [Meister et al., 2002], section 4.7 for a discussion of the effect. The primary standard is still the NIST FEL 514 with the calibration from December 2000.

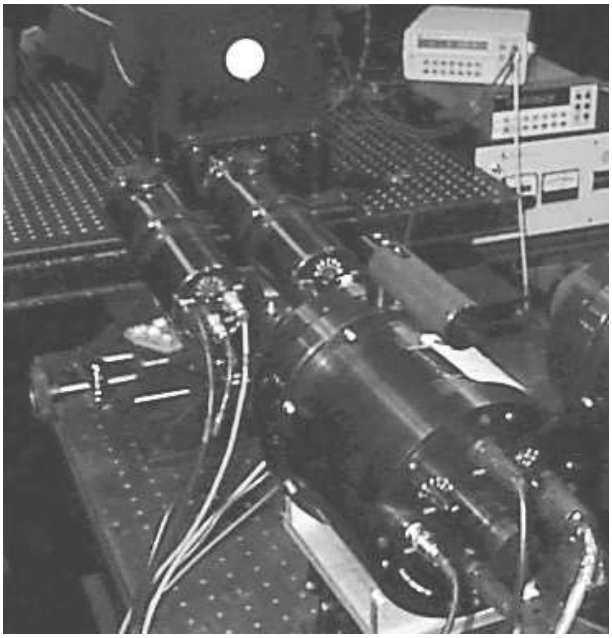

Figure 3.5: *The two SLMs (center of the picture, in front of the SXR-II) on an optical table in the calibration cabin in Snug Harbor, Honululu.*

3.2.8 USF

Kendall Carder's lab at the College of Marine Science, University of South Florida (USF) in St. Petersburg, Florida does not calibrate their handheld radiometers at the St. Petersburg facility. Their radiometers are calibrated at the University of Arizona, usually with a so-called 'Solar-Reflectance-Based' calibration method [Cattral et al., 2002]. At USF, the radiometers are checked for long-term stability and linearity. A uniform radiance standard from Labsphere (URS-600 shown in Fig. 3.6) is used for this purpose. Its exit port underfills the FOV of the SXR-II. Thus the measurements of the SXR-II do not give absolute radiance values. Still the SXR-II measurements can be used to check for (short-term) stability and linearity. The SXR-II was placed 50 cm away from the exit port of the URS-600. The integrating sphere of the URS-600 contains a photopic detector that measures the light intensity in foot lambert (FL) in the ISS. The lamp chamber of the URS-600 contains a regulated lamp and is separated from the integrating sphere by a variable attenuator. A micrometer adjusts the variable attenuator to limit the flux of light into the sphere. For this report, the attenuator was set to produce a flux of 500, 3,000, 5,000, 10,000, and 20,000FL. Radiance calibrations from Labsphere are available for the URS-600 at flux levels of 500, 3,000, 10,000, and 20,000FL for wavelengths from the UV to the IR. These calibrations are used when checking a radiometer for linearity.

3.2.9 UM

The Experimental Environmental Optics Group at the Atmospheric and Ocean Optics Laboratory at the Physics Department of the University of Miami (UM) uses a Spectralon plaque illuminated by a 1000 W modified type FEL for radiance calibrations. Two calibrated irradiance standards are available from OL, F-258 from June 1990 and F-161 from May 1984. UM transfers the scale to working standards with a monochromator from OL (Optical Radiation Measurement System, OL 740 A). It was planned to do the transfer right after the SIMRIC-2 measurements, but the monochromator malfunctioned and had to be repaired. A calibration transfer could not be done before this report was finished. A new primary standard from OL was purchased after the SIMRIC-2.

The power supply (OL 83 DS) is warmed up with a ballast lamp for at least 20 minutes. Prior to the SIMRIC-2, the FEL lamps were warmed up for 5 minutes immediately after the 20 minute warmup of the power supply. The FEL warmup time was extended to 10 minutes starting with the SIMRIC-2. All lamps are run at 8 Ampere. The current is monitored with a voltmeter and a shunt. The voltage across the lamp is recorded as well.

UM uses mechanical devices for alignment purposes instead of a laser. An FEL holder from OL is placed on a

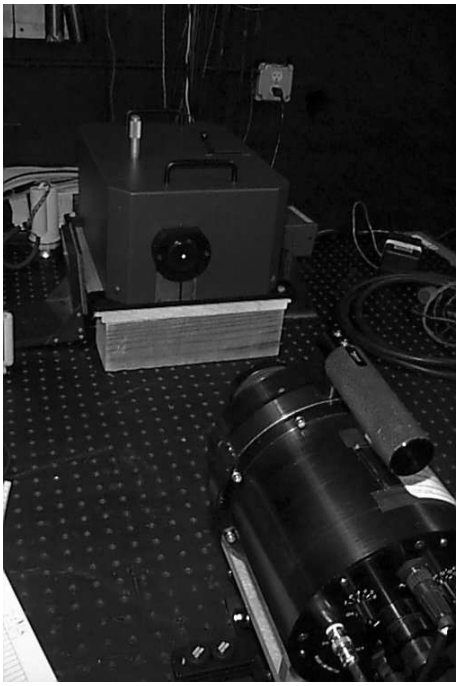

Figure 3.6: *The SXR-II looks at the ISS at USF. The wooden block is not part of the usual calibration procedures at USF and was only introduced to bring the exit aperture (closed by a black cover with a white point in the middle in the above picture) to the same height as the SXR-II. The micrometer screw to adjust the light level can be seen on top of the ISS.*

sled, which can be moved on two parallel optical rails of 3 m length, see Fig. 3.7. On one end of the rail, a Spectralon plaque is placed. A marker on the sled indicates the distance (printed next to the optical rail) between front of the pins of the FEL and the plaque. Two vertical wires (see Fig. 3.8) allow an easy alignment of the plaque at right angles to the optical rail. The wires can be turned to an angle of 45° to align a radiometer, a feature that made the alignment of the SXR-II (looking through the SXR-II eyepiece) easier than in any other laboratory visited during SIMRIC-1 or SIMRIC-2. An FEL alignment jig is placed in the FEL holder, and again the vertical wires are used to align the front surface of the alignment jig at right angles to the optical rail. The center of the crosshairs in the alignment jig is positioned using the left side of the horizontal pointer shown in Fig. 3.8. The pointer can be moved to any position on the optical rails. The right side of the horizontal pointer is used to align the radiometer to the center of the Spectralon plaque by moving the pointer as close to the Spectralon plaque as possible without touching it. A baffle (see Fig. 3.9) is placed between the lamp and the plaque, except for measurements at a distance of 50 cm. The size of the aperture in the baffle is adjusted until the plaque is fully illuminated. It is planned to replace this baffle with a baffle that has a square aperture rather than the diamond aperture of Fig. 3.9. The whole measurement area is surrounded by black curtains.

The reflectance of the Spectralon plaque is assumed to be 0.98, but no valid calibration is available. UM has resolved this deficiency by acquiring a new, calibrated plaque. It was not available for SIMRIC-2, so the value of 0.98 was used as reflectance factor in the calculations of this report.

3.2.10 Satlantic

The same protocols and facility as described in [Meister et al., 2002] were used. Two new FEL irradiance standards from OL were used, and the plaque had a new reflectance calibration from September 2002. Satlantic switched to using the effective distance correction (see [Meister et al., 2002], section 4.7) in 2003, but the values from SIMRIC-2 are not affected.

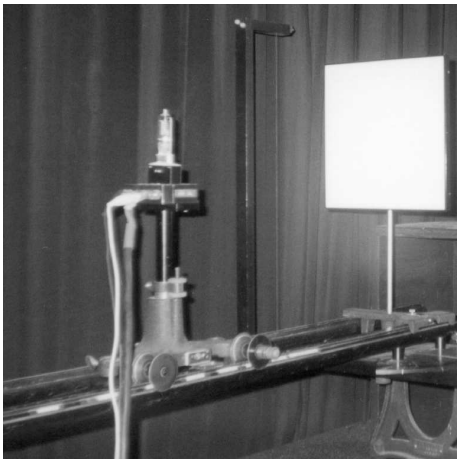

Figure 3.7: *At UM, a sled with an FEL holder rolls on two parallel optical rails. Between the two right hand wheels of the sled, a marker can be seen that indicates the distance to the plaque.*

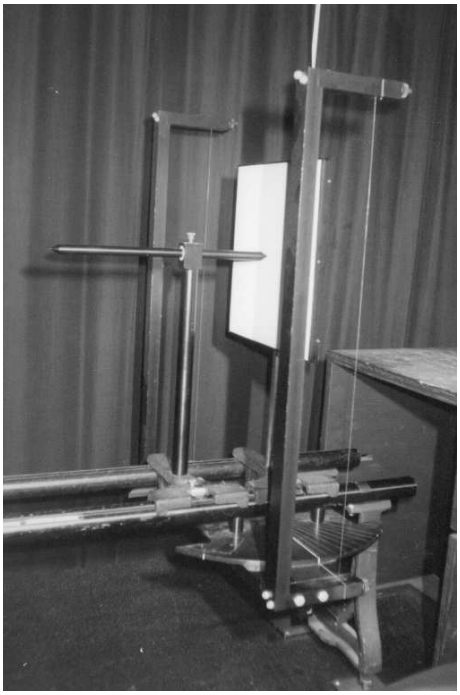

Figure 3.8: *Two vertical wires to the left and right of the Spectralon are used at UM to align the Spectralon plaque at right angles to the optical rail. The wires can be rotated to* 45° *to allow the alignment of the radiometer.*

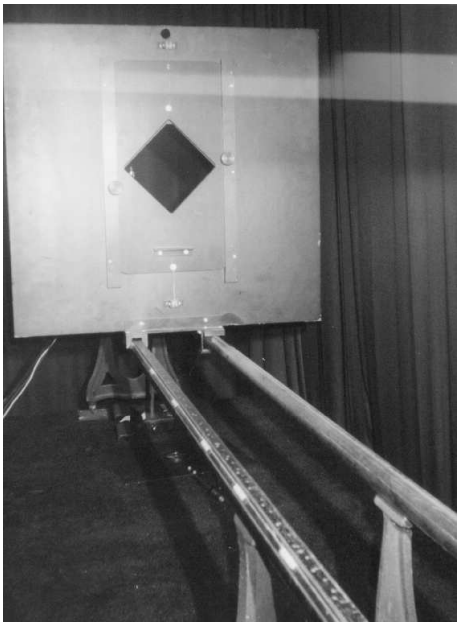

Figure 3.9: *The baffle at the UM is placed on the optical rails. The FEL lamp is behind the baffle (note the cables on the bottom left in the picture). The distance to the plaque can be seen printed on the left optical rail.*

3.3 SXR-II Specific Procedures

The same procedures as described in [Meister et al., 2002] were used during SIMRIC-2, they are repeated here for completeness. The SXR-II was positioned about 1 m apart from the plaque or sphere (Fig. 3.3). A 45° viewing angle relative to the plaques was obtained by projecting the adjacent leg and the opposite leg (both of length $\sqrt{0.5}$ m for a triangle with a right angle and a hypotenuse of 1 m) onto a common horizontal plane. The SXR-II was usually mounted on a tripod or labjack. An on-axis-cavity was placed in the center of the FOV to perform a measurement (called 'ambient measurement' from here on) that determines the size-of-source effect, see appendix [Meister et al., 2002]. The ambient measurement was subtracted from the measurement with the cavity removed (i.e. the actual measurement of the plaque/sphere, called 'signal measurement' from here on). A cap is placed in front of the SXR-II lens to obtain background measurements. They were not used in this report, as the subtraction of the ambient measurement includes the background signal.

The following setting was chosen in the SXR-II control software:

- 11 samples are taken for a given gain and channel.
- The delay between sample readings was set to 0.5 seconds.
- Do several consecutive wavelength scans (i.e. read channels 1 to 6 in ascending order). Typically 4 scans were chosen for the signal measurements, which resulted in a total measurement time of 5 minutes for the light source. Ambient measurements were usually 2 scans or less, background measurements were 3 scans or more.

The standard order of measurements is

1. Background
2. Ambient
3. Signal
4. Background,

but this sequence was not always used. During the light source warmup, the appropriate gain was chosen for each of the channels. The optimal gain gives a voltage reading between 100 mV and 1 V, because in this range the accuracy of the voltmeter is highest. All types of measurements (signal, ambient, background) used the gain setting optimized for the signal measurement.

The SXR-II noise uncertainty u_{stat} (Type A uncertainty) is calculated as

$$u_{\text{stat}} = \sqrt{\sigma_I^2 + \sigma_A^2} \tag{3.1}$$

where σ_I is the standard deviation of the signal readings of all samples and scans, and σ_A is the standard deviation of the ambient measurements. u_{stat} is less than 0.1% of the signal measurements for all measured radiances of the SIMRIC-2, except in a few cases for channel 1, where it is still close to 0.1%.

Chapter 4

Results

4.1 Radiance Calculation

The formula for calculating the band-averaged *expected radiances* L_e is

$$L_e(\text{channel}) = \int_0^\infty L_r(\lambda) \cdot S(\lambda, \text{channel}) \mathrm{d}\lambda \tag{4.1}$$

where $L_r(\lambda)$ is the radiance reflected from either a plaque or out of a sphere, $S(\lambda, \text{channel})$ is the responsivity of the respective radiometer channel (1-6 in the case of the SXR-II). The responsivity is normalized to one:

$$\int_0^\infty S(\lambda, \text{channel}) \mathrm{d}\lambda = 1 \tag{4.2}$$

Note that $S(\lambda, \text{channel})$ has the unit nm^{-1}, because it is sensitivity per wavelength interval. In reality, $S(\lambda, \text{channel})$ and $L_r(\lambda)$ are not given as continuous functions, but only at discrete wavelengths. Thus interpolation becomes necessary. For this study, for $L_r(\lambda)$ the interpolated data calculated by the laboratory in which the measurement was taken is used.

$S(\lambda, \text{channel})$ was measured by NIST in about 0.2 nm intervals in the high sensitivity regions, and in 5 to 10 nm intervals in low sensitivity regions. The wavelength range varies with channel, from about 400 nm to 940 nm. A dataset interpolated to 0.2 nm by NIST was used for the calculations. The actual calculation of eqs. 4.1-4.2 was carried out as a sum by the main author of this study, linearly interpolating to 0.1 nm wavelength intervals.

To account for the size-of-source effect (see [Meister et al., 2002], appendix A), measurements with an open cavity (see section 3.3) placed in the FOV of the SXR-II were subtracted from the actual signal measurements. The difference was divided by the calibration factors in Table 2.1 after a time dependent correction, see section 2.4.3. The resulting values are called *SXR-II measured radiances* L_m in this report.

4.2 Radiance Comparisons

4.2.1 NASA Code 920.1

There is a strong variation of the differences for channel 1 (411 nm) at NASA Code 920.1, see Fig. 4.1 and Table 4.1. The transfer radiometer used by NASA Code 920.1 is not very sensitive around 410nm, which results in a relatively high uncertainty estimate of 3.0% for 16 lamps for Hardy and 2.4% for 16 lamps for Slick at 410nm. The measurements were taken with 6 lamps and 2 lamps for Hardy, and 8 lamps and 4 lamps for Slick, because most channels of the SXR-II saturate at 16 lamps. Thus the uncertainty of the expected radiances is expected to be higher than 3% and 2.4%, resp., but no estimates are available.

The SXR-II measured the spheres on 4/24/02 and 4/25/02. The closest calibration transfers made by Code 920.1 are from 4/8/02 for Hardy and 5/1/02 for Slick. The closest dates were chosen for the calculation of the difference: for Hardy, the SXR-II measurements from 4/24/02 were chosen; for Slick, the SXR-II measurements from 4/25/02. The repeatability of the SXR-II measurements from the two dates is better than 0.5% for Hardy, but

Slick 8 lamps

λ_m [nm]	410.7	441.5	487.6	546.9	661.9	776.7
L_m	2.695	4.564	8.267	14.181	26.379	36.309
L_e	2.706	4.535	8.182	14.042	25.741	35.278
$\Delta(L_e - L_m)[\%]$	0.8	-0.2	-0.6	0.6	-2.0	-2.4

Slick 4 lamps

λ_m [nm]	410.7	441.5	487.6	546.9	661.9	776.7
L_m	1.189	2.018	3.667	6.315	11.832	16.42
L_e	1.208	1.974	3.577	6.192	11.501	15.848
$\Delta(L_e - L_m)[\%]$	2.9	-1.0	-1.2	-0.8	-1.8	-2.5

Hardy 6 lamps

λ_m [nm]	410.7	441.5	487.6	546.9	661.9	776.7
L_m	3.979	7.772	14.892	24.69	40.585	48.232
L_e	4.113	7.854	14.929	24.707	39.931	47.155
$\Delta(L_e - L_m)[\%]$	3.4	1.1	0.3	0.1	-1.6	-2.2

Hardy 2 lamps

λ_m [nm]	410.7	441.5	487.6	546.9	661.9	776.7
L_m	1.165	2.292	4.422	7.38	12.236	14.62
L_e	1.242	2.3	4.408	7.382	12.053	14.327
$\Delta(L_e - L_m)[\%]$	6.6	0.3	-0.3	0.	-1.5	-2.

Table 4.1: *Results at NASA Code 920.1 from 4/24/02 (Hardy) and 4/25/02 (Slick). Radiance unit is $\mu W/(cm^2\ sr\ nm)$. L_m is the SXR-II measured radiance, L_e is the expected radiance. Δ is the difference $L_e - L_m$ in %.*

the SXR-II measurements of Slick are up to 1.2% lower on the 25th than on the 24th (for 4 lamps, SXR-II channels 1 to 4). In effect, the previous calibration transfer by Code 920.1 for Slick (4 lamps) from 3/29/02 yielded values that are 2.4% to 3.6% higher in the SXR-II channels 1 to 4, thus the differences measured by the SXR-II between 4/24/02 and 4/25/02 for Slick may be part of a long term trend.

It is interesting to see that the differences at NASA Code 920.1 are spectrally very similar for SIMRIC-1 (see appendix A, Table A.2) and SIMRIC-2, and the additional measurement in August 2002 (shown in Fig. 4.1 as a dashed line): channels 5 and 6 are lowest (expected radiances are too low), channels 2,3,4 are very similar (close to 0% difference), and channel 1 is highest (expected radiances are too high). Although the differences between the expected radiances and the SXR-II measured radiances for SXR-II channels 5 and 6 are just within the combined uncertainties, the consistency of the differences (SIMRIC-1, SIMRIC-2, August 2002) suggests that there is a systematic bias at the wavelengths 662nm and 777nm.

4.2.2 ICESS / UCSB

The results from ICESS/UCSB are presented in table 4.2 and Fig. 4.2. There is a strong wavelength pattern in the differences: for the blue wavelengths below 600nm, the agreement is excellent, better than 1%. In the red and NIR, larger differences can be seen, up to about -3%. This wavelength pattern is often associated with stray light reflected from the baffles. But independent measurements done with UCSB equipment do not suggest such a strong presence of stray light.

A comparison with the results from SIMRIC-1 [Meister et al., 2002] shows that the measured radiances are about 1 to 2% lower for SIMRIC-2 than for SIMRIC-1 for all measured FELs, with no clear wavelength dependence. Thus it is likely that the new baffling described in section 3.2.7 has reduced the level of stray light, although it was expected that the improvement would be larger in the NIR than in the blue. The adoption of the new distance correction added 0.95% to the expected radiance, which increased the difference in the blue and decreased the

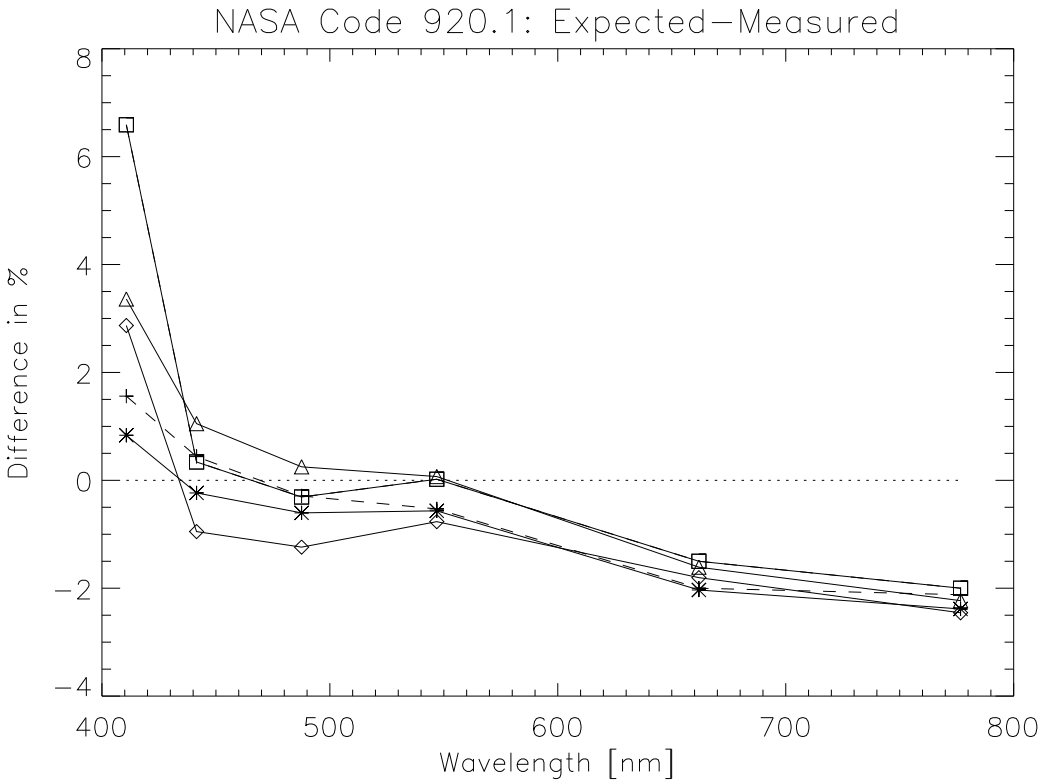

Figure 4.1: *The solid lines show the differences of the expected radiances of the NASA Code 920.1 spheres and the SXR-II measured radiances (stars: Slick 8 lamps, diamonds: Slick 4 lamps, triangles: Hardy 6 lamps, squares: Hardy 2 lamps). The dashed line shows the difference of the expected radiance of Hardy 6 lamps and the SXR-II measured radiances for 8/15/02.*

difference in the NIR. The new reflectance coefficients are about 0.5% lower for the shorter wavelengths (decreasing the expected radiances) and little changed in the NIR.

The consistency between the primary standard (F-514) and the two secondary standards (F-473 and F-305) is excellent, the strongest disagreement is in channel 6 (0.6% and 0.3%, resp.), all other channels are within ±0.2%.

4.2.3 WFF

The large differences seen in the comparison results from WFF in table 4.3 and Fig. 4.3 are largely due to an error in the setup of the lamp, an outdated reflectance calibration of the plaque, and some problems in the baffling, see section 3.2.3 for more details.

4.2.4 NRL

The results from NRL are shown in Fig. 4.4 and table 4.4. Channels 1 to 5 show differences of less than 2%, a very good agreement, and a significant improvement compared to the results from SIMRIC-1, especially in the blue. At channel 6, there is no improvement compared to SIMRIC-1, the expected radiances are about 3% lower than the measured radiances. Although this is just within the combined uncertainties, we suspect that there may be a problem with the baffling material. The results from the two FELs are very consistent. There is a difference of up to 1% between the differences for the FELs and the differences for the sphere. During SIMRIC-1, the difference was negligible.

FEL F-514

λ_m [nm]	410.7	441.5	487.6	546.9	661.9	776.7
L_m	0.04814	0.07435	0.12406	0.19813	0.33798	0.43883
L_e	0.04866	0.07543	0.12550	0.20033	0.33814	0.42827
$\Delta(L_e - L_m)[\%]$	1.1	1.5	1.2	1.1	0.1	-2.4

FEL F-473

λ_m [nm]	410.7	441.5	487.6	546.9	661.9	776.7
L_m	0.04527	0.07017	0.11762	0.18853	0.32316	0.42123
L_e	0.04580	0.07130	0.11915	0.19094	0.32415	0.41363
$\Delta(L_e - L_m)[\%]$	1.2	1.6	1.3	1.3	0.3	-1.8

FEL F-305

λ_m [nm]	410.7	441.5	487.6	546.9	661.9	776.7
L_m	0.04987	0.07645	0.12644	0.19996	0.33664	0.43452
L_e	0.05037	0.07748	0.12769	0.20184	0.33624	0.42265
$\Delta(L_e - L_m)[\%]$	1.0	1.4	1.0	0.9	-0.1	-2.7

SIMBIOS FEL F-474

λ_m [nm]	410.7	441.5	487.6	546.9	661.9	776.7
L_m	0.04401	0.06825	0.11444	0.18355	0.31492	0.41051
L_e	0.04525	0.07050	0.11800	0.18916	0.31929	0.40487
$\Delta(L_e - L_m)[\%]$	2.8	3.3	3.1	3.1	1.4	-1.3

Table 4.2: *Results at UCSB from 9/25/02. Radiance unit is $\mu W/(cm^2\ sr\ nm)$. L_m is the SXR-II measured radiance, L_e is the expected radiance. Δ is the difference $L_e - L_m$ in %.*

Oriel 7-1399

λ_m [nm]	410.7	441.5	487.6	546.9	661.9	776.7
L_m	0.212	0.3195	0.5159	0.7928	1.2877	1.6598
L_e	0.1959	0.2976	0.4822	0.7492	1.2223	1.5173
$\Delta(L_e - L_m)[\%]$	-7.6	-6.8	-6.5	-5.5	-5.1	-8.6

Oriel 7-1026

λ_m [nm]	410.7	441.5	487.6	546.9	661.9	776.7
L_m	0.2091	0.3165	0.5142	0.7939	1.2945	1.652
L_e	0.1967	0.2997	0.4874	0.7598	1.2428	1.5423
$\Delta(L_e - L_m)[\%]$	-5.9	-5.3	-5.2	-4.3	-4.	-6.6

Table 4.3: *Results at WFF from 7/16/02. Radiance unit is $\mu W/(cm^2\ sr\ nm)$. L_m is the SXR-II measured radiance, L_e is the expected radiance. Δ is the difference $L_e - L_m$ in %.*

FEL F-400

λ_m [nm]	410.7	441.5	487.6	546.9	661.9	776.7
L_m	0.712	1.109	1.867	3.	5.15	6.664
L_e	0.711	1.108	1.859	2.982	5.083	6.461
$\Delta(L_e - L_m)[\%]$	-0.1	0.	-0.5	-0.6	-1.3	-3.

FEL F-399

λ_m [nm]	410.7	441.5	487.6	546.9	661.9	776.7
L_m	0.737	1.145	1.921	3.073	5.245	6.764
L_e	0.735	1.143	1.911	3.049	5.161	6.540
$\Delta(L_e - L_m)[\%]$	-0.3	-0.2	-0.5	-0.8	-1.6	-3.3

USS 4000 sphere

λ_m [nm]	410.7	441.5	487.6	546.9	661.9	776.7
L_m	1.033	1.826	3.472	6.208	11.973	16.166
L_e	1.017	1.812	3.426	6.113	11.727	15.727
$\Delta(L_e - L_m)[\%]$	-1.5	-0.8	-1.3	-1.6	-2.1	-2.8

SIMBIOS FEL F-474

λ_m [nm]	410.7	441.5	487.6	546.9	661.9	776.7
L_m	0.723	1.12	1.881	3.015	5.16	6.675
L_e	0.74	1.152	1.926	3.082	5.207	6.57
$\Delta(L_e - L_m)[\%]$	2.4	2.8	2.4	2.2	0.9	-1.6

Table 4.4: *Results at NRL from 3/11/02 and 3/12/02. Radiance unit is $\mu W/(cm^2\ sr\ nm)$. L_m is the SXR-II measured radiance, L_e is the expected radiance. Δ is the difference $L_e - L_m$ in %.*

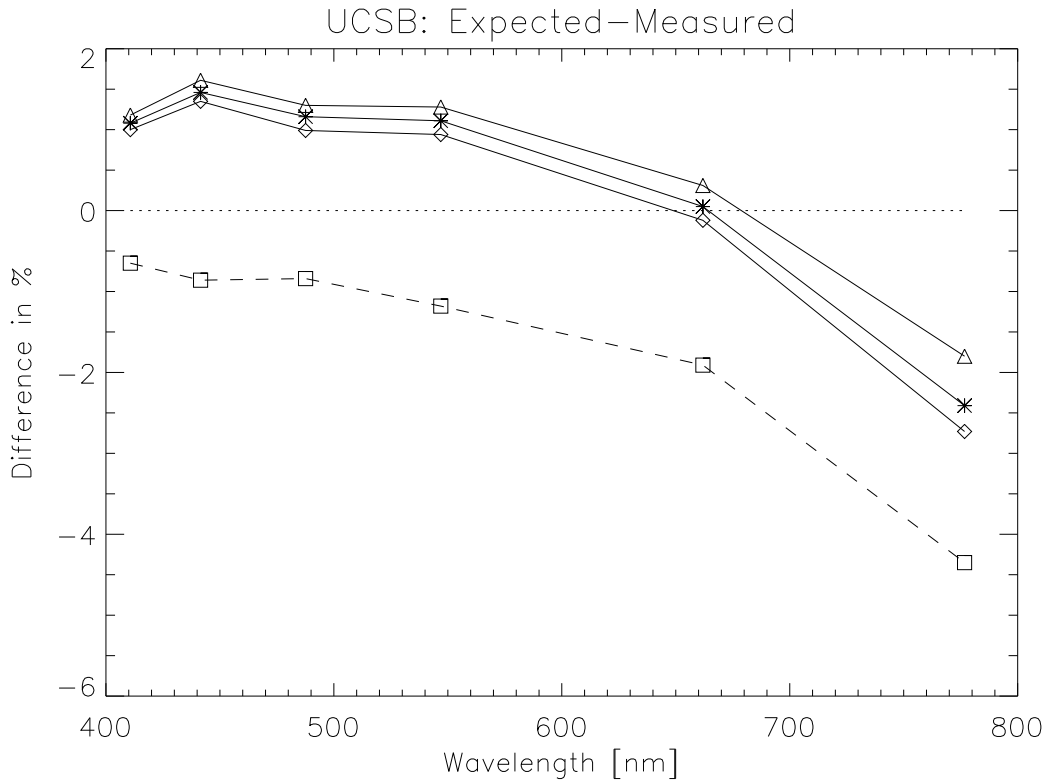

Figure 4.2: *The solid lines show the differences of the expected radiances at ICESS/UCSB and the SXR-II measured radiances (stars: F-514, diamonds: F-305, triangles: F-473). The dashed line shows the difference of the expected radiance of F-514 and the SXR-II measured radiances from SIMRIC-1.*

4.2.5 Scripps

During the measurements at Scripps, the PC recording the internal monitor data of the Scripps sphere failed, thus only manually recorded internal monitor values are available to correct the expected radiances. Three measurements were done. The internal monitor values decreased from the first to the second measurement by 0.6%, from the second to the third by 0.1%. These decreases correspond well to the change of the differences seen in Fig. 4.5. Overall, the differences between expected and measured radiances are very small, less than 1.3%. However, the range between the differences is almost 1%, which is surprisingly large. It may be due to the manual recording of the internal monitor readings. The failure of the PC was only noticed after the first two measurements, so during the third measurement the internal monitor values were recorded three times (only once during the first two measurements). The three readings from the third measurement are identical (only 4 significant digits can be read from the display), thus we put the highest confidence in the third measurement and report its value in table 4.5.

Labsphere sphere

λ_m [nm]	410.7	441.5	487.6	546.9	661.9	776.7
L_m	7.891	(saturated)	21.225	34.746	59.345	74.614
L_e	7.822	12.539	21.278	34.851	59.588	74.554
$\Delta(L_e - L_m)$[%]	-0.9	N/A	0.2	0.3	0.4	-0.1

Table 4.5: *Results at Scripps from 9/26/02. Radiance unit is $\mu W/(cm^2\ sr\ nm)$. L_m is the SXR-II measured radiance of the third measurement, L_e is the expected radiance of the third measurement. Δ is the difference $L_e - L_m$ in %. Channel 2 of the SXR-II saturated.*

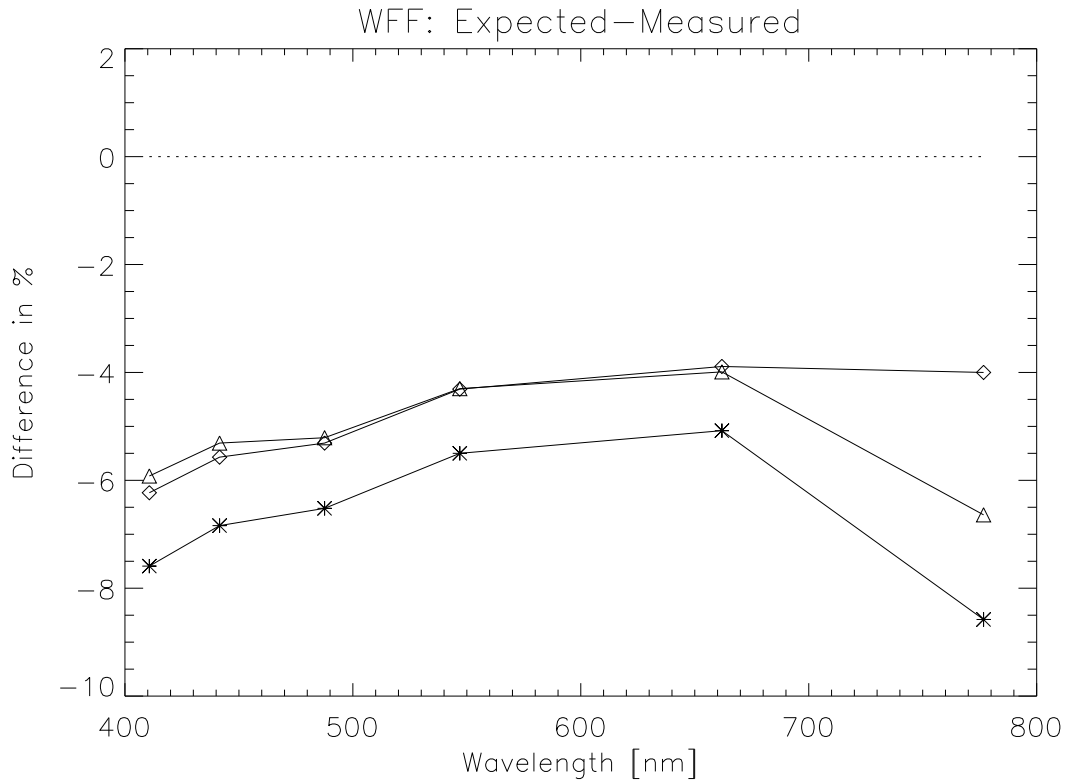

Figure 4.3: *The solid lines show the differences of the expected radiances at WFF and the SXR-II measured radiances (stars: 7-1399, diamonds: 7-1399 with additional baffling, triangles: 7-1026).*

4.2.6 Biospherical

The results from Biospherical are shown in Fig. 4.6 and table 4.6. Most differences are within ±1.0%, an excellent agreement. The measured SXR-II radiances of the F-473 are 0.5 to 0.9% lower at SIMRIC-2 than at SIMRIC-1. The Spectralon plaque had been refinished after the SIMRIC-1, which is a possible cause for a change of the reflected radiance in that magnitude.

The F-714 does not belong to Biospherical directly, it is an FEL from a Biospherical representative (K-Engineering, Tokyo, Japan) that was at Biospherical during the SIMRIC-2. It was measured, because it does have the NIST 2000 irradiance calibration, whereas the Biospherical primary standard (F-473) was calibrated by NIST in 1997, and is therefore based on the NIST 1992 irradiance scale. Comparisons between the NIST 1992 irradiance scale and the NIST 2000 irradiance scale have shown higher irradiances for the 2000 scale by about 0.5 to 1.0% [Yoon et al., 2002]. Assuming there are no measurement errors, the expected difference for the F-714 is 0%, since the SXR-II is also on the NIST 2000 scale, and the expected difference for the F-473 is up to -1.0%, i.e. the expected radiances should be lower than the measured radiances. Assuming that the same measurement errors were made for the F-473 and the F-714 during the SIMRIC-2, we expect the difference for the F-473 to be *lower* than the difference for the F-714 by up to 1.0%. But the differences from the F-473 are about 0.2 to 1.0% *higher* than the differences from the F-714. Several reasons are possible for this, most notably a drift in the F-473 (it was calibrated in 1997, i.e. 5 years before the measurements took place), a different scaling of the irradiance of the two FELs from 0.5m (the distance of the NIST calibration) to 2.952m (the distance of the SIMRIC-2 measurements at Biospherical), or uncertainties in the SXR-II measured radiances (estimated uncertainty is 0.8 to 1.0% see table 2.2).

4.2.7 MLML/MOBY

The results from the MLML spheres measured at NIST are shown in Fig. 4.7 and Table 4.7. The differences are 2% or less, with the worst agreement in channel 1 for the OL425 sphere. It can be seen in Fig. 4.7 that the OL420

FEL F-473

λ_m [nm]	410.7	441.5	487.6	546.9	661.9	776.7
L_m	0.02487	0.03805	0.06269	0.09870	0.16480	0.20826
L_e	0.02496	0.03844	0.0633	0.09958	0.16544	0.20873
$\Delta(L_e - L_m)[\%]$	0.4	1.0	1.0	0.9	0.4	0.2

FEL F-91773

λ_m [nm]	410.7	441.5	487.6	546.9	661.9	776.7
L_m	0.02185	0.03354	0.05555	0.08787	0.14794	0.18847
L_e	0.02171	0.03347	0.05531	0.08762	0.14704	0.1858
$\Delta(L_e - L_m)[\%]$	-0.6	-0.2	-0.4	-0.3	-0.6	-1.4

SIMBIOS FEL F-474

λ_m [nm]	410.7	441.5	487.6	546.9	661.9	776.7
L_m	0.02066	0.03202	0.05358	0.08565	0.14628	0.18772
L_e	0.02124	0.03308	0.05531	0.08858	0.14966	0.18923
$\Delta(L_e - L_m)[\%]$	2.8	3.3	3.2	3.4	2.3	0.8

FEL F-714 (NIST 2000 scale)

λ_m [nm]	410.7	441.5	487.6	546.9	661.9	776.7
L_m	0.02854	0.04298	0.06945	0.10713	0.17398	0.21636
L_e	0.02859	0.04329	0.06988	0.10776	0.17395	0.21382
$\Delta(L_e - L_m)[\%]$	0.2	0.7	0.6	0.6	0.	-1.2

Table 4.6: *Results at Biospherical from 9/27/02. Radiance unit is* $\mu W/(cm^2\ sr\ nm)$. L_m *is the SXR-II measured radiance,* L_e *is the expected radiance.* Δ *is the difference* $L_e - L_m$ *in %.*

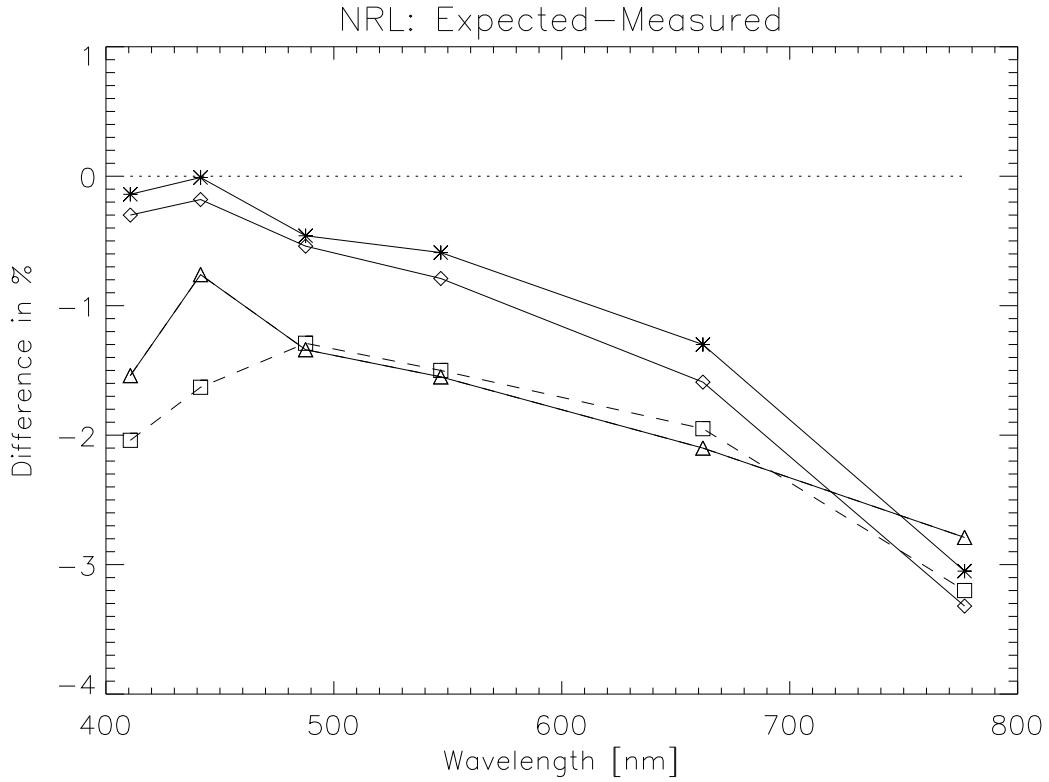

Figure 4.4: *The solid lines show the differences of the expected radiances at NRL and the SXR-II measured radiances (stars: F-400, diamonds: F-399, triangles: USS-4000). The dashed line shows the difference of the expected radiance of F-400 and the SXR-II measured radiances from SIMRIC-1.*

(both settings, W5 and W6) agree very well with the differences calculated for the NPR, which was measured in the same laboratory one day before the MLML spheres. On average, the OL425 sphere shows greater differences than the OL420 sphere. The internal monitor readings are 0.3% lower for OL425W6, and 1.1% lower for OL425W5. If the internal monitor readings from the OL425 had not been used to correct the expected radiances, the differences would decrease by the above given percentages. The uncertainties given by NIST (k=2) range from 0.4% to 0.9% for the wavelengths from 400, 500 and 600 nm for the two spheres, 0.4% to 2.2% at the wavelengths 700 and 800 nm. Combining these uncertainties with the SXR-II uncertainties (see table 2.2) shows that the differences are within the combined uncertainties, with the possible exception of OL425 at 412 nm (combined uncertainty is 1.9%, difference is 2.0%)

The results presented here are from the first round of measurements. A second round of measurements was taken immediately following the completion of the first round, i.e. the lamps were turned off after the first round, and the SXR-II was repositioned for each lamp. The repeatability of the SXR-II measured radiances is remarkably good, with a typical agreement of better than 0.1%. The highest differences found were in channels 3 and 6 of up to 0.15%.

4.2.8 University of Miami

Fig. 4.8 and Table 4.8 show the results at UM. UM was the only laboratory were FELs were measured at varying distances from the plaque. At the closest distance (0.5m), the expected values from the F-161 are significantly lower than the measured radiances, by about 1% to 6%, increasing with wavelength. The SIMBIOS F-474 seems to give better results, but the OL calibration of the F-474 gives typically about 2% higher expected radiances than the measured radiances, so the results from the two FELs are not as inconsistent as the plot seems to indicate. Furthermore, UM uses a reflectance factor of only 0.98, which is about 3% less than typically used in other laboratories. An increase of the reflectance factor would result in higher expected radiances, reducing the difference to the measured radiances.

OL 425 W6

λ_m [nm]	410.7	441.5	487.6	546.9	661.9	776.7
L_m	0.05549	0.09238	0.16602	0.28187	0.5114	0.70388
L_e	0.05438	0.09127	0.16442	0.28044	0.51009	0.69562
$\Delta(L_e - L_m)[\%]$	-2.	-1.2	-1.	-0.5	-0.3	-1.2

OL 425 W5

λ_m [nm]	410.7	441.5	487.6	546.9	661.9	776.7
L_m	0.03318	0.05524	0.09927	0.16854	0.3055	0.41414
L_e	0.0325	0.05439	0.09857	0.16713	0.3037	0.41003
$\Delta(L_e - L_m)[\%]$	-2.	-1.5	-0.7	-0.8	-0.6	-1.

OL 420 W6

λ_m [nm]	410.7	441.5	487.6	546.9	661.9	776.7
L_m	0.08017	0.1364	0.24642	0.41798	0.75348	1.00077
L_e	0.07911	0.13542	0.24518	0.41688	0.74809	0.99882
$\Delta(L_e - L_m)[\%]$	-1.3	-0.7	-0.5	-0.3	-0.7	-0.2

OL 420 W5

λ_m [nm]	410.7	441.5	487.6	546.9	661.9	776.7
L_m	0.02606	0.04437	0.0802	0.13597	0.24511	0.3265
L_e	0.02577	0.04411	0.07986	0.13579	0.24368	0.32535
$\Delta(L_e - L_m)[\%]$	-1.1	-0.6	-0.4	-0.1	-0.6	-0.4

Table 4.7: *Radiances of the MLML spheres from 8/8/02. Radiance unit is $\mu W/(cm^2\ sr\ nm)$. L_m is the SXR-II measured radiance, L_e is the expected radiance. Δ is the difference $L_e - L_m$ in %.*

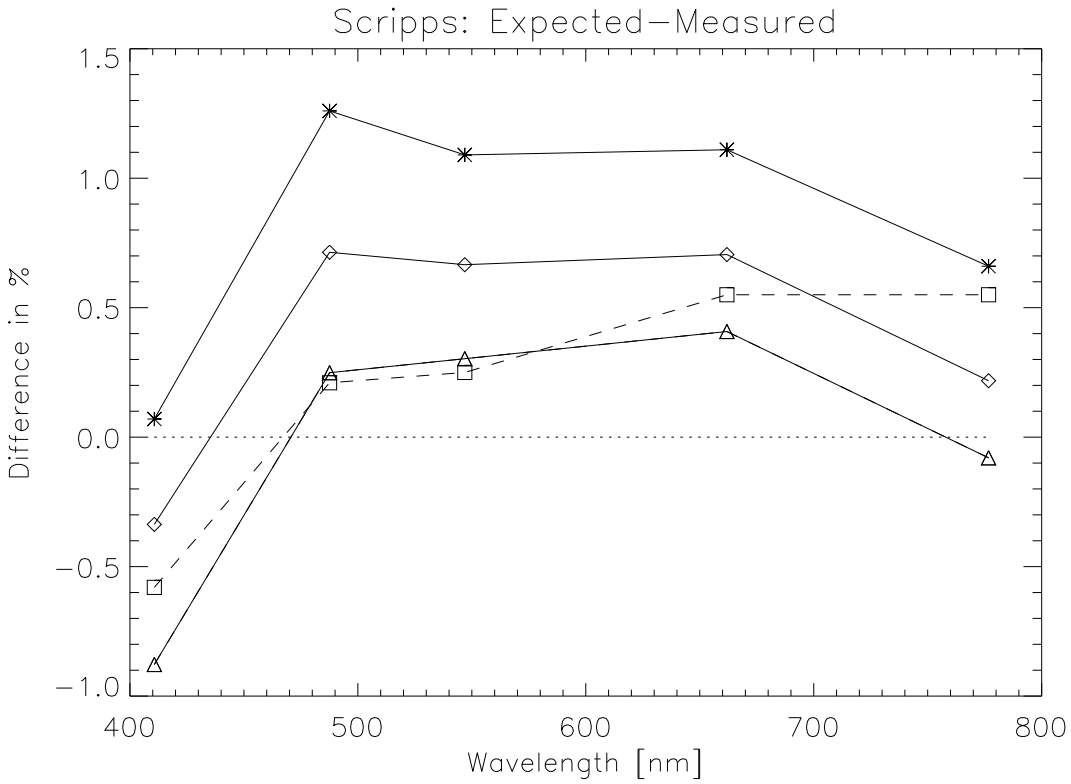

Figure 4.5: *The solid line shows the differences of the expected radiances of the Scripps sphere and the SXR-II measured radiances from SIMRIC-2 (stars: first measurement, diamonds: second measurement, triangles: third measurement). The dashed line shows the difference of the expected radiances of the sphere and the SXR-II measured radiances from SIMRIC-1.*

There is a very large difference for the F-161 at 770 nm, about 6% at 0.5m. This is often a sign of a baffling problem, as many baffling materials reflect strongly in the NIR. The increase of the difference with distance plaque/FEL to 14% at 3m also supports the assumption of a baffling problem, because with a greater distance there is more baffling material between plaque and FEL that can produce scattered light.

In addition to the primary standard F-161 (with an OL calibration), two secondary standards (FELs F-91793 and F-91794) were measured. It was planned to transfer the calibration from F-161 to the secondary standards after the SIMRIC-2 measurements with a monochromator from UM, but the system malfunctioned and had to be sent to the manufacturer. No calibration transfer could be made until April 2003, so no expected radiances are available for the secondary standards. Thus we do not report the measured radiances here. Similar trends when increasing the distance plaque/FEL were found as for the F-161 and the F-474.

As a result of the SIMRIC-2, several changes were implemented at UM, including the purchase of a new FEL, a calibrated plaque, and improvements to the baffling.

4.2.9 Satlantic

The differences between expected and measured radiances are within the combined uncertainties at Satlantic (2.3% at Satlantic, see Table 2.2 for SXR-II). There are several interesting points that can be derived from the results presented in Table 4.9 and Fig. 4.9:

- The spectral shape of the differences is very similar for channels 2 to 5 between SIMRIC-1 and SIMRIC-2, but there is a variation for channels 1 and 6. This may be a sign of a stable relative calibration between channels 2 to 5, and a less stable calibration of channels 1 and 6. Note that if the SQM-II had been used in SIMRIC-1 to correct the SXR-II, channel 1 would have been stable relative to channels 2 to 5.

- The spectral shape of the differences for channels 1 to 5 for SIMRIC-2 is very similar to the average difference

FEL F-161 (0.5m)

λ_m [nm]	410.7	441.5	487.6	546.9	661.9	776.7
L_m	0.84	1.302	2.143	3.347	5.534	7.076
L_e	0.834	1.272	2.075	3.244	5.31	6.661
$\Delta(L_e - L_m)[\%]$	-1.1	-2.4	-3.4	-3.5	-4.6	-6.3

FEL F-161 (3m)

λ_m [nm]	410.7	441.5	487.6	546.9	661.9	776.7
L_m	0.02368	0.03668	0.06041	0.09434	0.1569	0.21511
L_e	0.02316	0.03534	0.05764	0.09011	0.14751	0.18504
$\Delta(L_e - L_m)[\%]$	-2.2	-3.7	-4.6	-4.5	-6.	-14.

SIMBIOS FEL F-474 (0.5m)

λ_m [nm]	410.7	441.5	487.6	546.9	661.9	776.7
L_m	0.699	1.102	1.854	2.959	5.039	6.564
L_e	0.711	1.107	1.851	2.965	5.01	6.33
$\Delta(L_e - L_m)[\%]$	1.3	0.2	-0.4	0.	-0.7	-3.7

SIMBIOS FEL F-474 (3m)

λ_m [nm]	410.7	441.5	487.6	546.9	661.9	776.7
L_m	0.0199	0.03134	0.05269	0.08409	0.14417	0.20382
L_e	0.01976	0.03075	0.05142	0.08235	0.13918	0.17584
$\Delta(L_e - L_m)[\%]$	-0.5	-1.5	-2.	-1.6	-2.8	-10.9

Table 4.8: *Results at the University of Miami from 10/17/02 for distances FEL/plaque of 0.5m and 3m. Radiance unit is $\mu W/(cm^2\ sr\ nm)$. L_m is the SXR-II measured radiance, L_e is the expected radiance. Δ is the difference $L_e - L_m$ in %.*

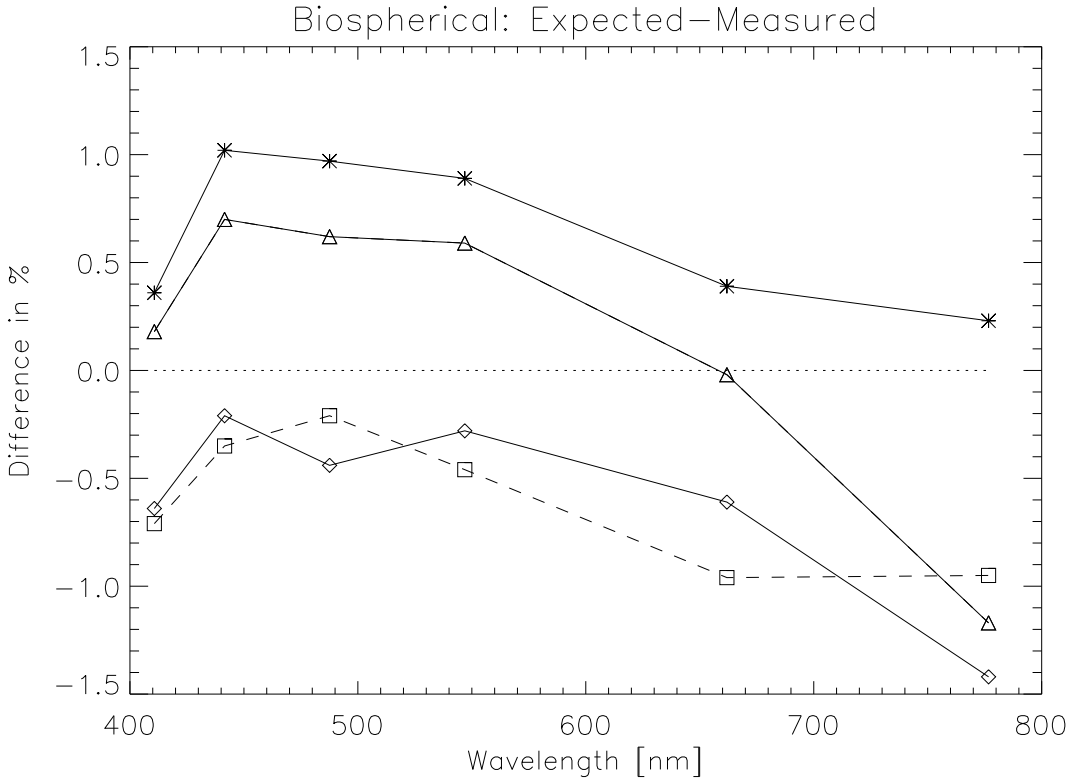

Figure 4.6: *The solid lines show the differences of the expected radiances at Biospherical and the SXR-II measured radiances (stars: F-473, diamonds: F-91773, triangles: F-714). The dashed line shows the difference of the expected radiance of F-473 and the SXR-II measured radiances from SIMRIC-1.*

found in SIRREX-7, Fig. 5, page 25 ([Hooker et al., 2002]): the difference in channels 2 and 3 is almost identical, in channel 4 it is about 0.3% greater than in channel 5, in channels 2 and 3 it is about 0.8% better than in channel 4, and in channel 1 it is about 0.3% better than in channels 2 and 3. In both studies (SIMRIC-2 and SIRREX-7), the measured values are higher than the expected values. The cause for the average differences found in SIRREX-7 was never discovered.

Satlantic started to use the effective distance correction for the offset of the lamp center relative to the front of the pins (see [Meister et al., 2002], section 4.7) in 2003, but it did not use it for the SIMRIC-2. If the effective distance correction had been used, the expected radiances at Satlantic would have increased by about 0.8%, improving the agreement with the SXR-II measured radiances.

4.3 SIMBIOS FEL F-474

FEL type lamps of 1000 W, modified to a medium bipost stage are the most common type of source used as spectral irradiance standards. The SIMBIOS Project owns an FEL lamp calibrated by Optronics Laboratories (OL) in September 1997, labeled as F-474. This lamp was used at all those participating laboratories who also used FEL lamps as calibration source. It illuminated a Spectralon plaque and the radiance reflected from the Spectralon plaque was measured by the SXR-II and a local radiance radiometer, except at the NASA Code 920.1 laboratory, where no plaque is used, thus the lamp was only measured by the Code 920.1 irradiance radiometer.

The calibration by OL is invalid since September 1998. The OL calibration is used nonetheless, and the results from all other laboratories are compared against it, keeping in mind that our goal is not to verify the OL calibration, but to compare how the laboratories are doing relative to each other. The OL calibration data of selected wavelengths is given in Table 4.10, page 49.

The FEL-474 was handcarried to and from the laboratories. On the return flight from Miami, the suitcase

FEL F-711

λ_m [nm]	410.7	441.5	487.6	546.9	661.9	776.7
L_m	0.1616	0.2429	0.3899	0.5952	0.9541	1.1794
L_e	0.1574	0.2373	0.3807	0.5871	0.9443	1.1609
$\Delta(L_e - L_m)[\%]$	-2.6	-2.3	-2.4	-1.4	-1.	-1.6

FEL F-719

λ_m [nm]	410.7	441.5	487.6	546.9	661.9	776.7
L_m	0.1571	0.2366	0.3808	0.5828	0.938	1.1631
L_e	0.1533	0.2316	0.3726	0.5765	0.9311	1.1482
$\Delta(L_e - L_m)[\%]$	-2.4	-2.1	-2.1	-1.1	-0.7	-1.3

FEL F-409

λ_m [nm]	410.7	441.5	487.6	546.9	661.9	776.7
L_m	0.1018	0.1585	0.2658	0.4244	0.7255	0.9361
L_e	0.0989	0.1545	0.2596	0.4174	0.7145	0.9172
$\Delta(L_e - L_m)[\%]$	-2.9	-2.5	-2.3	-1.7	-1.5	-2.

SIMBIOS FEL F-474

λ_m [nm]	410.7	441.5	487.6	546.9	661.9	776.7
L_m	0.1071	0.1662	0.2774	0.4411	0.7496	0.9637
L_e	0.1065	0.1662	0.2786	0.4465	0.7556	0.9596
$\Delta(L_e - L_m)[\%]$	-0.5	0.	0.4	1.2	0.8	-0.4

Table 4.9: *Results at Satlantic from 11/07/02. Radiance unit is $\mu W/(cm^2\ sr\ nm)$. L_m is the SXR-II measured radiance, L_e is the expected radiance. Δ is the difference $L_e - L_m$ in %.*

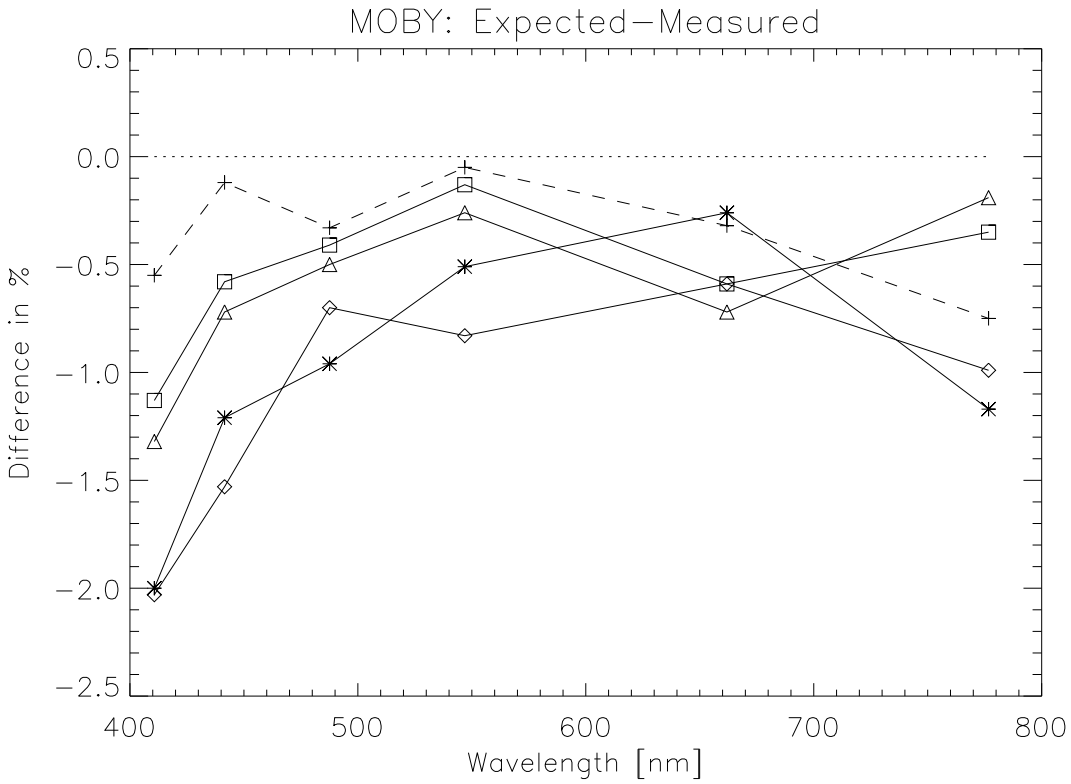

Figure 4.7: *The solid lines show the differences of the expected radiances of the MLML spheres and the SXR-II measured radiances (stars: OL425 W6, diamonds: OL425 W5, triangles: OL420 W6, squares: OL420 W5). The dashed line shows the difference of the expected radiance of the NPR and the SXR-II measured radiances, measured one day before the MLML spheres in the same laboratory at NIST.*

containing the FEL-474 was dropped by an airport security employee. The only laboratory visited after this incident was Satlantic.

The differences of the OL calibration and the SXR-II measured radiances are shown in Fig. 4.10. The laboratory to laboratory variations are stronger than from SIMRIC-1 (about 4% in Fig. 4.10 versus about 2% for SIMRIC-1, see Fig. 4.12 in [Meister et al., 2002]). The overall trend is similar, the differences decrease for higher wavelengths.

The most positive differences in the first four SXR-II channels are from the F-474 measurements at Biospherical, up to 3.4%. Above 450nm, the most negative differences are at UM, ranging from 0 to –4%. This is probably due to a baffling problem, see section 4.2.8. The shape of the differences of the F-474 measured at UCSB is quite similar to the shape of the other FELs measured at UCSB. This suggests that the primary standard at UCSB is not the reason for the strong decrease of the differences with wavelength. Except for Satlantic and NASA Code 920.1, the differences at 777nm are at least 1% smaller than at 662nm, and smaller at 547nm than at 662nm by at least 0.7%.

The results from NASA Code 920.1 for the F-474 are given in table 4.10. They were not measured by the SXR-II, but by the NASA Code 920.1 transfer spectrometer OL746, thus the wavelengths shown in Fig. 4.10 (dashed lines) are different from the SXR-II center wavelengths. A look at the data from NASA Code 920.1 shows that from 400 to 600nm (SXR-II channels 1-4), the differences are similar to results from other laboratories, but around SXR-II channel 6 (777nm), the difference is significantly different from the results of the other laboratories, it is about 4% higher. In order to compare this difference to the difference found in the sphere comparisons at NASA Code 920.1 (Fig. 4.1, page 36), it is important to keep in mind that in Fig. 4.10 the measured values are provided by NASA Code 920.1, but in Fig. 4.1 the expected values are provided by NASA Code 920.1. This means that the sign of the differences is expected to be reversed, which is in fact the case.

For channel 6, the differences expected minus measured radiance of the main calibration standards at UCSB, NRL, Biospherical, and Satlantic are: [-2.4%, -3.0%, 0.2%, -1.4%], the differences of the F-474 are: [-1.3%, -1.6%, 0.8%, -0.4%]. Assuming that the SXR-II measured radiances and the irradiance calibration data of the

SIMBIOS FEL F-474 measured by 746, calibrated by OL in 1997

λ [nm]	E_m(8/18/02)	E_e	Δ(8/18/02)[%]	E_m(9/12/02)	Δ(9/12/02)[%]	Stabil. [%]
400	1.861	1.91	2.7	1.873	2.0	0.7
450	3.841	3.94	2.6	3.871	1.8	0.8
500	6.460	6.54	2.9	6.504	2.2	0.7
600	12.298	12.7	3.3	12.380	2.6	0.7
700	17.138	17.9	4.4	17.244	3.8	0.6
800	20.038	21.0	4.8	20.193	4.0	0.8

Table 4.10: *Irradiance of the SIMBIOS FEL F-474 for a distance of 50 cm, measured by the OL 746. E_m is the measured irradiance of the respective date. Irradiance unit is $\mu W/(cm^2\ nm)$. Expected irradiance E_e is from the OL 1997 calibration. Common wavelengths of OL calibration and 746 are shown. Stability is the difference E_m(9/12/02)–E_m(8/18/02).*

main calibration standards are correct, it follows that the differences found for the main calibration standards are due to protocol, setup or baffling issues that will apply to all FELs measured in that laboratory. Thus we can use the differences of the main calibration standards to correct the differences of the F-474, which yields [+1.1%, +1.4%, +0.6%, +1.0%] for the respective laboratories, which averages to +1.0%. This average value shall be called 'corrected F-474 difference'. The average difference of the expected irradiance and the two measured irradiances from NASA Code 920.1 (8/18/02 and 9/12/02) is 4.1% at 700nm and 4.4% at 800nm. This is about 3.3% higher than the corrected F-474 difference. The average difference at 777nm for the sphere comparisons (table 4.1, page 35) is -2.3%. As mentioned above, the sign needs to be reversed, so the F-474 irradiance measurements at NASA Code 920.1 are 1.0% (=3.3% - 2.3%) lower than it was expected from the sphere comparisons.

NASA Code 920.1 measured the F-474 on two different dates, 8/18/02 and 9/12/02. The maximum difference between the two measurements is 0.8%, a significant improvement compared to the SIMRIC-1. Comparing the results from NASA Code 920.1 for the F-474 from the SIMRIC-1 and SIMRIC-2, it can be seen that the measurements from 9/12/02 and 6/19/01 agree within 0.3%. This suggests that the F-474 measurement at 6/18/01 is abnormal, because the difference between the irradiances of the F-474 measured by the OL746 during SIMRIC-1 on 6/18/01 and 6/19/01 ranges from 1.6 to 3.0%. Thus the conclusion drawn in section 4.3.7 in [Meister et al., 2002] concerning the better quality of the Hardy sphere measurements on 6/18/01 compared to the measurements on 6/19/01 cannot be sustained. In the appendix, the results for the Hardy spheres from SIMRIC-1 are given for both days.

4.4 Linearity Comparison

The sphere at the University of South Florida (USF) is not used for absolute calibrations, thus the SXR-II could only be used to check the linearity of the sphere. The sphere exit aperture underfilled the SXR-II field of view. This was not a problem since neither the sphere nor the SXR-II were moved between the measurements, and absolute radiances are not required for a linearity check.

The SXR-II measured the sphere at 5 levels: 500, 3,000, 5,000, 10,000 and 20,000 FL. The data processing involved several steps:

- First, the SXR-II measured radiances of all levels were normalized by the SXR-II measured radiances of 500FL. The SXR-II saturated in 2 channels at 10,000FL and in 4 levels at 20,000FL.
- Second, the calibration radiances were normalized to the calibrated radiances of the 500FL level. The sphere was calibrated at 4 levels by Labsphere: 500, 3,000, 10,000 and 20,000FL, at wavelength intervals of about 50 nm.
- Third, these normalized values were interpolated to the 6 wavelengths of the SXR-II channels.

The ratio of these interpolated, normalized calibration radiances (S_C) to the normalized SXR-II measured radiances (S_M) is shown in the top 4 plots of Fig. 4.11. By definition, at 500FL the ratio is one. For higher levels, the deviations are within a range of $\pm$1%.

The 5,000 and 10,000FL levels were measured twice by the SXR, separated by about 25 minutes. In the two lower plots of Fig. 4.11, the ratios of these SXR-II measured radiances are shown for each level. It can be seen

Time [hh:mm]	Level [FL]
10:26	20,000
10:33	10,000
10:39	5,000
10:46	3,000
10:53	500
10:59	10,000
11:05	5,000

Table 4.11: Timetable for the start of the SXR-II measurements at USF. Each measurement lasted about 3 minutes. The lamp of the sphere was turned on at 10:15, the power supply was turned on at 10:04.

that the radiances of the second measurement are about 0.5% higher in some channels. The lamp was ramped up about 10 minutes before the first measurement, the power supply was ramped up about 20 minutes before the first measurement. It is likely that the warmup time for the sphere was too short, compromising the results of this comparison. However, the SXR-II measurements used in Fig. 4.11 for the 500, 3,000 and 10,000 FL level were acquired within 15 minutes, 30 minutes after the lamp was turned on (see Table 4.11). Thus for these two levels, the warmup should have been adequate, but probably not for the 20,000FL level. The repeatability uncertainty for the SXR-II is about 0.1%, the uncertainty for the linearity of the SXR-II is about 0.1% as well [Johnson et al., 1998]. Thus from the measurements made, we can conclude that the calibration of the sphere is linear from 500FL to 10,000FL to within about $\pm 0.5\%$.

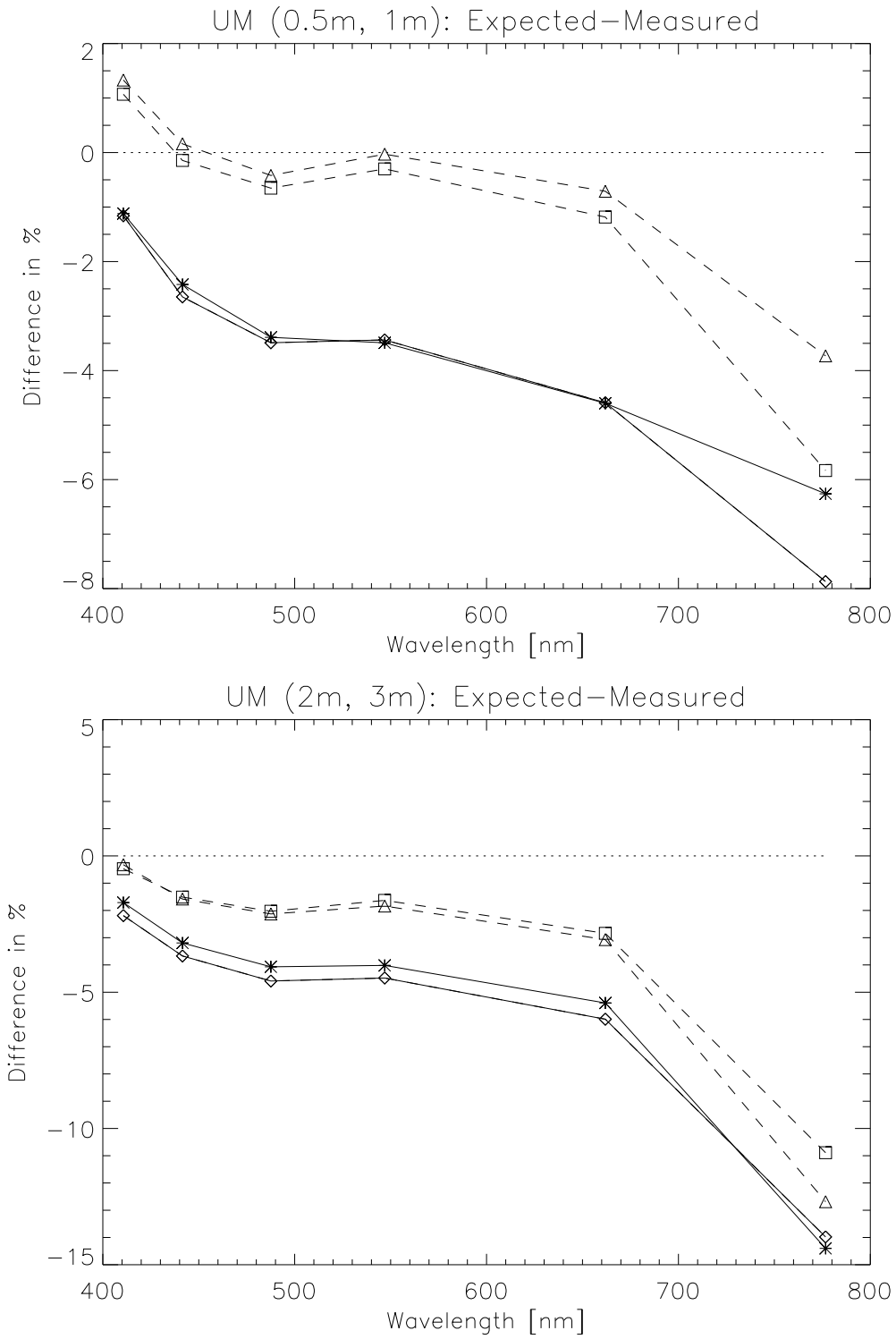

Figure 4.8: *The solid lines show the differences of the expected radiances at the University of Miami and the SXR-II measured radiances for the F-161. The dashed line shows the difference of the expected radiance at UM and the SXR-II measured radiances for the SIMBIOS FEL F-474. The top plot shows the results for the standard distance 0.5m (stars and triangles) and 1m (diamonds and squares) between plaque and FEL, the bottom plot for a distance of 2m (stars and triangles) and 3m (diamonds and squares).*

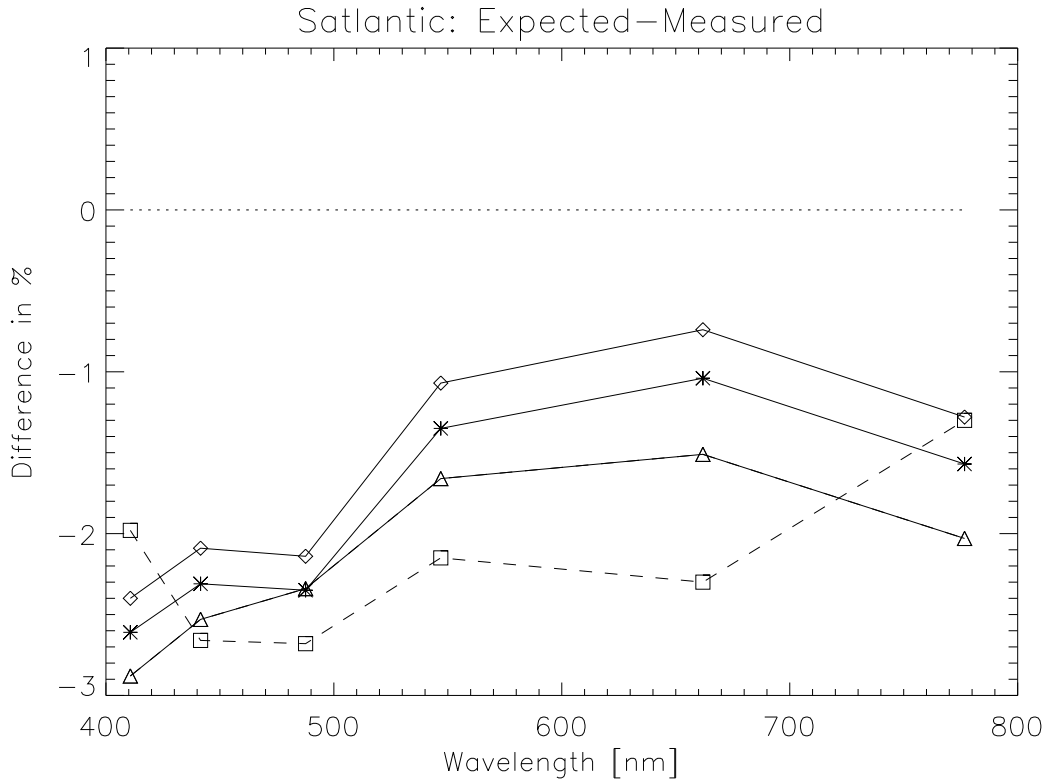

Figure 4.9: *The solid lines show the differences of the expected radiances at Satlantic and the SXR-II measured radiances (stars: F-711, diamonds: F-719, triangles: F-409). The dashed line shows the difference of the expected radiance at Satlantic of F-409 and the SXR-II measured radiances from SIMRIC-1. A correction with the SQM-II measurements of the SXR-II SIMRIC-1 measurements similar to the corrections applied for the SIMRIC-2 would change the difference for channel 1 by approximately -1.0% to about -3.0%.*

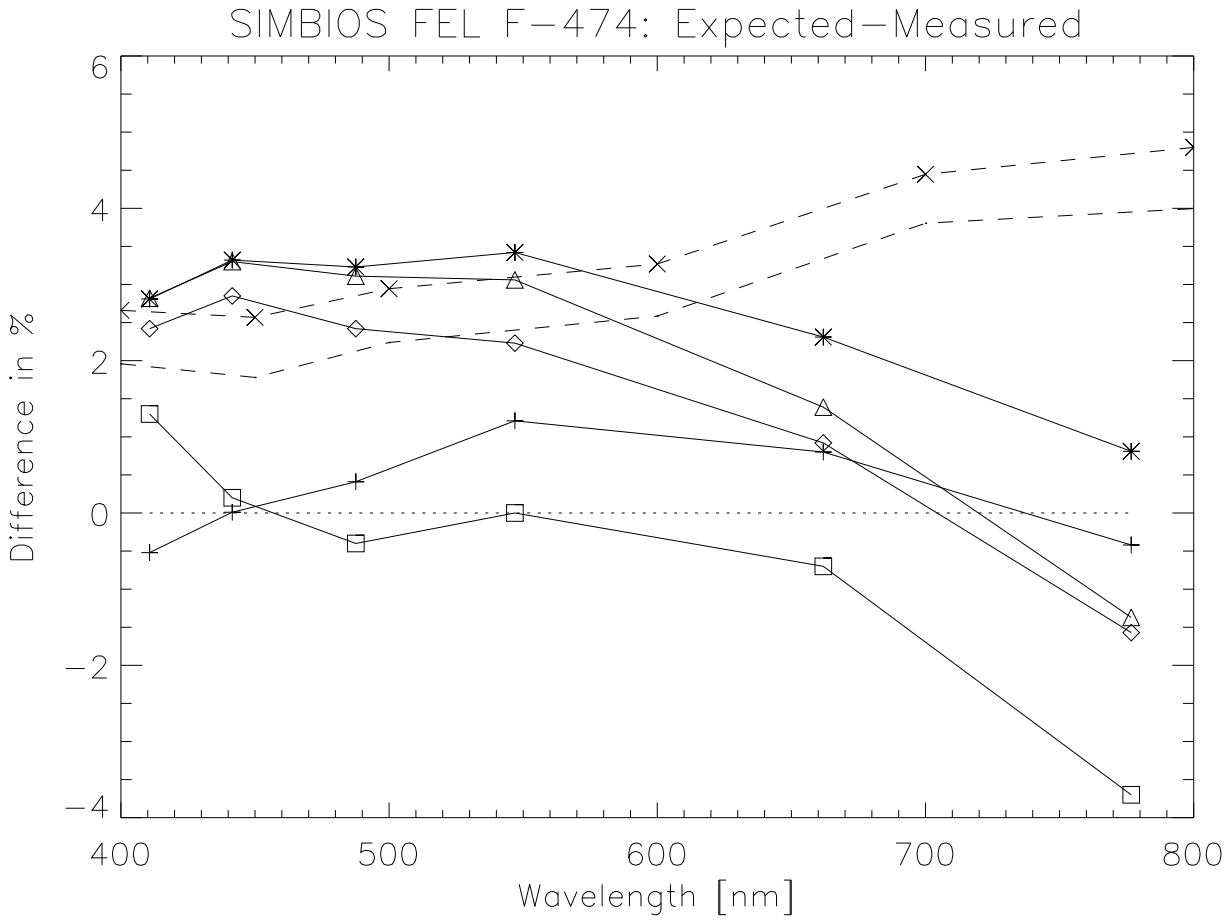

Figure 4.10: *The solid lines show the differences of the expected radiances from the OL calibration of the SIMBIOS FEL F-474 and the SXR-II measured radiances at the following laboratories: Biospherical (stars), NRL (diamonds), UCSB (triangles), UM (squares), Satlantic (plus signs). The dashed line shows the difference of the expected irradiance from the OL calibration of the SIMBIOS FEL F-474 and the measured irradiance of the F-474 using the NASA Code 920.1 transfer spectrometer (crosses for 8/18/02, no symbols for 9/12/02).*

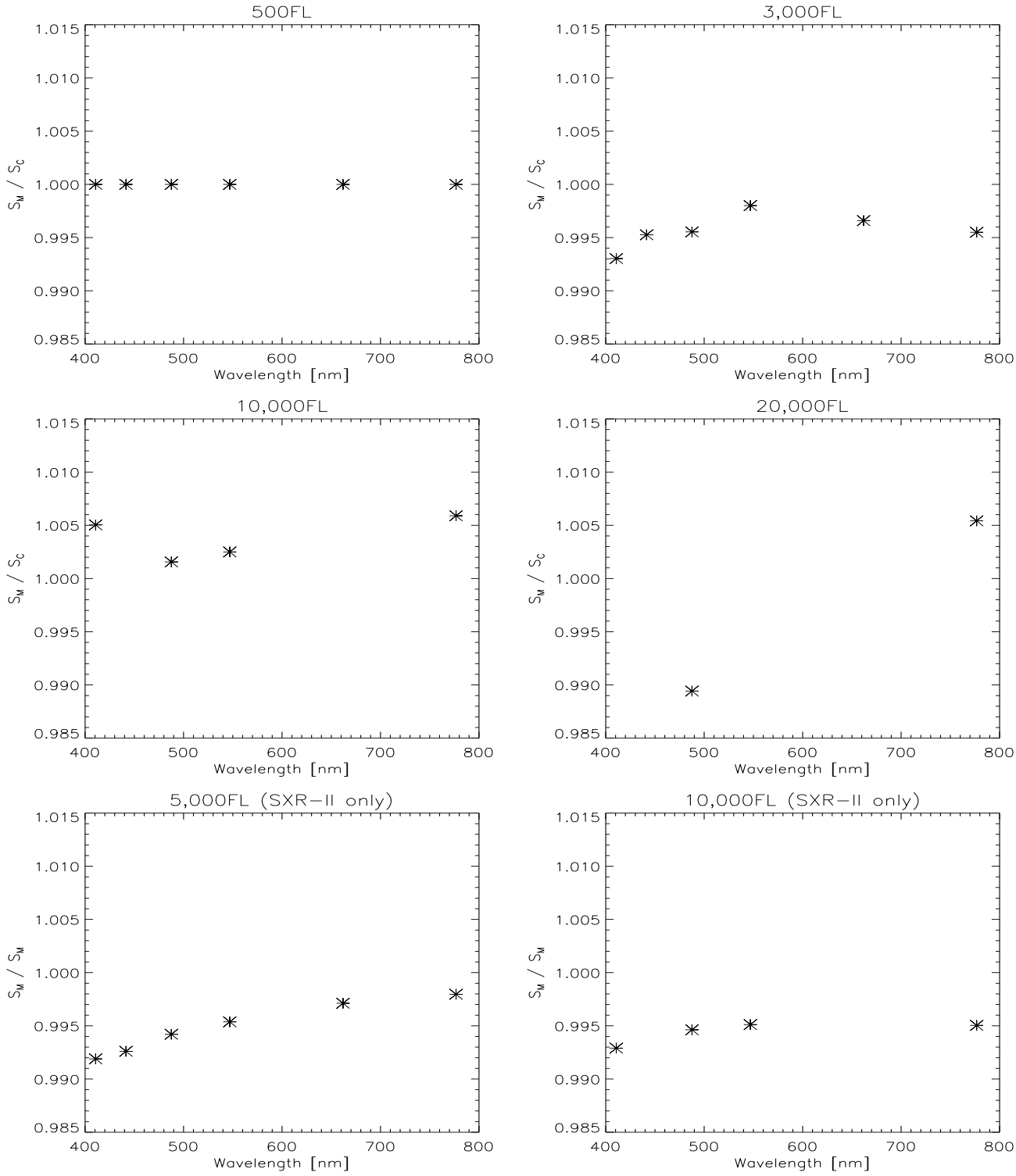

Figure 4.11: *Results of the measurements at USF. The top four plots show the normalized SXR-II measured radiances (S_M) divided by the normalized calibration radiances (S_C, see text). The lower two plots show the S_M ratios of those levels measured twice. A timetable for all SXR-II measurements is given in Table 4.11.*

Chapter 5

Spectralon Plaques

5.1 Background

Radiance calibrations are can be made by illuminating a reflectance standard normally (i.e. an incidence angle of 0°) and viewing the plaque at an angle of 45°. Spectralon plaques are widely used as reflectance standards. Unfortunately, there is no agreement in the oceanographic community on the usage of reflectance factors for these plaques. The plaques are produced by Labsphere, which advertises their reflectance as 'highly lambertian', i.e independent of the illumination and viewing geometry. If the plaques were truly lambertian, the '8°/ Hemispherical Reflectance Factor' usually provided by Labsphere would be the correct quantity to use in the above described calibration setup. However, the deviations from a lambertian reflector are found to be so significant ([Johnson et al., 1996], [Jackson et al., 1992]) that either a correction to the specific illumination and viewing geometry is necessary, or the bidirectional reflectance factor should be measured directly for the required illumination and viewing angles. Upon request, Labsphere provides a so called 'Spectral Reflectance Factor' for illumination/viewing angles of 0°/45°, but there is not enough documentation made available by Labsphere to show that this quantity is indeed the required 'Bidirectional Reflectance Factor' as defined in [Nicodemus et al., 1977]. The Spectral Reflectance Factor is typically about 2% higher than the 8°/ Hemispherical Reflectance Factor.

5.2 Reflectance calibrations of the SIMBIOS plaque

The SIMBIOS Project purchased a Spectralon plaque with two reflectance calibrations made in September 2001 from Labsphere: the 8°/ Hemispherical Reflectance Factor and the Spectral Reflectance Factor, see [Meister et al., 2002], chapter 4.6. Labsphere estimates an uncertainty of 0.5% for the 8°/ Hemispherical Reflectance Factor and 1.5% to 1.8% for the Spectral Reflectance Factor. In April 2002, the SIMBIOS plaque was calibrated at the Diffuser Calibration Facility (DCaF) of NASA Code 920.1 for both quantities as well. At DCaF, the plaque was illuminated by a broadband xenon arc lamp. A monochromator provided light from 400 to 800 nm in 100 nm steps with 12 nm bandwidths. The measurements were made relative to a Labsphere Spectralon plaque (S/N 20471-1-1, calibrated by NIST on a regular basis). The uncertainty at DCaF is given as 1.0 % for the measurement of both quantities [Georgiev and Butler, 2002]. An 8°/ directional/hemispherical integrating sphere is used for the measurement of the 8°/ Hemispherical Reflectance Factor. The same light source and scatterometer as for the directional/directional measurements are used. More information on the setup can be found at 'http://spectral.gsfc.nasa.gov' and [Georgiev and Butler, 2002].

The reflectance calibrations are compared in Fig. 5.1. It can be seen that the calibration for the 8°/ Hemispherical Reflectance Factor agree very well, the maximum difference is only 0.2 %, with no obvious trend in the differences. The bidirectional reflectance factors measured at DCaF are about 1 % higher than the Spectral Reflectance Factor measured by Labsphere. They show a similar spectral trend, a rise of about 1 % from 400 nm to 770 nm for Labsphere, a rise of about 0.5 % from 400 nm to 800 nm for DCaF. The lower plot in Fig. 5.1 also contains an approximation of the bidirectional reflectance factor suggested in [Johnson et al., 1996], the 8°/ Hemispherical Reflectance Factor multiplied by 1.028, shown as a dashed line. It is interesting to see that the DCaF measurements are closer to the dashed line than to the Labsphere measurements, especially above 500 nm.

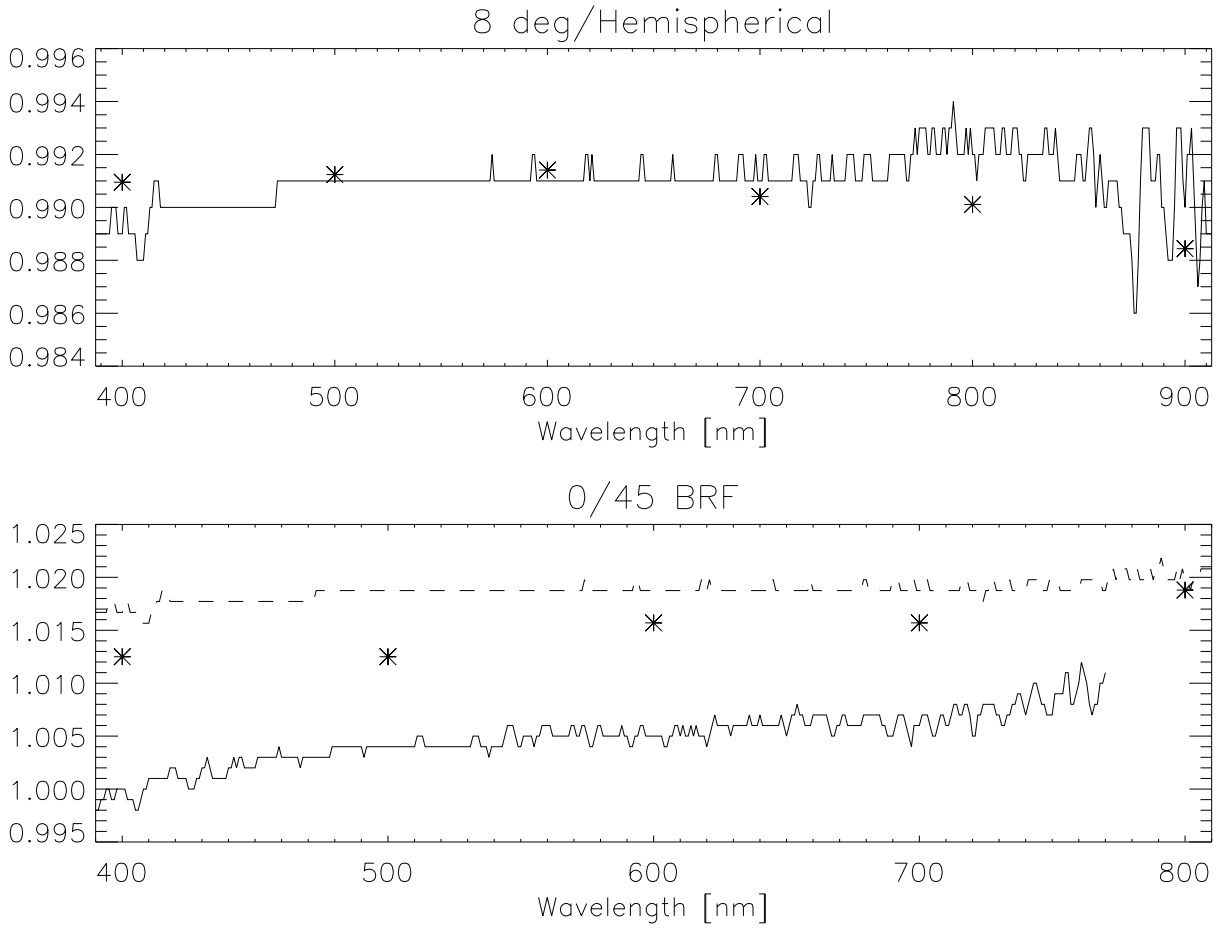

Figure 5.1: *Reflectance calibrations of the SIMBIOS Spectralon Plaque S/N 34079. The stars show the NASA Code 920.1 DCaF measurements from April 2002, the solid line shows the Labsphere measurements from September 2001. The top plot shows the* 8°/ *Hemispherical Reflectance Factors, the lower plot shows the* 0°/45° *bidirectional reflectance factors. The dashed line in the lower plot shows the Labsphere* 8°/ *Hemispherical Reflectance Factor multiplied by 1.028, a correction suggested in [Johnson et al., 1996]. The dotted line shows the average value*

Independently of the SIMRIC-2 activities, Spectralon plaques have been sequentially sent to NIST by DCaF over a period of several years, for calibrations of directional/ hemispherical (R(6°/hem.)) and directional/directional (R(0°/45°)) reflectance. The average of the ratios at 400, 500, 600, 700, 800, and 900 nm was calculated to be 1.025± 0.003, taking into account typical NIST uncertainties for directional/hemispherical and directional/directional reflectance (Jim Butler, private communication, 2002). This value agrees well with the measurements taken at DCaF of the SIMBIOS Spectralon plaque.

Chapter 6

Conclusions

The comparisons between the expected radiances (based on the calibration data provided by the respective laboratory) and the measured radiances (based on the NIST calibrated SXR-II transfer radiometer) showed that most laboratories agree well within the combined uncertainties (the uncertainties for the laboratories are typically about 2%, see [Meister et al., 2002], the uncertainties for the SXR-II are up to 1%, see table 2.2, page 6). Exceptions are the laboratories at Wallops Flight Facility and the University of Miami. The most likely error sources have been identified (sections 3.2.3 and 3.2.9) and have been addressed by these laboratories.

For most laboratories, the measured radiance at 777nm is higher than the expected radiance. This may indicate a bias in the calibration of the SXR-II. But the mid-year comparison at NIST (Fig. 2.12, page 22) seems to limit this bias to less than 1%. Another possible explanation is stray light problems in these laboratories caused by the reflectance spectrum of the baffling material. For NASA Code 920.1, ICESS at UCSB, NRL, and UM the measured radiances increase significantly relative to the expected radiances above 600nm than in the shorter wavelengths. The comparison using the F-474 (Fig. 4.10, page 53) shows an increase of the SXR-II measured radiances relative to the expected radiances for the longer wavelengths compared to the shorter wavelengths. But the transfer radiometer from NASA Code 920.1 shows an increase of its measured irradiance relative to the expected radiances for longer wavelengths. Ambient stray light is an unlikely error source for irradiance measurements at NASA Code 920.1, because the stray light level for the FELs for which the calibration transfer is done is similar (e.g. if the measurement of the primary standard contains significant stray light, the measurement of the secondary standard is expected to contain a similar amount). The source for the bias between expected radiances and SXR-II measured radiances in channel 6 in the above mentioned laboratories cannot be determined from the available data: it may be a different error source for each laboratory, or it may be a bias in the SXR-II measurements of unknown origin.

It is interesting to note that most measured radiances are higher than the expected radiances, for SIMRIC-1 as well as for SIMRIC-2. This may indicate that stray light or a brightness increase of the irradiance or reflectance standards is a more common problem than a brightness decrease of the irradiance or reflectance standards.

According to the NIST calibrations on SIRCUS, the SXR-II has been more stable in 2002 than in 2001. The maximum difference between the December 2000 and the December 2001 NIST calibration is 1.6% (see appendix, table A.1), the maximum difference between the December 2001 and the January 2003 NIST calibration is only 0.7%. The uncertainties of the NIST calibrations of the SXR-II are not exactly known (no calibration report has been delivered by NIST until June 2003 for either calibration), but the differences seen in 2002 are probably close to the combined uncertainties of the December 2001 and the January 2003 NIST calibrations.

The time series of the SXR-II measurements of the two SQMs (OCS-5002 and SQM-II) in the SIMBIOS Optical Laboratory showed a dip of the channel 1 (411nm) radiances in the summer of 2002 by about 2%, see section 2.4.2. A very similar dip of channel 1 was observed in the summer of 2001 when monitoring the SQM-II [Meister et al., 2002]. The blue internal monitor of the OCS-5002 did not show a dip during that period. Thus we have evidence from four different light sources (SQM-II and OCS-5002, each with HiBank and LoBank) and from the blue internal monitor of the OCS-5002 that this dip is indeed caused by a change in the responsivity of the SXR-II. The SXR-II looked at a NIST light source calibrated at FASCAL in August 2002 (Fig. 2.12, page 22). The difference of the expected and measured radiance also suggests that the SXR-II measured radiance in channel 1 was too low at that time. Thus it was decided to correct the SXR-II measurements with the SQM time series (see section 2.4.2). It was decided to do this for all channels, because this improved the mid-year comparison at NIST for all channels (no change in channel

2). The corrections to the SXR-II measured radiances are less than 0.5% for all channels (see Fig. 2.10, page 20), except for channel 1 with a correction of up to 2%.

The performance of the two SQMs of the SIMBIOS Project has been comparable. The short term (weeks to months) evolution of the SXR-II responsivity derived from either SQM is extremely similar, see Fig. 2.10, page 20. But for long term monitoring, the radiances produced by the two SQMs are significantly different, with an increase of up to about 1% for both SQM-II HiBank and LoBank, a decrease of up to 0.6% for the OCS-5002 LoBank and a decrease of up to 2% for the OCS-5002 HiBank. Unfortunately, the long term stability of the internal monitors of neither the SQM-II (Fig. 2.8, page 15) nor the OCS-5002 internal blue monitor (table 2.7, page 19) agreed well with the stability of the respective SXR-II channels.

The bidirectional reflectance factor and the hemispherical reflectance factor of a SIMBIOS Spectralon reflectance plaque was measured at NASA Code 920.1 (section 5). The hemispherical reflectance factors agree very well with the hemispherical reflectance factors from a recent Labsphere calibration. But the directional reflectance factor from Code 920.1 is about 1% higher than the Spectral Reflectance Factors from the Labsphere calibration. The directional reflectance factor from Code 920.1 is about 0.5% lower than a directional reflectance factor calculated using a method suggested in [Johnson et al., 1996], which uses the hemispherical reflectance factor. An independent study with 4 Spectralon plaques being calibrated by NIST yielded similar results. This means that it is uncertain if those SIMRIC-2 participants using the method from [Johnson et al., 1996] would increase their accuracy if they switched to using the Spectral Reflectance Factors from Labsphere. More research is needed on this subject.

FELs are calibrated by NIST at a distance of 50cm. Many of the SIMRIC-2 participants illuminate Spectralon plaques at distances greater than 50cm. The method for scaling the irradiance from 50cm to the distance used to illuminate the plaque has recently been described by NIST [Yoon et al., 2003] and [Mueller et al., 2003] (Volume 6, page 23). ICESS at UCSB and Satlantic adopted this method. The main author of this study hopes that this method will disseminate quickly to all laboratories which use FELs at distances greater than 50cm.

Acknowledgements

Thanks to Jim Butler and Georgi Georgiev from NASA Code 920.1 for measuring the SIMBIOS Spectralon plaque and providing the data from their plaques, and to Carol Johnson and Steve Brown from NIST, Optical Technology Division, for their support with the SXR-II, and to K-Engineering, Tokyo, Japan, for their permission to use their FEL lamp.

Appendix A

Corrected SIMRIC-1 results

A.1 Calibration coefficients

NIST provided corrected SXR-II calibration coefficients for the calibrations on SIRCUS in December 2000 and December 2001. The changes for the December 2000 calibration are negligible (less than 0.1 %), still the numbers are given in table A.1 below. The changes for December 2001 are up to 0.4 %, thus it is justified to recalculate the major radiance comparison results for the SIMRIC-1 from 2001.

	Channel 1	Channel 2	Channel 3	Channel 4	Channel 5	Channel 6
λ_m [nm]	410.69	441.51	487.58	546.89	661.91	776.71
$< D_{cs}^{2000}$ [V cm^{2}sr nm/μW] $>$	0.65511	0.92577	0.11749	0.20207	0.17642	0.017722
$\delta < D_{cs}^{2000} >$ [%]	-0.1	-0.1	-0.1	-0.1	-0.1	0
$< D_{cs}^{2001} >$ [V cm^{2}sr nm/μW]	0.65595	0.94123	0.11818	0.20419	0.17758	0.017694
$\delta < D_{cs}^{2001} >$ [%]	-0.4	0	-0.4	-0.4	-0.4	-0.4
$\Delta < D > (2001 - 2000)$ [%]	0.1	1.6	0.6	1.0	0.7	-0.2

Table A.1: *Corrected SXR-II calibration coefficients* $< D_{cs} >$ *for gain 1 on the SXR-II amplifier (multiplied by -1, the radiometer provides negative voltages) and moment wavelengths* λ_m *for the 6 SXR-II channels. The difference* δ *gives the difference in % of the corrected calibration coefficients minus the initial calibration coefficients for the respective year. The difference* Δ *in the coefficients between the two dates is calculated as* $< D_{cs}^{2001} >$ *minus* $< D_{cs}^{2000} >$ *and given in %.*

A.2 Radiance comparison results

The measured radiances are calculated by dividing the measured voltages by the calibration coefficients, thus a reduction of the calibration coefficient leads to an increase in the measured radiances. Measurements at the end of the year of 2001 (e.g. at Satlantic) are more affected by the changes than measurements at the beginning of the year (e.g. at NRL) because only the calibration coefficients from December 2001 changed significantly. Note that a linear interpolation of the SXR-II calibration coefficients between December 2000 and December 2001 was used, thus the maximum change for the measured radiance is less than the change of the December 2001 calibration coefficient.

Table A.2 shows the corrected measured radiances and the relative differences of the expected radiances (unchanged from the SIMRIC-1 report, [Meister et al., 2002]) minus the corrected measured radiances.

The expected radiances of the F-473 (a secondary standard) at UCSB were calculated incorrectly (the error is probably due to a problem when transferring the parameters from UCSB to the main author of this study). The correct expected radiances (using the UCSB protocol from SIMRIC-1) for the six SXR-II channels are [μW/(cm^2 sr nm]: [0.04580, 0.07111, 0.11873, 0.18991, 0.32247, 0.41039].

NRL, FEL F-400, 04/24/01:

Wavelength [nm]	410.69	441.51	487.58	546.89	661.91	776.71
L_m [μW/(cm^2 sr nm]	0.72544	1.12677	1.88286	3.02773	5.18413	6.67494
Difference ($L_e - L_m$) [%]	-2.0	-1.6	-1.3	-1.5	-2.0	-3.2

Scripps, Labsphere sphere, 05/01/01:

Wavelength [nm]	410.69	441.51	487.58	546.89	661.91	776.71
L_m [μW/(cm^2 sr nm]	7.9141	sat.	21.3548	34.9646	59.6094	74.5831
Difference ($L_e - L_m$) [%]	-0.6	sat.	0.2	0.3	0.5	0.5

Biospherical, FEL F-473, 05/03/01:

Wavelength [nm]	410.69	441.51	487.58	546.89	661.91	776.71
L_m [μW/(cm^2 sr nm]	0.025000	0.038365	0.063072	0.099547	0.166100	0.209729
Difference ($L_e - L_m$) [%]	-0.7	-0.3	-0.2	-0.5	-1.0	-1.0

UCSB, FEL F-514, 05/08/01:

Wavelength [nm]	410.69	441.51	487.58	546.89	661.91	776.71
L_m [μW/(cm^2 sr nm]	0.048974	0.075881	0.126115	0.201634	0.342929	0.444233
Difference ($L_e - L_m$) [%]	-0.7	-0.9	-0.8	-1.2	-1.9	-4.3

HOBI Labs, Oriel 7-1259, 05/10/01:

Wavelength [nm]	410.69	441.51	487.58	546.89	661.91	776.71
L_m [μW/(cm^2 sr nm]	0.245352	0.367841	0.585362	0.892488	1.41382	1.72806
Difference ($L_e - L_m$) [%]	-2.0	-2.0	-1.6	-1.2	-0.7	-1.5

NASA Code 920.1, Hardy (6 lamps), 6/18/01:

Wavelength [nm]	410.69	441.51	487.58	546.89	661.91	776.71
L_m [μW/(cm^2 sr nm]	3.74222	7.69253	15.1028	25.2661	40.7930	48.2187
Difference ($L_e - L_m$) [%]	3.6	0.1	-0.2	0.4	-0.4	-1.6

NASA Code 920.1, Hardy (6 lamps), 6/19/01:

Wavelength [nm]	410.69	441.51	487.58	546.89	661.91	776.71
L_m [μW/(cm^2 sr nm]	3.77232	7.73375	15.1263	25.3149	40.9339	48.2095
Difference ($L_e - L_m$) [%]	3.7	0.5	-0.4	-0.4	-1.9	-2.8

Satlantic, FEL F-662, 09/05/01:

Wavelength [nm]	410.69	441.51	487.58	546.89	661.91	776.71
L_m [μW/(cm^2 sr nm]	(0.153200)	0.233377	0.376427	0.578462	0.936355	1.14818
Difference ($L_e - L_m$) [%]	(-1.6)	-2.0	-2.2	-1.5	-1.6	-0.6

Satlantic, FEL F-409 (NIST calibration from 1996), 09/05/01:

Wavelength [nm]	410.69	441.51	487.58	546.89	661.91	776.71
L_m [μW/(cm^2 sr nm]	(0.100668)	0.158370	0.265818	0.425410	0.729120	0.928410
Difference ($L_e - L_m$) [%]	(-2.0)	-2.7	-2.7	-2.1	-2.3	-1.3

Table A.2: *Corrected SXR-II measured radiances of the highest level calibration sources which were measured in the participating laboratories. Values in brackets are questionable due to a suspected instability in channel 1 of the SXR-II late in 2001, see [Meister et al., 2002], chapter 2.3.2. L_m is the measured radiance, L_e is the expected radiance. L_e did not change and is given in the tables in [Meister et al., 2002].*

A.3 SQM-II time series

The corrected changes of the SQM-II radiance as measured by the SXR-II are shown in Table A.3 and Fig. A.1. The two curves in Fig. A.1 are extremely similar: both show a decrease in the blue and an increase in the red/NIR. The SQM-II LoBank has increased about 0.5 % more than the SQM-II HiBank. This can be explained by a decrease in the color temperature of the SQM-II light bulbs. It is remarkable that even the 'spikes' at 488 nm and 662 nm are very similar. A likely reason for the spikes is the NIST calibration. The spikes are so small (less than 0.5 %) that they are within the combined uncertainties of the two NIST calibrations.

SXR-II wavelength [nm]	410.69	441.51	487.58	546.89	661.91	776.71
SQM-II HiBank increase [%]	-0.8	-0.8	0	0	0.6	0.3
SQM-II LoBank increase [%]	-0.3	-0.2	0.6	0.6	1.1	0.8

Table A.3: *Corrected change of the SXR-II measured radiance of the SQM-II HiBank and LoBank from December 2000 to December 2001. The differences were calculated using the averages of the 3 SXR-II/SQM-II measurement sessions before and after the NIST calibrations in December 2000 and December 2001 (subtracting the December 2000 average from the December 2001 average). See Fig. A.1 for a graphical illustration.*

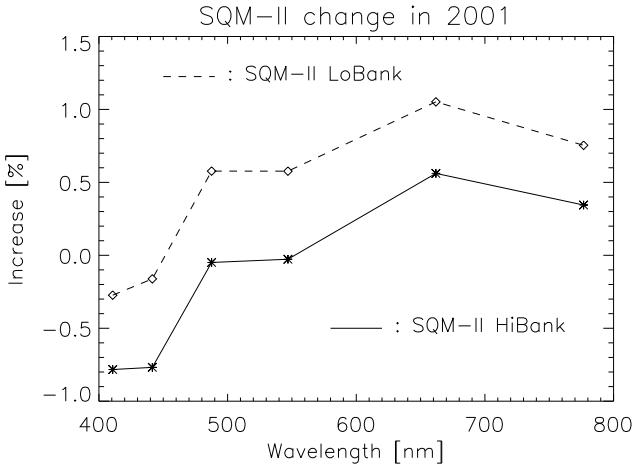

Figure A.1: *Corrected change of the SXR-II measured radiance of the SQM-II HiBank and LoBank from December 2000 to December 2001 (values from Table A.3).*

Appendix B

SIMRIC-2 Participants

The SIMRIC-2 participants are listed below in alphabetical order:

Peter Abel, NASA Goddard Space Flight Center, Code 920.1
Greenbelt Rd, Greenbelt, MD 20771
Tel: 301 614 5943, peter.abel.1@gsfc.nasa.gov

Kendall Carder, College of Marine Science, University of South Florida
St. Petersburg, FL 33701-5016
Tel: 757 553 3952, kcarder@monty.marine.usf.edu

Albert Chapin, Physics Department, University of Miami
Coral Gables, Fl 33146
Tel: 305 284 2325 ext 3, chapin@physics.miami.edu

Dennis Clark, Oceanic Research and Applications Div., NOAA/NESDIS/ORA
Camp Springs, MD 20746
Tel: 301 763 8102, dennis.k.clark@noaa.gov

John Cooper, Raytheon Information Technology and Science Services, NASA Code 920.1
Greenbelt Rd, Greenbelt, MD 20771
Tel: 301 284 5949, john.w.cooper.1@gsfc.nasa.gov

Curtiss Davis, Naval Research Laboratory, Optical Sensing Section, Code 7203
4555 Overlook Avenue, SW, Washington, DC 20375
Tel: 202 767 9269, curtiss.davis@nrl.navy.mil

David English, College of Marine Science, University of South Florida
St. Petersburg, FL 33701-5016
Tel: 757 553 3954, denglish@marine.usf.edu

Michael Feinholz, Physical Oceanography, Moss Landing Marine Laboratories
University Hawaii Marine Center c/o MOBY Project, 1 Sand Island Road, Honolulu, HI 96819
Tel: 808 847 3449, feinholz@nsf.mlml.calstate.edu

Giulietta Fargion, SAIC / SIMBIOS, Goddard Space Flight Center Code 970.1
Greenbelt Rd, Greenbelt, MD 20771
Tel: 301 286 0744, gfargion@simbios.gsfc.nasa.gov

Robert Frouin, Scripps Institution of Oceanography, University of California, San Diego
8810 La Jolla Shores Drive, La Jolla, CA 92037
Tel: 858 534 6243, rfrouin@ucsd.edu

Frank Hoge, AOL Project, NASA Wallops Flight Facility Code 972
Wallops Island, VA 23337-5099
Tel: 757 824 1567, Frank.E.Hoge@nasa.gov

Daniel Korwan, Naval Research Laboratory, Optical Sensing Section, Code 7218
4555 Overlook Avenue, SW, Washington, DC 20375
Tel: 202 404 1391, korwan@nrl.navy.mil

Gordana Lazin, Satlantic Inc., Richmond Terminal, Pier 9, 3481 North Marginal Road
Halifax, Nova Scotia, Canada, B3K 5X8
Telephone: 902 492 4780, gogo@satlantic.com

Charles McClain, Office for Global Carbon Studies, NASA Goddard Space Flight Center Code 971
Greenbelt Rd, Greenbelt, MD 20771
Tel: 301 286 0758, chuck@seawifs.gsfc.nasa.gov

Scott McLean, Satlantic Inc., Richmond Terminal, Pier 9, 3481 North Marginal Road
Halifax, Nova Scotia, Canada, B3K 5X8
Telephone: 902 492 4780, scott@satlantic.com

Gerhard Meister, Futuretech / SIMBIOS, Goddard Space Flight Center Code 970.1
Greenbelt Rd, Greenbelt, MD 20771
Tel: 301 286 0758, meister@simbios.gsfc.nasa.gov

David Menzies, The Institute for Computational Earth System Science (ICESS)
University of California at Santa Barbara (UCSB), Santa Barbara, CA 93106-3060
Tel: 805 893 8496, davem@icess.ucsb.edu

Antoine Poteau, Scripps Institution of Oceanography
8810 La Jolla Shores Drive, La Jolla, CA 92037
Tel: 858 822 1416, poteau@genius.ucsd.edu

James Robertson, Biospherical Instruments Inc.
5340 Riley St, San Diego, CA 92110
Tel: 619 686 1888, robertson@biospherical.com

Jennifer Sherman, Satlantic Inc., Richmond Terminal, Pier 9, 3481 North Marginal Road
Halifax, Nova Scotia, Canada, B3K 5X8
Telephone: 902 492 4780, jennifer@satlantic.com

Kenneth Voss, Physics Department, University of Miami
Coral Gables, FL 33146
Tel: 305 284 2323 ext 2, voss@miami.rsmas.miami.edu

James Yungel, AOL Project, Wallops Flight Facility Code 972
Wallops Island, VA 23337-5099
Tel: 757 824 1026, yungel@osb.wff.nasa.gov

Bibliography

[Biggar, 1998] Biggar S.F., Calibration of a visible and near-infrared portable transfer radiometer, *Metrologia*, 1998, vol. 35, 701-706.

[Brown et al., 2000] Brown S.W., Eppeldauer G.P., Lykke K.R., NIST facility for spectral irradiance and radiance responsivity calibrations with uniform sources, *Metrologia*, 2000, vol. 37, 579-582.

[Clark et al., 2001] Clark D.K., Feinholz M.E., Yarbrough M.A., Johnson B.C., Brown S.W., Kim Y.S., Barnes R.A., *Overview of the Radiometric Calibration of MOBY*, SPIE's 46th Annual Meeting, San Diego, California, July/August 2001

[Clark et al., 2002] Clark D.K., Feinholz M.E., Yarbrough M.A., Johnson B.C., Brown S.W., Kim Y.S., Barnes R.A., Overview of the radiometric calibration of MOBY, In Proceedings of SPIE 4483, pages 64-76, 2002.

[Cattral et al., 2002] Cattral C., Carder K.L., Thome K.J., Gordon H.R., Solar Reflectance-based calibration of spectral radiometers, *Geophysical Research Letters*, vol. 29, no. 20, 2002.

[Fargion et al., 2002] Fargion G.S. and McClain C.R. (editors), SIMBIOS Project 2001 Annual Report, NASA Tech. Memo. 2002-210005, Goddard Space Flight Center, Greenbelt, Md., 2002.

[Georgiev and Butler, 2002] Georgiev G. and Butler J., Bidirectional reflectance distribution function and hemispherical reflectance of JSC Mars-1, Presented at SPIE Annual meeting, Seattle 2002, published in *Proceedings of SPIE*, Zu-Han G., Maradudin A., Surface Scattering and Diffraction for Advanced Metrology II, Volume 4780, pp.165-175, 2002

[Hooker et al., 1998] Hooker S.B., Aiken J., Calibration and Evaluation of field radiometers with the SeaWiFS Quality Monitor (SQM), *Journal of Atmospheric and Oceanic Technology*, 15:995-1007, 1998.

[Hooker et al., 2002] Hooker S.B. et al., The Seventh SeaWiFS Intercalibration Round-Robin Experiment (SIRREX-7), March 1999, NASA Tech. Memo. 2002-206892, Vol. 17, Goddard Space Flight Center, Greenbelt, Md., 2002, 69 p., edited by S.B. Hooker and E.R. Firestone

[Jackson et al., 1992] Jackson R.D., Clarke T., Moran S., Bidirectional Calibration Results for 11 Spectralon and 16 $BaSO_4$ Reference Reflectance Panels, *Remote Sensing of Environment*, 1992, vol. 40, 231-239

[Johnson et al., 1996] Johnson B.C. et al., The Fourth SeaWiFS Intercalibration Round-Robin Experiment (SIRREX-4), May 1995, NASA Tech. Memo. 104566, Vol. 37, Goddard Space Flight Center, Greenbelt, Md., 1996, 65 p., edited by S.B. Hooker and E.R. Firestone

[Johnson et al., 1998] Johnson B.C., Fowler J.B., Cromer C.L., The SeaWiFS Transfer Radiometer (SXR), NASA Tech. Memo. 1998-206892, Vol. 1, NASA/Goddard Space Flight Center, Greenbelt, Md., 1998, 58 p., edited by S.B. Hooker and E.R. Firestone

[Johnson et al., 1998b] Johnson B.C., Shaw P-S., Hooker S.B., Lynch D., Radiometric and engineering performance of the SeaWiFS quality monitor (SQM): A portable light source for field radiometers, *J. Atmospheric Oceanic Technol.*, 1998, vol. 15, 1008-1022.

[Meister et al., 2002] Meister G., Abel P., Barnes R., Cooper J., Davis C., Godin M., Goebel D., Fargion F., Frouin R., Korwan D., Maffione R., McClain C., McLean S., Menzies D., Poteau A., Robertson J., Sherman J., The First SIMBIOS Radiometric Intercomparison (SIMRIC-1), April-September 2001, NASA Tech. Memo. 2002-210006, Goddard Space Flight Center, Greenbelt, Md., 2002, 60p.

[Meister et al., 2003] Meister G. et al., Comparison of spectral radiance calibrations at oceanographic and atmospheric research laboratories, *Metrologia*, 2003, vol. 40, 93-96.

[Mueller et al., 2003] Mueller J.L., Fargion G.S. and C.R. McClain (editors), Ocean Optics Protocols For Satellite Ocean Color Sensor Validation, Revision 4, Volumes I-VI, NASA Tech. Memo. 2003-211621/Rev4-Vol1-6, Goddard Space Flight Center, Greenbelt, Md., January 2003.

[Nicodemus et al., 1977] Nicodemus F.E. et al., Geometric Considerations and Nomenclature for Reflectance, US Department of Commerce, National Bureau of Standards, Monogram 160:52, 1977, 52 p.

[Riley and Bailey, 1998] Riley T., Bailey S., The Sixth SeaWiFS/SIMBIOS Intercalibration Round-Robin Experiment (SIRREX-6), August-December 1997, NASA Tech. Memo. 1998-206878, NASA/Goddard Space Flight Center, Greenbelt, Md., 1998, 26 p., edited by S.B. Hooker and E.R. Firestone

[Yoon et al., 2002] Yoon H.W., Gibson C.E., Barnes P.Y., The realization of the NIST detector-based spectral irradiance scale, *Applied Optics*, 41:5879-5890, 2002.

[Yoon et al., 2003] Yoon H.W., Proctor J.E., Gibson C.E., FASCAL 2: a new NIST facility for the calibration of the spectral irradiance of sources, *Metrologia*, 2003, vol. 40, 30-34.